



National Library  
of Canada

Acquisitions and  
Bibliographic Services Branch

395 Wellington Street  
Ottawa, Ontario  
K1A 0N4

Bibliothèque nationale  
du Canada

Direction des acquisitions et  
des services bibliographiques

395, rue Wellington  
Ottawa (Ontario)  
K1A 0N4

*Your file* *Votre référence*

*Our file* *Notre référence*

## NOTICE

**The quality of this microform is heavily dependent upon the quality of the original thesis submitted for microfilming. Every effort has been made to ensure the highest quality of reproduction possible.**

**If pages are missing, contact the university which granted the degree.**

**Some pages may have indistinct print especially if the original pages were typed with a poor typewriter ribbon or if the university sent us an inferior photocopy.**

**Reproduction in full or in part of this microform is governed by the Canadian Copyright Act, R.S.C. 1970, c. C-30, and subsequent amendments.**

## AVIS

**La qualité de cette microforme dépend grandement de la qualité de la thèse soumise au microfilmage. Nous avons tout fait pour assurer une qualité supérieure de reproduction.**

**S'il manque des pages, veuillez communiquer avec l'université qui a conféré le grade.**

**La qualité d'impression de certaines pages peut laisser à désirer, surtout si les pages originales ont été dactylographiées à l'aide d'un ruban usé ou si l'université nous a fait parvenir une photocopie de qualité inférieure.**

**La reproduction, même partielle, de cette microforme est soumise à la Loi canadienne sur le droit d'auteur, SRC 1970, c. C-30, et ses amendements subséquents.**

**Canada**

**Synthesis and Evaluation of Antibody-Albumin-Methotrexate Ternary  
Conjugates For Cancer Treatment**

by

**Leslie Henry Kondejewski**

**Submitted in partial fulfillment of the requirements for the degree of Doctor of Philosophy**

at

**Dalhousie University  
Halifax, Nova Scotia  
February, 1994**

**© Copyright by Leslie Henry Kondejewski, 1994**



National Library  
of Canada

Acquisitions and  
Bibliographic Services Branch

395 Wellington Street  
Ottawa, Ontario  
K1A 0N4

Bibliothèque nationale  
du Canada

Direction des acquisitions et  
des services bibliographiques

395, rue Wellington  
Ottawa (Ontario)  
K1A 0N4

Your file    Votre référence

Our file    Notre référence

**The author has granted an irrevocable non-exclusive licence allowing the National Library of Canada to reproduce, loan, distribute or sell copies of his/her thesis by any means and in any form or format, making this thesis available to interested persons.**

**L'auteur a accordé une licence irrévocable et non exclusive permettant à la Bibliothèque nationale du Canada de reproduire, prêter, distribuer ou vendre des copies de sa thèse de quelque manière et sous quelque forme que ce soit pour mettre des exemplaires de cette thèse à la disposition des personnes intéressées.**

**The author retains ownership of the copyright in his/her thesis. Neither the thesis nor substantial extracts from it may be printed or otherwise reproduced without his/her permission.**

**L'auteur conserve la propriété du droit d'auteur qui protège sa thèse. Ni la thèse ni des extraits substantiels de celle-ci ne doivent être imprimés ou autrement reproduits sans son autorisation.**

ISBN 0-315-93780-7

**Canada**

Name Leslie Henry Kondejewska

Dissertation Abstracts International is arranged by broad, general subject categories. Please select the one subject which most nearly describes the content of your dissertation. Enter the corresponding four-digit code in the spaces provided.

Biochemistry

0487

U·M·I

SUBJECT TERM

SUBJECT CODE

**Subject Categories**

**THE HUMANITIES AND SOCIAL SCIENCES**

**COMMUNICATIONS AND THE ARTS**

Architecture 0729  
 Art History 0377  
 Cinema 0900  
 Dance 0378  
 Fine Arts 0357  
 Information Science 0723  
 Journalism 0391  
 Library Science 0399  
 Mass Communications 0708  
 Music 0413  
 Speech Communication 0459  
 Theater 0465

**EDUCATION**

General 0515  
 Administration 0514  
 Adult and Continuing 0516  
 Agricultural 0517  
 Art 0273  
 Bilingual and Multicultural 0282  
 Business 0688  
 Community College 0275  
 Curriculum and Instruction 0727  
 Early Childhood 0518  
 Elementary 0524  
 Finance 0277  
 Guidance and Counseling 0519  
 Health 0680  
 Higher 0745  
 History of 0520  
 Home Economics 0278  
 Industrial 0521  
 Language and Literature 0279  
 Mathematics 0280  
 Music 0522  
 Philosophy of 0998  
 Physical 0523

Psychology 0525  
 Reading 0535  
 Religious 0527  
 Sciences 0714  
 Secondary 0533  
 Social Sciences 0534  
 Sociology of 0340  
 Special 0529  
 Teacher Training 0530  
 Technology 0710  
 Tests and Measurements 0288  
 Vocational 0747

**LANGUAGE, LITERATURE AND LINGUISTICS**

Language 0679  
 General 0289  
 Ancient 0290  
 Linguistics 0290  
 Modern 0291  
 Literature 0401  
 General 0294  
 Classical 0294  
 Comparative 0295  
 Medieval 0297  
 Modern 0298  
 African 0316  
 American 0591  
 Asian 0305  
 Canadian (English) 0352  
 Canadian (French) 0355  
 English 0593  
 Germanic 0311  
 Latin American 0312  
 Middle Eastern 0315  
 Romance 0313  
 Slavic and East European 0314

**PHILOSOPHY, RELIGION AND THEOLOGY**

Philosophy 0422  
 Religion 0318  
 General 0321  
 Biblical Studies 0319  
 Clergy 0320  
 History of 0322  
 Philosophy of 0469  
 Theology 0323

**SOCIAL SCIENCES**

American Studies 0323  
 Anthropology 0324  
 Archaeology 0326  
 Cultural 0327  
 Physical 0310  
 Business Administration 0272  
 General 0770  
 Accounting 0454  
 Banking 0338  
 Management 0385  
 Marketing 0501  
 Canadian Studies 0503  
 Economics 0505  
 General 0508  
 Agricultural 0509  
 Commerce Business 0510  
 Finance 0511  
 History 0358  
 Labor 0366  
 Theory 0351  
 Folklore 0578  
 Geography 0578  
 Gerontology 0578  
 History 0578  
 General 0578

Ancient 0579  
 Medieval 0581  
 Modern 0582  
 Black 0328  
 African 0331  
 Asia, Australia and Oceania 0332  
 Canadian 0334  
 European 0335  
 Latin American 0336  
 Middle Eastern 0337  
 United States 0585  
 History of Science 0398  
 Law 0615  
 Political Science 0616  
 General 0617  
 International Law and Relations 0814  
 Public Administration 0452  
 Recreation 0626  
 Social Work 0627  
 Sociology 0938  
 General 0631  
 Criminology and Penology 0628  
 Demography 0629  
 Ethnic and Racial Studies 0630  
 Individual and Family Studies 0700  
 Industrial and Labor Relations 0344  
 Public and Social Welfare 0709  
 Social Structure and Development 0999  
 Theory and Methods 0453  
 Transportation 0999  
 Urban and Regional Planning 0453  
 Women's Studies 0453

**THE SCIENCES AND ENGINEERING**

**BIOLOGICAL SCIENCES**

Agriculture 0473  
 General 0285  
 Agronomy 0475  
 Animal Culture and Nutrition 0476  
 Animal Pathology 0359  
 Food Science and Technology 0478  
 Forestry and Wildlife 0479  
 Plant Culture 0480  
 Plant Pathology 0817  
 Plant Physiology 0777  
 Range Management 0746  
 Wood Technology 0306  
 Biology 0287  
 General 0308  
 Anatomy 0309  
 Biostatistics 0379  
 Botany 0329  
 Cell 0353  
 Ecology 0369  
 Entomology 0793  
 Genetics 0410  
 Limnology 0307  
 Microbiology 0317  
 Molecular 0416  
 Neuroscience 0433  
 Oceanography 0821  
 Physiology 0778  
 Radiation 0472  
 Veterinary Science 0786  
 Zoology 0760  
 Biophysics 0786  
 General 0760  
 Medical 0760

**EARTH SCIENCES**

Biogeochemistry 0425  
 Geochemistry 0996

Geodesy 0370  
 Geology 0372  
 Geophysics 0373  
 Hydrology 0388  
 Mineralogy 0411  
 Paleobotany 0345  
 Paleocology 0426  
 Paleontology 0418  
 Paleozoology 0985  
 Palynology 0427  
 Physical Geography 0368  
 Physical Oceanography 0415

**HEALTH AND ENVIRONMENTAL SCIENCES**

Environmental Sciences 0768  
 Health Sciences 0566  
 General 0300  
 Audiology 0992  
 Chemotherapy 0567  
 Dentistry 0350  
 Education 0769  
 Hospital Management 0758  
 Human Development 0982  
 Immunology 0564  
 Medicine and Surgery 0347  
 Mental Health 0569  
 Nursing 0570  
 Nutrition 0380  
 Obstetrics and Gynecology 0354  
 Occupational Health and Therapy 0381  
 Ophthalmology 0571  
 Pathology 0419  
 Pharmacology 0572  
 Pharmacy 0382  
 Physical Therapy 0573  
 Public Health 0574  
 Radiology 0575  
 Recreation 0575

Speech Pathology 0460  
 Toxicology 0383  
 Home Economics 0386

**PHYSICAL SCIENCES**

**Pure Sciences**  
 Chemistry 0485  
 General 0749  
 Agricultural 0486  
 Analytical 0487  
 Biochemistry 0488  
 Inorganic 0738  
 Nuclear 0490  
 Organic 0491  
 Pharmaceutical 0494  
 Physical 0495  
 Polymer 0754  
 Radiation 0405  
 Mathematics 0605  
 Physics 0986  
 General 0606  
 Acoustics 0608  
 Astronomy and Astrophysics 0748  
 Atmospheric Science 0607  
 Atomic 0798  
 Electronics and Electricity 0759  
 Elementary Particles and High Energy 0609  
 Fluid and Plasma 0610  
 Molecular 0752  
 Nuclear 0756  
 Optics 0611  
 Radiation 0463  
 Solid State 0346  
 Statistics 0984  
**Applied Sciences**  
 Applied Mechanics 0346  
 Computer Science 0984

Engineering 0537  
 General 0538  
 Aerospace 0539  
 Agricultural 0540  
 Automotive 0541  
 Biomedical 0542  
 Chemical 0543  
 Civil 0544  
 Electronics and Electrical 0348  
 Heat and Thermodynamics 0545  
 Hydraulic 0546  
 Industrial 0547  
 Marine 0794  
 Materials Science 0548  
 Mechanical 0743  
 Metallurgy 0551  
 Mining 0552  
 Nuclear 0549  
 Packaging 0765  
 Petroleum 0554  
 Sanitary and Municipal System Science 0770  
 Geotechnology 0428  
 Operations Research 0796  
 Plastics Technology 0795  
 Textile Technology 0994

**PSYCHOLOGY**

General 0621  
 Behavioral 0384  
 Clinical 0622  
 Developmental 0620  
 Experimental 0623  
 Industrial 0624  
 Personality 0625  
 Physiological 0989  
 Psychobiology 0349  
 Psychometrics 0632  
 Social 0451



**To my loving parents**

## Table of Contents

Table of Contents	v
List of Figures	x
List of Tables	xii
Abstract	xiii
List of Abbreviations	xiv
Acknowledgements	xvii
<b>I. Introduction</b>	<b>1</b>
1. Immunotherapy of cancer	1
2. IgG structure	1
3. Tumor antigens	6
4. Use of antibodies for immunotherapy	9
4.1 Criteria for antibody selection	9
4.2 Unconjugated antibodies as therapeutic agents	10
4.3 Radiolabeled antibodies as therapeutic agents	13
4.4 Antibody-bound drugs as therapeutic agents	14
5. Methotrexate	15
6. Direct linkage of methotrexate to antibodies	18
7. Linkage of drugs to antibodies through a carrier	22
8. Chemistry of antibody-protein conjugation	23
9. Non-site-specific linkage of carriers to antibodies	28
Serum albumin	28
Dextran	30
Polyglutamate	31
Polylysine	32
Antibody-bound toxins	33
Antibody-bound liposomes	34
10. Site-specific linkage of carriers to antibodies	34
Polyglutamate	37
Dextran	38
Antibody-bound liposomes	38
Antibody-bound toxins	39
11. Project rationale and objectives	39

<b>II. Materials and Methods</b>	<b>41</b>
Materials	41
Methods	43
1. General methods	43
1.1 Protein assays	43
1.2 Polyacrylamide gel electrophoresis	43
1.3 Desalting	44
1.4 Iodination of proteins	44
2. Cell lines	45
3. Production and isolation of IgG	45
3.1 Hybridoma growth and ascites formation	45
3.2 Purification of antibodies	46
Fractionation with caprylic acid	46
Chromatography using Protein A-Sepharose	46
4. Characterization of mAb K20	47
4.1 Determination of the immunoreactive fraction	47
4.2 Determination of the number of binding sites per cell and the apparent affinity constant	48
4.3 Isoelectric focusing	48
5. Coupling of MTX to HSA	49
5.1 Synthesis of MTX-AE	49
5.2 Incorporation of MTX-AE into HSA	50
Effect of molar ratio of MTX-AE over HSA	50
Effect of pH	50
Routine synthesis of HSA-MTX	51
5.3 Incorporation of MTX into HSA using EDCI	51
6. Direct incorporation of MTX into IgG	52
7. Activation of HSA for conjugation to IgG	52
7.1 Direct reduction of HSA with DTT	52
7.2 Incorporation of thiols into HSA using SPDP	53
8. Synthesis of MTX-HSA-SPDP for conjugation to IgG	53
9. Synthesis of non-site-specific IgG-HSA and IgG-HSA-MTX conjugates	54
9.1 Incorporation of SPDP and GMBS spacers into IgG	54
9.2 Non-site-specific conjugation of spacer-derivatized IgG to HSA and HSA-MTX	54

<b>10. Synthesis of heterobifunctional site-specific spacers</b>	<b>55</b>
10.1 Synthesis of SPDP	55
10.2 Synthesis of HPDP	56
10.3 Synthesis of AUPDP	56
11-[3-(2-pyridyldithio)propionyl]aminoundecanoic acid	56
11-[3-(2-pyridyldithio)propionyl]aminoundecanoic acid hydrazide	57
10.4 Synthesis of DNP-AU-hydrazide	57
11-aminoundecanoic acid methyl ester	57
11-(2,4-dinitrophenyl)aminoundecanoic acid methyl ester	58
11-(2,4-dinitrophenyl)aminoundecanoic acid hydrazide	58
<b>11. Synthesis of site-specific IgG-HSA and IgG-HSA-MTX conjugates</b>	<b>58</b>
11.1 Oxidation of IgG with sodium periodate	58
11.2 Incorporation of HPDP and AUPDP spacers into oxidized IgG	59
11.3 Site-specific conjugation of spacer-derivatized IgG to HSA and HSA-MTX	59
<b>12. Stability of site-specific conjugates</b>	<b>60</b>
12.1 Native PAGE and elution of conjugates from the gels	60
12.2 Dialysis of IgG containing DNP-AU-hydrazide as a reporter group	61
12.3 Competitive release of DNP-AU-hydrazide with propanal	62
12.4 Time required for hydrazone stabilization with cyanoborohydride	62
<b>13. Purification of conjugates</b>	<b>62</b>
13.1 Binary mAb K20-HSA conjugates	62
13.2 Ternary mAb K20-HSA-MTX conjugates	62
<b>14. Characterization of conjugates</b>	<b>63</b>
14.1 Measurement of antibody activity	63
Antibody activity by ELISA	63
Antibody activity by competition with <sup>125</sup> I-mAb K20	64
Antibody activity by competition with mAb K20-biotin	64
14.2 Measurement of cytotoxicity of conjugates	65
14.3 DHFR inhibition assay	66
14.4 Establishment of conjugate composition	66
Native PAGE and Western blot analysis of conjugates	66

Dual labelling experiments to determine conjugate composition	67
14.5 Evidence for site-specificity in site-specific conjugates	68
Labelling of mAb K20 with biotin	68
Digestion with papain	68
Digestion with pepsin	68
Western blot analysis of digested mAb K20-biotin	69
14.6 Long term stability of mAb K20-HSA binary conjugates	69
<b>III. Results</b>	<b>70</b>
1. Rationale for IgG-HSA-MTX conjugate construction	70
2. Activation of MTX	73
2.1 Formation of MTX-AE	73
2.2 Isolation of MTX-AE	75
3. Coupling of MTX to HSA	75
3.1 Effect of coupling conditions on MTX-AE incorporation into HSA	75
3.2 Coupling of MTX to HSA using EDCI	77
3.3 Purification of HSA-MTX monomer	77
4. Activation of HSA and HSA-MTX for conjugation with IgG	78
4.1 Introduction of thiols using SPDP	78
4.2 Introduction of thiols by direct reduction of HSA with DTT	79
5. Site-specific IgG-HSA-MTX conjugates	80
5.1 Synthesis of the site-specific spacers HPDP and AUPDP	80
5.2 Site-specific modification of IgG with HPDP and AUPDP	83
5.3 Site-specific conjugation of HSA and HSA-MTX to IgG	83
Conjugation of mAb K20 with HSA	83
Conjugation of mAb K20 with HSA-MTX	85
Conjugation of NRG with HSA	87
5.4 Evaluation of hydrazone bond stability and stabilization with cyanoborohydride	87
Elution of conjugates from native PAGE gels	87
Model studies with DNP-AU-hydrazide	89
5.5 Synthesis of stabilized site-specific conjugates	92
mAb K20-HSA conjugates	92

mAb K20-HSA-MTX conjugates	93
6. Non-site-specific IgG-HSA-MTX conjugates	101
6.1 Incorporation of SPDP and GMBS spacers into IgG	102
6.2 Non-site-specific conjugation of IgG with HSA	102
6.3 Non-site-specific conjugation of IgG with HSA-MTX	104
7. Synthesis of direct IgG-MTX conjugates	106
8. Characterization of mAb K20 conjugates	106
8.1 Determination of the ratio of HSA-MTX to IgG	106
8.2 Evidence for carbohydrate linkage in site-specific conjugates	107
8.3 Effect of modifications and conjugation on mAb K20 binding activity	110
8.4 DHFR inhibition by MTX-containing conjugates	117
8.5 Cytotoxicity of MTX-containing conjugates	118
8.6 Long term stability of mAb K20-HSA binary conjugates	120
9. Characterization of native mAb K20	120
9.1 Isolation of mAb K20	120
9.2 Immunoreactive fraction	122
9.3 Number of binding sites and apparent affinity constant for Caki-1 cells	122
9.4 IEF of mAb K20	123
<b>IV. Discussion</b>	126
1. Synthesis of HSA-MTX	127
2. Synthesis of conjugates	132
3. Characterization of conjugates	142
4. Future directions	153
<b>V. Conclusions</b>	154
<b>VI. References</b>	155

## List of Figures

Figure 1.	Schematic representation of IgG structure.	2
Figure 2.	Sites of action of MTX.	16
Figure 3.	Synthesis of MTX-AE and its reaction with proteins.	21
Figure 4.	Reactions of SPDP and GMBS with proteins.	72
Figure 5.	Structure of synthesized site-specific cross-linkers and a site specific stability probe.	81
Figure 6.	Effect of oxidation level on incorporation of AUPDP into NRG.	84
Figure 7.	Analysis of site-specific conjugation efficiency by native PAGE.	86
Figure 8.	SDS PAGE analysis of conjugates eluted from native gels.	88
Figure 9.	Stabilization of hydrazone-linked DNP reporter groups with cyanoborohydride.	91
Figure 10.	Scheme for the synthesis of site-specific mAb K20-HSA binary conjugates.	94
Figure 11.	Purification of a site-specific mAb K20-HSA binary conjugate by gel filtration chromatography.	95
Figure 12.	Comparison of purified mAb K20-HSA site-specific and non-site-specific binary conjugates by SDS PAGE.	96
Figure 13.	Scheme for the synthesis of site-specific IgG-HSA-MTX ternary conjugates.	97
Figure 14.	SDS PAGE analysis of a site-specific mAb K20-HSA-MTX ternary conjugation mixture and conjugate purification.	98
Figure 15.	SDS PAGE analysis of purified ternary conjugates and direct IgG-MTX conjugates.	100
Figure 16.	Scheme for the synthesis of non-site-specific IgG-HSA-MTX ternary conjugates.	103
Figure 17.	SDS PAGE analysis of a non-site-specific mAb K20-HSA-MTX ternary conjugation mixture and conjugate purification.	105
Figure 18.	Localization of sites on mAb K20 reactive toward site-specific and non-site-specific derivatives of biotin.	108

<b>Figure 19. Digestion of mouse IgG1 by pepsin and papain.</b>	<b>109</b>
<b>Figure 20. Binding analysis of conjugates using a direct cell-binding ELISA technique.</b>	<b>112</b>
<b>Figure 21. Competitive binding of binary conjugates measured with <sup>125</sup>I-mAb K20.</b>	<b>113</b>
<b>Figure 22. Competitive binding of ternary conjugates measured with mAb K20-biotin.</b>	<b>115</b>
<b>Figure 23. Long term stability of site-specific and non-site-specific mAb K20 binary conjugates.</b>	<b>121</b>
<b>Figure 24. Analysis of mAb K20 binding to Caki-1 cells.</b>	<b>124</b>
<b>Figure 25. Isoelectric focusing analysis of mAb K20.</b>	<b>125</b>

## **List of Tables**

<b>Table 1.</b>	<b>Effect of reactant ratio on activation of methotrexate.</b>	<b>74</b>
<b>Table 2.</b>	<b>Effect of MTX-AE excess on incorporation into HSA.</b>	<b>76</b>
<b>Table 3.</b>	<b>Effect of pH on MTX-AE incorporation into HSA.</b>	<b>76</b>
<b>Table 4.</b>	<b>Reduction of HSA disulfides with DTT.</b>	<b>79</b>
<b>Table 5.</b>	<b>Reduction of NRG aldehyde groups with cyanoborohydride.</b>	<b>90</b>
<b>Table 6.</b>	<b>Stabilization of DNP-NRG hydrazone bonds with cyanoborohydride.</b>	<b>92</b>
<b>Table 7.</b>	<b>Recovery of IgG in conjugates.</b>	<b>104</b>
<b>Table 8.</b>	<b>Retention of mAb K20 antigen binding activity following chemical modifications and conjugation.</b>	<b>111</b>
<b>Table 9.</b>	<b>DHFR inhibition by MTX-containing conjugates.</b>	<b>116</b>
<b>Table 10.</b>	<b>Cytotoxicity of conjugates toward Caki-1 and D10-1 cells.</b>	<b>119</b>

## **Abstract**

The anticancer drug methotrexate (MTX) was conjugated to the monoclonal antibody (mAb) K20 directed against a cell surface antigen on the human kidney cancer cell line, Caki-1, for the purpose of obtaining effective targeting agents. Linkage of MTX to mAb K20 was through the use of human serum albumin (HSA) as an intermediary, in which HSA containing between 28 and 35 mol MTX/mol HSA (HSA-MTX) was linked to the mAb. The hypothesis was that carrier-based conjugates would be more effective targeting agents than direct mAb K20-MTX conjugates on the basis of increased drug load and greater retention of antigen binding activity of the mAb. The conjugation of HSA-MTX to mAb K20 was carried out using a site-specific method in which HSA-MTX was linked to the carbohydrate moiety of the mAb. It was predicted that site-specific conjugates would retain greater antibody activity than non-site-specific conjugates in which HSA-MTX was linked to amino groups of the mAb since the carbohydrate moiety is located at a distance from the antigen binding site.

Two site-specific heterobifunctional spacers were synthesized to allow conjugation to the carbohydrate moiety of mAb K20. These were 3-(2-pyridyldithio)propionic acid hydrazide (HPDP) and 11-[3-(2-pyridyldithio)propionyl]aminoundecanoic acid hydrazide (AUPDP). Use of the longer AUPDP gave higher yields of ternary mAb K20-HSA-MTX conjugates, suggesting that steric factors limited conjugation of HSA to the carbohydrate of mAb K20 when using HPDP. Hydrazone-linked conjugates prepared using AUPDP were unstable and could not be isolated without prior stabilization by cyanoborohydride. Following stabilization, 1:1 site-specific mAb K20:HSA-MTX conjugates were isolated. Non-site-specific ternary conjugates were also synthesized using 3-(2-pyridyldithio)propionic acid succinimidyl ester as the cross-linker. The non-site-specific conjugates retained only one third the antibody activity of the corresponding site-specific conjugates. The site-specific mAb K20-HSA-MTX conjugate was more cytotoxic to target Caki-1 cells than either the non-site-specific mAb K20-HSA-MTX conjugates, or direct conjugates in which MTX was linked directly to mAb K20 amino groups. The site-specific conjugate also displayed the greatest selectivity for the target cell line Caki-1, compared to D10-1, a non-target cell line. It is likely that the greater cytotoxicity to Caki-1 cells as well as the increased selectivity was the result of the increased retention of antigen binding activity in the site-specific conjugate.

## List of Abbreviations

125I	radioactive iodine 125
131I	radioactive iodine 131
A280	absorbance at 280nm
AICAR	aminoimidazole carboxamide ribonucleotide transformylase
AUPDP	11-[3-(2-pyridyldithio)propionyl]aminoundecanoic acid hydrazide
BSA	bovine serum albumin
Buffer A	0.1 M sodium acetate, pH 4.0
CDR	complementarity determining region
CMD	carboxymethyl dextran
cpm	counts per minute
DCC	dicyclohexylcarbodiimide
DEAE	diethylaminoethyl
dH <sub>2</sub> O	distilled water
DHF	dihydrofolate
DHFR	dihydrofolate reductase
DME	Dulbecco's Modified Eagle's Medium
DMF	N,N-dimethylformamide
DMSO	dimethylsulfoxide
DNP	dinitrophenyl
DNP-AU-hydrazide	11-(2,4-dinitrophenyl)aminoundecanoic acid hydrazide
DNP-cys	N-(2,4-dinitrophenyl)-cysteine
DNP-OMe	11-(2,4-dinitrophenyl)aminoundecanoic acid methyl ester
DPBS	Dulbecco's phosphate buffered saline
DTNB	5,5'-dithiobis(2-nitrobenzoic acid)
DTT	dithiothreitol
EDCI	1-ethyl-3-(3'-dimethylaminopropyl)carbodiimide
EDTA	ethylenediaminetetraacetic acid
ELISA	enzyme linked immunosorbant assay
FCS	fetal calf serum
FDNB	1-fluoro-2,4-dinitrobenzene
Fuc	fructose
Gal	galactose

<b>GAM IgG-HRP</b>	<b>goat anti-mouse IgG conjugated to horse radish peroxidase</b>
<b>GAR</b>	<b>glycinamide ribonucleotide transformylase</b>
<b>GlcNAc</b>	<b>N-acetylglucosamine</b>
<b>GMBS</b>	<b><math>\gamma</math>-maleimidobutyric acid succinimidyl ester</b>
<b>h</b>	<b>hour(s)</b>
<b>HAMA</b>	<b>human anti-mouse antibody</b>
<b>HBSS</b>	<b>Hank's buffered saline solution</b>
<b>HPDP</b>	<b>3-(2-pyridyldithio)propionic acid hydrazide</b>
<b>HSA</b>	<b>human serum albumin</b>
<b>i.p.</b>	<b>intraperitoneally</b>
<b>IC<sub>50</sub></b>	<b>concentration for 50% inhibition</b>
<b>IEF</b>	<b>isoelectric focusing</b>
<b>IgG</b>	<b>immunoglobulin G</b>
<b>IRF</b>	<b>immunoreactive fraction</b>
<b>K<sub>a</sub></b>	<b>affinity constant</b>
<b>mAb IgG1</b>	<b>non-specific mouse mAb of IgG1 subclass</b>
<b>mAb K20</b>	<b>monoclonal antibody K20 against RCC</b>
<b>mAb</b>	<b>monoclonal antibody</b>
<b>Man</b>	<b>mannose</b>
<b>min</b>	<b>minute(s)</b>
<b>mp</b>	<b>melting point</b>
<b>MTX</b>	<b>methotrexate</b>
<b>MTX-AE</b>	<b>methotrexate active ester</b>
<b>MW</b>	<b>molecular weight</b>
<b>NADPH</b>	<b>nicotinamide adenine dinucleotide phosphate (reduced form)</b>
<b>ND</b>	<b>not determined</b>
<b>NHS</b>	<b>N-hydroxysuccinimide</b>
<b>NMR</b>	<b>nuclear magnetic resonance</b>
<b>H</b>	<b>hydrogen(s)</b>
<b>s</b>	<b>singlet</b>
<b>bs</b>	<b>broad singlet</b>
<b>d</b>	<b>doublet</b>
<b>m</b>	<b>multiplet</b>
<b>t</b>	<b>triplet</b>
<b>q</b>	<b>quartet</b>

n	pentet
NRG	normal rabbit globulin
OPD	o-phenylenediamine
PAD	polyaldehyde dextran
PAGE	polyacrylamide gel electrophoresis
PBS	phosphate buffered saline (pH 7.2, 0.01M phosphate, 0.15M NaCl)
PGA	polyglutamate
RCC	renal cell carcinoma
Rf	retardation factor
RT	room temperature
SD	standard deviation
SDS	sodium dodecyl sulfate
sec	seconds
Sia	sialic acid (N-acetylneuramic acid)
SPDP	3-(2-pyridyldithio)propionic acid succinimidyl ester
TCA	trichloroacetic acid
THF	tetrahydrofolate
TLC	thin layer chromatography
TS	thymidylate synthase
V	volts
v/v	volume per volume
w/v	weight per volume
°C	degrees Celsius
$\lambda_{max}$	wavelength of maximum absorbance
$\epsilon$	molar extinction coefficient

## **Acknowledgements**

I would like to thank Dr. Blair and Dr. Ghose for their supervision and support throughout the course of the project and their input during the writing of this thesis. I would also like to thank Dr. Kralovec for his advice in many areas of the project. Special thanks to Drs. Byers, Wallace, and Yeung who served as members of my supervisory committee. Finally, I am grateful to all those who were involved in one way or another, including Molly Mammen, Helen Nolido-Cruz, Tsedale Weyhnot, and Drs. Ashim Guha, Steve Luner, Lan Chen, and Zhen Ping Zhu.

## **I. Introduction**

### **1. Immunotherapy of cancer**

One of the shortcomings of traditional cancer treatment with anti-cancer drugs is that these agents have limited specificity for cancer cells. Anti-cancer drugs are preferentially toxic to rapidly dividing cells which include many vital normal cell populations as well as cancer cells. This lack of specificity limits the doses which can be used to levels which result in acceptable toxicity to normal cells. Often these doses are insufficient to destroy all cancer cells. One approach to attain greater specificity has been to link the drug to a suitable targeting agent which can deliver it specifically to cancer cells (1). Targeting agents which have been used include growth factors (2,3), cytokines (4), LDL particles (2,5), lectins (6), hormones (7), and antibodies (8,9). Of these agents, antibodies have become the most widely used due to the ability to produce large amounts of homogeneous antibody preparations directed against virtually any cell-surface antigen.

### **2. IgG structure**

Immunoglobulins of the G class (IgG) are proteins made up of four polypeptide chains; two identical light chains and two identical heavy chains (Figure 1). Each heavy chain is composed of one variable region ( $V_H$ ) and three constant regions ( $C_{H1}$ ,  $C_{H2}$ , and  $C_{H3}$ ). The light chain has one variable region ( $V_L$ ) and one constant region ( $C_L$ ). The heavy and light chains of IgG typically have MWs of 50 kDa and 25 kDa, respectively, resulting in an overall MW of 150 kDa for an intact IgG (10). IgGs differ from the immunoglobulins of other classes (IgA, IgD, IgE and IgM) on the basis of the type of heavy chain which they contain. The different heavy chains of immunoglobulins are associated with differences in normal physiological roles, abundance in serum and, in the cases of IgA and IgM, the degree of polymerization as these are found as dimers and

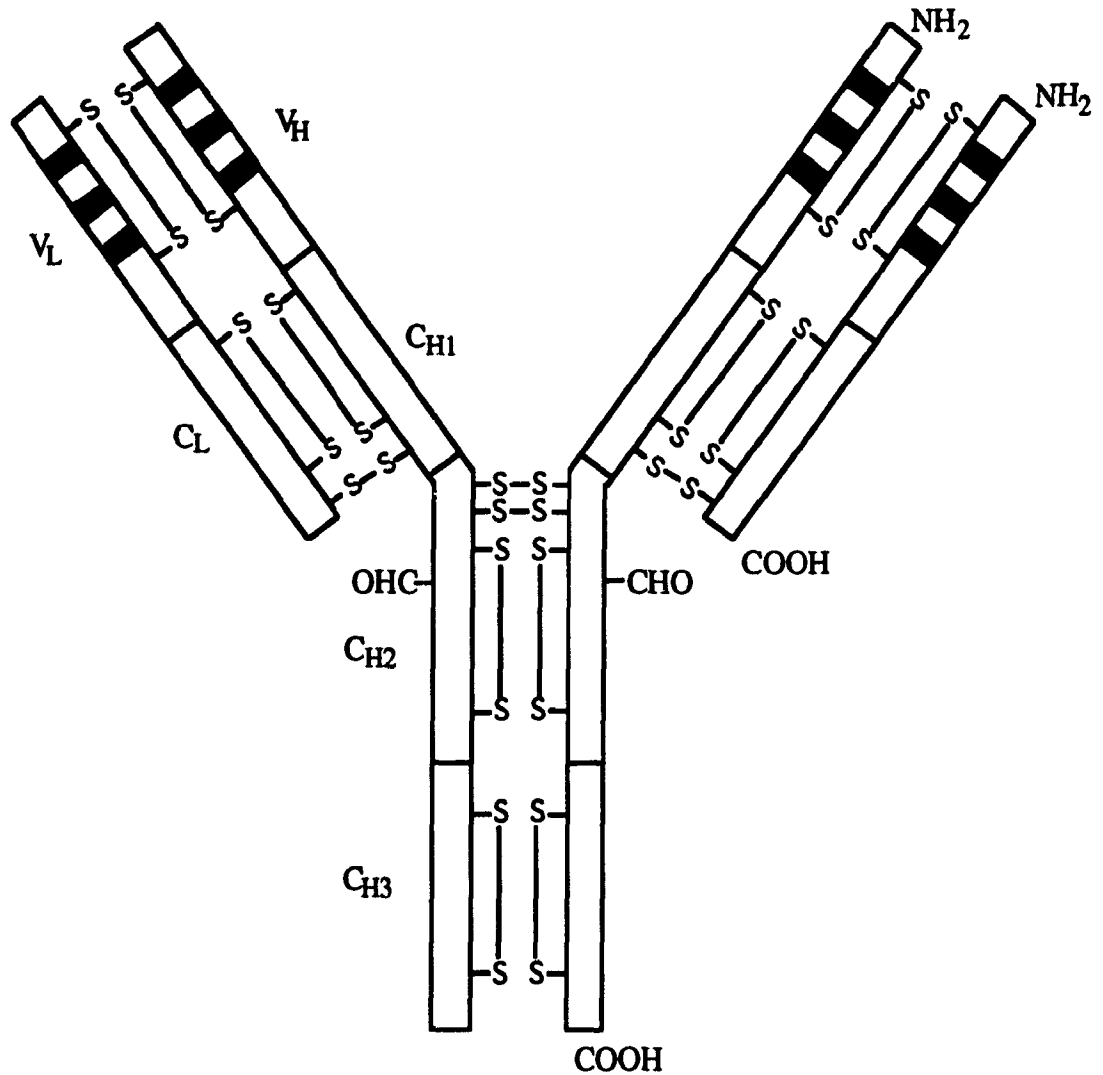


**Figure 1. Schematic representation of IgG structure.**

Each heavy (H) and light (L) chain of the IgG molecule is divided into constant (C) and variable (V) regions and each region contains an intrachain disulfide bond. The two heavy chains are disulfide bonded in the hinge region and each light chain is disulfide bonded to one heavy chain. Shown also are the amino and carboxyl termini of the heavy and light chains as well as the conserved N-linked glycosylation site in the  $C_{H2}$  domain. The antigen binding site is defined by the complementarity determining regions (shaded) of both heavy and light chains. See text for greater detail.

pentamers, respectively. IgG can be further divided into subclasses in which  $C_H$  sequences are different, but these differences are not as great as those between immunoglobulins of other classes. The subclasses of mouse IgG are IgG<sub>1</sub>, IgG<sub>2a</sub>, IgG<sub>2b</sub> and IgG<sub>3</sub>. These differ in relative abundance in serum, half-life, locations of disulfide bonds, flexibility and antigen-binding capability. Two types of light chains are known to occur, these being either kappa or lambda chains. In the mouse, the majority of immunoglobulins contain the kappa light chain (11).

Each light chain is disulfide bonded to one heavy chain near the carboxyl terminal of the light chain, and the two heavy chains are disulfide linked between  $C_{H1}$  and  $C_{H2}$ , this area forming the hinge region of the molecule. The constant and variable regions are similar in sequence and form compact, globular domains which are similar in tertiary structure. The conformation of these domains is known as the immunoglobulin fold, consisting of two layers of antiparallel  $\beta$ -sheets which interact with neighbouring domains of either the heavy or light chain. Each domain contains an intrachain disulfide bond which stabilizes the tertiary structure of that domain (12). Intact immunoglobulins are dynamic in nature and form a flexible Y- or T-shaped structure with the variable regions present at the ends of the arms of the Y (T). The Y-T transition is important as it allows for variable positioning of each antigen binding site. It arises from the flexibility of the hinge region. The structure of the hinge differs in immunoglobulins from different classes and members of different classes bind antigen with varying efficiency (13,14).

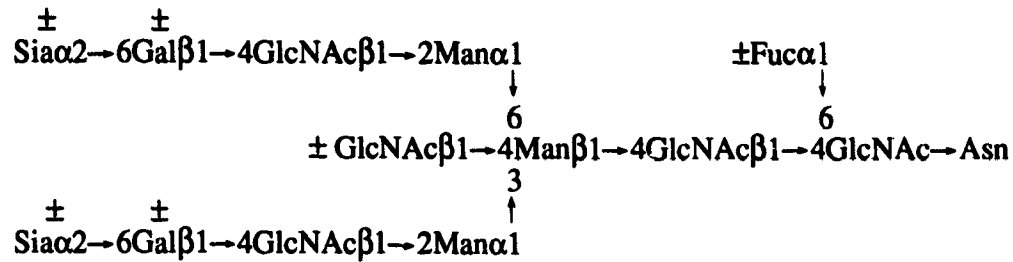
IgG can be proteolytically cleaved into characteristic fragments with pepsin and papain. Papain cleaves the heavy chains at a site above the interchain disulfide bonds, giving rise to two Fab fragments (fragment antigen binding) and an Fc fragment (fragment crystallizable). Pepsin cleaves the heavy chains below the interchain disulfide bonds resulting in the formation of a bivalent  $F(ab')_2$  fragment (11).

The antigen binding function of the IgG molecule is localized in the V regions. Each heavy and light chain V region is subdivided into four framework regions separated

by three hypervariable or complementarity-determining regions (CDRs). The CDRs form the  $\beta$ -loops or reverse turns which join the antiparallel  $\beta$ -sheets of the immunoglobulin fold. The amino acids contained within the six CDRs interact with antigen and the combination of interactions between the CDRs and the antigen comprise the antigen binding site of the immunoglobulin (10).

The C<sub>H2</sub> domain of IgG contains the conserved N-glycosylation site at Asn 297 in a number of species. A number of murine antibodies also possess the N-linked carbohydrate addition sequence Asn-X-Ser/Thr in the second CDR of the variable region of the heavy chain, although these are generally antibodies which are specific for carbohydrate (15-17). Conservation of this glycosylation sequence suggests a functional role, but the precise influence of these heavy chain oligosaccharides on Fc structure and function is still unclear. Glycosylation of IgG has been implicated in both its biological functions and physiochemical properties, including resistance to proteases, thermal stability, solubility, binding to macrophage and monocyte Fc receptors, interaction with complement component C1q, and circulatory lifetime *in vivo* (18-20). In addition to N-linked carbohydrate, O-linked carbohydrate has been reported within the hinge region of rabbit (21) and murine IgG (12,22).

IgGs from all species have been found to exhibit diversity in their oligosaccharide structures, both in the types and the arrangement of the sugars. The IgG molecule characterized by one amino acid sequence (i.e. monoclonal) is therefore a population of glycosylated variants or glycoforms in which, in any glycoform, the amino acid sequence is identical but the attached oligosaccharides are different. The N-linked oligosaccharides are of the biantennary complex type that have a pentasaccharide core structure consisting of three mannose (Man) and two N-acetylglucosamine (GlcNAc) residues. The presence or absence of a fucose (Fuc) residue attached to the Asn-linked GlcNAc residue ( $\pm$ Fuc $\alpha$ 1 $\rightarrow$ 6) and a bisecting GlcNAc at the Man branch ( $\pm$ GlcNAc $\beta$ 1 $\rightarrow$ 4) add to the diversity of the core structure. The complete N-linked oligosaccharide can be represented as:



In mouse IgG, 94% of N-linked carbohydrate is found to contain the Fuc, but the bisecting GlcNAc is not found (21,23). In contrast, IgG from bovine, rabbit and human serum have been found to contain various amounts of both the Fuc and the bisecting GlcNAc (23). Outer chain heterogeneity arises from the residues attached to the core structure, as both sialic acid (Sia) and galactose (Gal) may or may not be present. In addition to sialic acid, N-glycolylneuraminic acid has been found as the terminal sugar residue in a number of species (23). In IgG isolated from pooled mouse serum, the relative proportions of neutral, mono-sialylated and di-sialylated oligosaccharides was found to be 77%, 17% and 7%, respectively (23). However, a recent study of a mouse mAb IgG<sub>1</sub> has shown that the glycosylation pattern is highly dependent on the culture method employed to produce that mAb (24). The relative proportions of neutral to acidic oligosaccharides varied greatly depending on whether the hybridoma was obtained from ascites fluid or from cell culture. mAb from ascites fluid contained only neutral oligosaccharide chains whereas that from cell culture contained variable amounts of both mono- and di-sialylated components. The proportions were similar to that seen in pooled IgG from mouse serum, and dependent on whether the hybridoma was grown in serum-free or serum-containing medium. Differences in the relative amounts of both fucose and galactose were also seen, depending on the methods.

X-ray crystallographic studies have established the three-dimensional structure of the carbohydrate in rabbit (25) and human (26) Fc fragments and the protein-oligosaccharide interactions are consistent with the conformational analysis of free IgG

oligosaccharides determined by high resolution NMR (27). The carbohydrate is present between the two  $C_{H2}$  domains which prevents the interactions found between domains in other parts of the molecule. The  $\alpha 1 \rightarrow 6$  linkage can assume two conformations in solution, giving a flexible arm to the oligosaccharide. However, when the oligosaccharide is attached to Asn 297, the  $\alpha 1 \rightarrow 6$  antennae interact with hydrophobic and polar residues within the same  $C_{H2}$  domain giving rigidity to the structure. The  $\alpha 1 \rightarrow 3$  arms are also rigid in nature, with the  $\alpha 1 \rightarrow 3$  arm of one oligosaccharide chain interacting with the core of the opposing chain, and the remaining  $\alpha 1 \rightarrow 3$  arm extending outwards between the domains.

### **3. Tumor antigens**

To be useful as targeting agents, antibodies require specific targets present on cancer cells. Results obtained from studies on tumor transplantation and identification of antibody and T-cell responses against tumors support the existence of tumor associated antigens. Tumor-specific antigens have been demonstrated on chemically induced tumors by tumor transplantation in inbred mice (28). The majority of these studies used methylcholanthrene-induced sarcomas, which were shown to be immunogenic in inbred mice leading to rejection of tumor transplants in presensitized mice. A noteworthy feature of these tumor rejection antigens is that each chemically-induced tumor is antigenically distinct. A tumor can elicit an immune response against itself, but not against another tumor which was induced by the same carcinogen in the same animal (29).

The p53 tumor suppressor molecule is an example of a serologically detected tumor antigen. Antibodies to p53 were found in sera of mice immunized with methylcholanthrene-induced sarcomas, and p53 was immunoprecipitated from a number of transformed but not normal cells (30). Many mutations of p53 have been found to be clustered in four highly conserved regions of the molecule. Mutations in these regions may therefore induce common conformational changes that can be identified by antibodies (31).

Since p53 mutations are common to a number of human cancers, mAbs to mutant p53 should be useful in the diagnosis of malignancy.

At the present time, many tumor associated antigens detected by mAbs have been defined and can be classified by function: i) antigens with signalling or transport functions such as growth factor receptors (epidermal growth factor, transferrin) (3,32), cation-binding proteins (melanotransferrin) (33), and transport proteins (P-glycoprotein) (34); ii) cell-cell interacting tumor antigens such as carcinoembryonic antigen (CEA) (35) and intercellular adhesion molecule-1 (ICAM-1) (36); iii) cell matrix-interacting antigens such as the integrins (laminin and vitronectin receptors) (37); and iv) blood group antigens such as the Lewis antigens (33).

The structural identification of determinants recognized by T-cells is difficult due to the cell-bound nature of the T-cell antigen receptor and the MHC-restriction of T-cell recognition. Cloned tumor specific T-cell reactivities have recently been identified, and a small number of T-cell-defined antigens are beginning to be characterized (28). Tumor antigens of the P815 mastocytoma were the first T-cell-recognized antigens to be structurally defined. Cells which were mutagenized *in vitro* were found to be immunogenic *in vivo* as well as being susceptible to lysis by cytotoxic T-cells generated to each variant. Responses in both cases were variant-specific, indicating that the antigens expressed were different. The antigens of three such clones were subsequently identified and found to be different from each other, and each differed from normal cellular counterparts by a single amino acid substitution (28,38). Mucins represent another group of T-cell antigens present on a number of human cancers, where cytotoxic T-cells have been shown to recognize the polypeptide core of the mucin. There does not appear to be any change in the polypeptide itself in these mucins, but instead a change in O-linked glycosylation (31).

Until recently, it was generally believed that tumor antigens present on malignant cells were the same as antigens present on normal cells, but that their expression was higher on malignant cells. According to this view, there are no tumor specific antigens, but

instead, tumor associated antigens (33). A new concept which has arisen is that there are, in fact, tumor specific antigens, and that these are defined by tumor specific mutant proteins. The mutant proteins are encoded by oncogenes and tumor suppressor genes which have undergone various mutations. Evidence for this view comes from the demonstration of structural mutations in several oncogenes involving point mutations, chromosomal translocations, internal deletions, and viral insertional mutagenesis (31). Point mutations in the tumor suppressor genes, p53 and RB 1, have also been detected (39). Since proto-oncogenes and suppressor genes are important in normal cellular regulation and differentiation processes, their alteration may result in novel proteins with transforming activity (31). Some of these mutant proteins may represent tumor specific antigens that could be useful in immunotherapy.

Other tumor antigens which are possible targets for immunotherapy include those which are abnormally glycosylated. Surface glycoproteins on a number of human tumors display abnormal carbohydrate structures which may lead to the exposure of new epitopes (40). Still other potential targets include those which are amplified in certain tumors. For example, the epidermal growth factor receptor (41) and transferrin receptor are preferentially expressed on a number of tumors. Oncofetal antigens such as carcinoembryonic antigen and alpha-fetoprotein, which are generally not expressed by normal differentiated cells, are found in patients with colon and liver cancer, respectively (33).

While it is obvious that the tumor specific antigens defined by mutant proteins can serve as targets for antibody therapy on the basis of their restriction to tumor sites, tumor associated antigens which are only preferentially expressed on tumors may or may not be good targets. The utility of such tumor associated antigens as targets will depend on their level of expression relative to that on normal cells.

#### **4. Use of antibodies for immunotherapy**

A large number of mAbs have been produced against a wide variety of tumor antigens. The majority of these are of murine origin which have been generated by the immunization of mice with tumor extracts, whole cells, or purified antigen preparations. A number of human mAbs have also been produced, usually by fusion of lymphocytes obtained from lymph nodes of cancer patients with either human or murine myeloma cells. The advantages of human mAbs is that these may recognize antigenic determinants which are not immunogenic in mice, and these mAbs will not elicit the human anti-mouse response seen with murine mAbs.

##### **4.1 Criteria for antibody selection**

A number of variables determine whether a particular mAb will be suitable for the preparation of mAb conjugates for cancer therapy. The specificity of the mAb for the tumor itself is of importance in this regard. As discussed, certain tumor antigens are more tumor specific than others, and the effectiveness of agents targeted by mAbs directed against these antigens will therefore depend in part on the distribution of antigen between normal and tumor cells (1). The number of antigen molecules on the surface of tumor cells, the affinity with which the mAb binds, and the fate of the mAb-antigen complex are also factors which should also be considered for mAb selection (42). Many tumor antigens are present at approximately  $1 \times 10^6$  molecules per cell surface, although values between  $2.5 \times 10^4$  and  $7 \times 10^6$  have been reported (43). It is generally believed that a higher antigen density is desirable, since a greater number of mAbs can potentially bind to target cells. Along this same line, a greater proportion of high affinity mAbs will bind to cells compared to low affinity mAbs at a given concentration. mAbs with affinity constants below  $1 \times 10^8 \text{ M}^{-1}$  are thought to be inappropriate for drug targeting purposes (44). For therapeutic purposes, the immunoreactive fraction (IRF) of the mAb preparation is also important (45,46). The IRF defines the proportion of mAbs contained in the preparation

which are capable of binding to antigen. Preparations with a high IRF are desirable since they contain low amounts of non-specific antibody.

The fate of cell-bound mAb depends on the antigen to which the mAb is directed. Some tumor antigens are integral components of the cell surface and are not internalized (47), whereas others are endocytosed following cross-linking by mAbs (48,49). The use of non-internalized mAbs would be useful in applications where internalization is not desirable, such as in antibody-directed enzyme/prodrug therapy where cell-bound mAb-enzyme conjugates are used to activate circulating prodrugs in the vicinity of the tumor (50). For example, mAb-alkaline phosphatase conjugates have been used in combination with phenol mustard phosphate (51), doxorubicin phosphate (52), and mitomycin phosphate (53). MTX- $\alpha$ -alanine has also been used as a prodrug and activated with mAb-carboxypeptidase A (54). Certain anti-cancer agents such as the anthracyclines (doxorubicin, daunomycin), platinum complexes (cisplatin), and alkylating agents (nitrogen mustard, chlorambucil, nitrosoureas) may also have cell membrane effects, and may be useful with these non-internalized mAbs (55). The majority of anticancer drugs which are used in mAb-based drug targeting are active intracellularly, so mAbs that are internalized would appear to be the most appropriate choice for these drugs.

#### **4.2 Unconjugated antibodies as therapeutic agents**

Unconjugated mAbs can produce antitumor effects by a number of mechanisms. mAbs can cause activation of components of the immune system, such as triggering of complement- or antibody-dependent cytotoxicity, and can cause interference of growth or differentiation by direct binding to tumor cells (56).

It is well known that the proliferation of tumor cells in culture is controlled by various growth factors, and a similar control mechanism is postulated for the control of tumor cell growth *in vivo* (57). mAbs to growth factor receptors, such as epidermal growth factor receptor on carcinomas (58), interleukin-2 receptors on T-cell leukemias (59)

and bombesin receptors in small cell lung carcinoma (57), among others, are being evaluated as therapeutic agents. Antibodies to such receptors have been shown to inhibit growth of tumor cells both *in vitro* and *in vivo*. In most cases, the major mode of action of these mAbs *in vivo* appears to be the disruption of normal receptor functioning by blockage of ligand binding and not the recruitment of host effector mechanisms.

Unconjugated mAbs have been used to target the natural effector systems against specific cell types. *In vivo*, cells coated with antibody are susceptible to antibody-dependent cell-mediated cytotoxicity, complement-mediated cytotoxicity and phagocytosis. Clinical responses with mAbs have been seen in the treatment of certain hematologic (60) and solid tumors (56), but poorer responses have been seen in the treatment of solid tumors. The type of mAb used for treatment is of importance since mAbs from different species and of different isotypes activate human effector systems to various degrees.

A problem encountered with the use of mouse mAbs in human patients is that the patient usually produces antibodies against the mouse mAb, this being known as the human anti-mouse antibody (HAMA) response (57). HAMA greatly reduces the effectiveness of the mAb treatment since the mouse antibodies are complexed by human antibodies, resulting in degradation and excretion. mAb fragments such as Fab or F(ab')<sub>2</sub> are less immunogenic than whole IgG due to the lack of the Fc portion of the molecule, but their continued use still results in a HAMA response. Ideally, the use of human mAbs would be appropriate, but attempts to construct human hybridomas have met with limited success. Approaches to reduce the immunogenicity of murine mAbs have therefore been developed, these being the use of chimeric and humanized mAbs (61). Chimeric mAbs are constructed to contain the variable region of the original murine mAb and the constant region of a human antibody. The antibody retains the original antigen binding properties. Immunogenicity of chimeric mAbs is reduced to some degree, but the variable region of a number of chimeric mAbs has been found to be immunogenic. Humanized antibodies reduce the immunogenicity further, since they contain both human constant regions as well

as human framework regions, and only the hypervariable regions are of murine origin (62). These hybrid antibodies may also be more efficient than murine mAbs at eliciting host responses against the targeted cells, since it is known that murine mAbs are poor activators of human effector systems.

The use of bispecific mAbs represents another approach taken to target host effector systems against tumors. These mAbs are bifunctional in that each antibody binding site has specificity for a different ligand, typically for a tumor antigen and for an antigen present on an effector cell. These mAbs have been prepared either by chemical cross-linkage or through disulfide exchange of appropriate mAbs, and by the fusion of two appropriate hybridomas, resulting in the formation of hybrid-hybridomas (quadromas) (63). The most effective bispecific mAbs have been those with specificity for the CD3 antigen on cytotoxic T cells or the CD16 Fc $\gamma$ RIII receptor on natural killer cells. It has been demonstrated both *in vitro* and *in vivo* that these bispecific mAbs can result in selective lysis of target cells (63,64).

Antibodies termed anti-idiotypic antibodies have binding specificity for the antigen binding site of another antibody. The antigenic determinants on the target antibody are called idiotypes. Anti-idiotypic antibodies directed against cell-surface idiotypes present on malignant B cells have been used to regulate the proliferation of these cells *in vitro* and *in vivo* (65,66). Surface immunoglobulin on B cells typically serve as a growth stimulatory receptor where antigen binding results in proliferation of antigen-binding clones, however, antibodies directed against the idiotypes of these immunoglobulins appear to have a regulatory influence on proliferation, the mechanisms of which are still unknown (56).

Anti-idiotypic antibodies may also be immunologically identical to the antigen with which the primary antibody reacts. Anti-idiotypic antibodies have therefore been used as vaccines to immunize against tumors. Immunologic response to the anti-idiotypic antibody results in the production of anti-anti-idiotypic antibodies in the host which may bind the

original antigen. The advantage of this type of vaccine is that anti-idiotypic antibodies can be obtained in pure form in large quantities, and may also be more immunogenic than the original tumor antigen (56). This concept has met with some success in human clinical trials where patients with colorectal cancer were administered a goat anti-idiotypic antibody (67). All patients developed anti-anti-idiotypic antibodies and a number showed positive clinical responses.

#### **4.3 Radiolabeled antibodies as therapeutic agents**

mAbs coupled to radionuclides have been used for tumor detection and therapy. Factors important for tumor imaging include the radionuclide used, the antibody form, and the scanning method. The radionuclides used most often for imaging are  $^{131}\text{I}$ ,  $^{111}\text{In}$ ,  $^{123}\text{I}$ , and  $^{99\text{m}}\text{Tc}$  owing to their short half-lives and appropriate gamma-emitting properties. Although intact IgG are retained better by tumors and are therefore more desirable for drug or toxin immunotherapy,  $\text{F(ab')}_2$  and Fab fragments are preferred for imaging because both targeting and blood clearance are more rapid, thus reducing background. A number of mAbs have been developed which show sufficient tumor targeting properties to be useful for radioimmunodetection. Among the most widely used mAbs for imaging have been those directed against carcinoembryonic antigen. Apart from direct imaging of known or unknown tumors, radioimmunodetection is often used for the confirmation of tumor targeting by mAbs which are to be used for immunotherapy. Imaging resolution is typically in the range of 1.0 to 2.0 cm, although tumors as small as 0.5 cm have been detected (68).

One advantage of radiolabeled mAbs for therapy over drug- or toxin-mAb conjugates is that, with the appropriate choice of radionuclide, radiolabeled mAbs can kill cells from a distance of several cell diameters and may therefore kill antigen negative cancer cells contained within the tumor. Internalization of the mAb is also not necessary, allowing greater flexibility in the choice of mAb. Whereas a high target/nontarget ratio of counts is

required for optimal imaging, a high concentration of tissue radioactivity over a long duration is desirable for radioimmunotherapy (56). Cell killing by radiation is most closely related to the damage to DNA.  $\beta$ -emitting radionuclides such as  $^{131}\text{I}$ ,  $^{90}\text{Y}$  and  $^{67}\text{Cu}$  have been used in therapy. Although superior to  $\gamma$ -emitters,  $\beta$ -emitters are not the ideal choice due to inefficient local cell-killing and toxicity to distant normal tissues. Future use of radionuclides for immunotherapy will likely focus on  $\alpha$ -emitting particles as these may be the most effective at killing tumor targets without significantly penetrating normal tissues (69).

#### **4.4 Antibody-bound drugs as therapeutic agents**

Anti-cancer drugs have been covalently linked to mAbs in an effort to direct these agents to tumor sites. The chemistry involved in the linkage of these drugs to antibodies has been reviewed extensively (1,70,71) and will only be dealt with briefly (except for MTX-see below) to demonstrate the underlying principles involved. The major goal of conjugate construction is the retention of both drug and antibody activities while at the same time maximizing the load of drug carried by the mAb. A number of functional groups present in mAbs have been used as sites for conjugation, for example thiols (either derived from the mAb itself by limited reduction of disulfides, or by introduction of blocked thiols such as in SPDP), amino groups, and carboxyl groups. Of these, the  $\epsilon$ -amino groups of lysine residues have been used most often. mAbs differ widely in their sensitivity to chemical modifications (72,73) and appropriate mAbs as well as conjugation methods must be chosen accordingly. This sensitivity is especially a problem with monoclonal compared to polyclonal preparations because a decrease in binding activity is likely to be shared by all molecules in the monoclonal preparation due to their homogeneity.

In many cases, drug activity is also decreased following conjugation to mAbs (1,73). This may be due to steric hindrance because of the proximity of the drug to the mAb or to the blockage of important functional groups on the drug which are necessary

for full drug activity. A loss of drug activity following conjugation may not be a problem if drug is released at the target site in an active form. Methods to achieve such release have been incorporated into conjugate design and include the use of: i) acid-labile spacers between drug and mAb (for example a cis-aconitic spacer) (74); ii) hydrazone bonds which are cleaved in the acidic environment of the lysosome (75); iii) peptide linkers designed to be cleaved by lysosomal enzymes (76); and iv) disulfide linkage of the drug which allows release of free drug more readily in lysosomes (77).

Representatives from a number of different classes of anti-cancer drugs have been linked directly to mAbs for targeting purposes. Reports of these conjugations are numerous and include: antimetabolites (MTX, 5-fluorouridine) (73,78-80), anthracyclines (daunomycin, adriamycin, idarubicin) (81-84), antitumor antibiotics (mitomycin C) (85), alkylating agents (chlorambucil, melphalan) (86,87), and vinca alkaloids (vinblastine, vindesine) (88).

## **5. Methotrexate**

MTX belongs to a class of antimetabolites known as the antifolates. It has been widely used for the treatment of a number of cancers including leukemias, lymphomas and breast cancer . Newer antifolates such as trimetrexate, pyritrexim and 10-ethyl-5-deaza-aminopterin have basic structures similar to MTX but differ in their uptake, sites of action and intracellular processing (see below). These new antifolates are being evaluated for use as chemotherapeutic agents, but to this point MTX remains the most commonly used antifolate (89).

Folates are active in their reduced form as tetrahydrofolates (THF) and are used for the synthesis of thymidylate from deoxyuridylate as well as in the synthesis of the purine ring (Figure 2). In the case of purine synthesis, THF in the form of 10-formyl THF supplies a one-carbon group for purine ring synthesis. Similarly, THF in the form of 5,10-methylene THF supplies a methylene group as well two hydrogens in the synthesis of

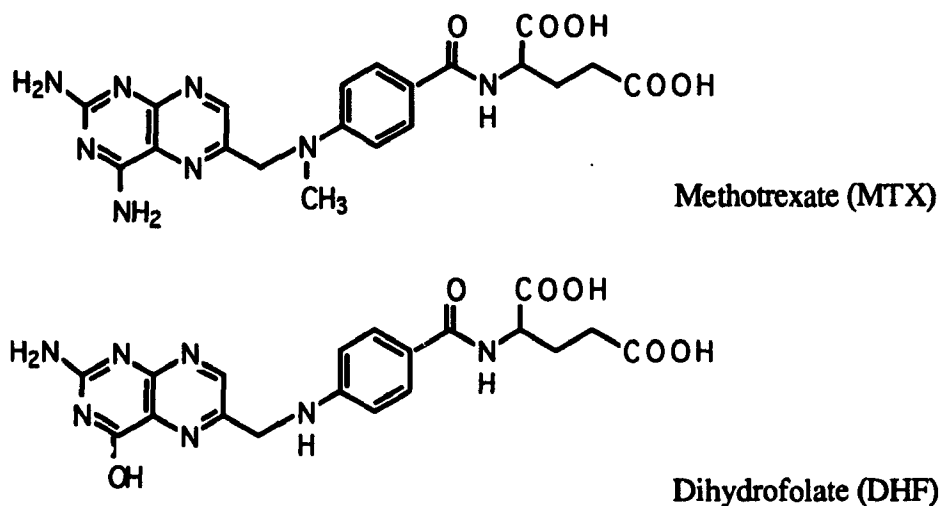
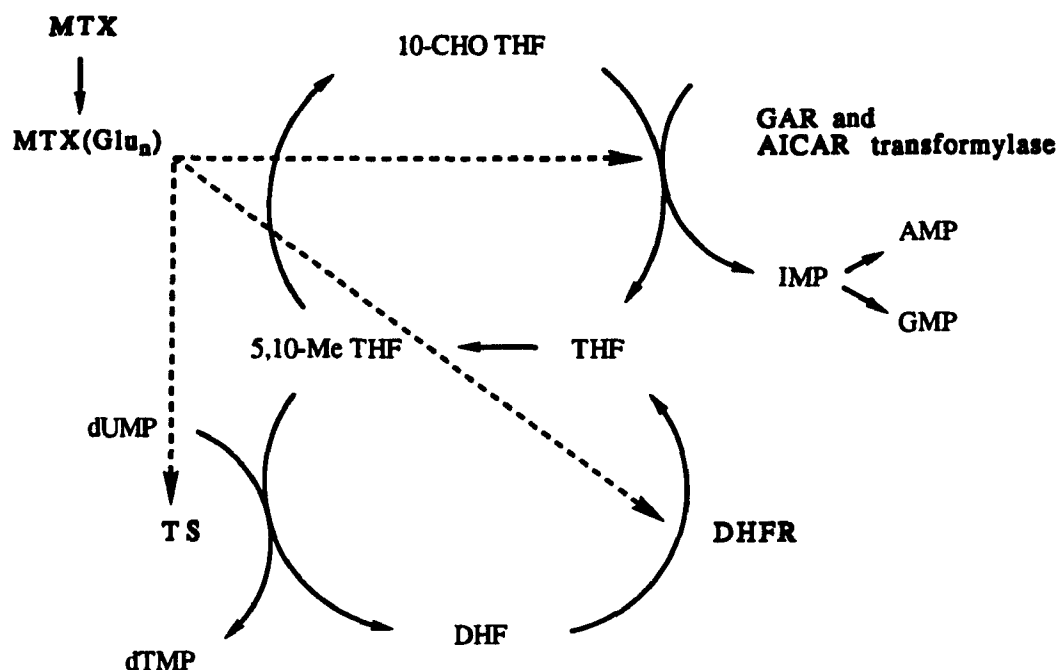


**Figure 2. Sites of action of Methotrexate.**

Intracellular MTX polyglutamates formed by the action of folylpolyglutamyl synthetase inhibit thymidylate synthesis by direct inhibition of dihydrofolate reductase (DHFR) and thymidylate synthase (TS) as indicated by the broken arrows. *de novo* purine synthesis is also disrupted by inhibition of glycinamide ribonucleotide (GAR) transformylase and aminoimidazole carboxamide ribonucleotide (AICAR) transformylase. DHF, dihydrofolate; THF, tetrahydrofolate; 10-CHO THF, 10-formyl THF; 5,10-Me THF, 5,10-methylen THF. Shown also are the structures of MTX and DHF.

thymidylate from deoxyuridylate. Both these reactions require a pool of reduced cofactor which is generated by dihydrofolate reductase (DHFR) (90). MTX is a structural analogue of dihydrofolate (DHF) as shown in Figure 2. The substitution of an amino group for the hydroxyl group at position 4 of the pteridine ring of DHF is the key feature of MTX which allows for the tighter binding of MTX to DHFR compared to DHF (91). By inhibiting DHFR, MTX reduces the available pool of reduced folates required for the synthesis of purines and thymidylate, thereby blocking cell division and ultimately causing cell death. In the presence of NADPH, MTX binds to DHFR in what has been characterized as a slow, tight binding process in which MTX first forms a rapid but weak complex with DHFR and NADPH, followed by a slow isomerization to a tightly bound complex (92). The binding of MTX to DHFR is tight but is reversible, and under therapeutic conditions where high levels of competitive substrate (DHF) are present, an excess of MTX over DHFR is required for total inhibition of the enzyme (93).

MTX enters cells by a high affinity influx mechanism which is both temperature sensitive and energy-dependent. This mechanism appears to be mediated by specific membrane proteins and is also responsible for the transport of naturally occurring reduced folates (94,95). It accounts for all MTX uptake at extracellular drug concentrations of up to 50  $\mu\text{M}$ . A second less efficient uptake mechanism has also been proposed which occurs at high extracellular MTX concentrations and may represent passive diffusion since it does not demonstrate competition with natural folates (96). Efflux of MTX appears to occur through at least two route-specific carriers, one of which is the uptake carrier protein. The second efflux mechanism is also energy-dependent and appears to be shared by cyclic nucleotides (90).

Naturally occurring folates are polyglutamated by the action of folylpolyglutamyl synthetase which adds from two to five glutamate residues in a  $\gamma$ -peptide linkage to the folates. Polyglutamation enhances both the intracellular retention of folates as well as their affinity for thymidylate synthetase and aminoimidazole carboxamide ribonucleotide

transformylase (97). Intracellular MTX is also polyglutamated by polyglutamyl synthetase, although the affinity for MTX is much lower than for normal physiological folates. MTX polyglutamates are better inhibitors of DHFR than free MTX, and also inhibit thymidylate synthase, GAR and AICAR transformylase, whereas free MTX has little effect on these enzymes (98). Cellular cytotoxicity appears to be a result of DHFR inhibition as well as MTX polyglutamate inhibition of the purine synthesis pathway (99,100) as shown in Figure 2. The two factors considered most important to the efficacy of MTX treatment of cancer are the intracellular concentration of drug and the duration of exposure (90). A high intracellular concentration is required to ensure total inhibition of DHFR and the purine-synthesizing enzymes, while the duration of exposure is important because the action of MTX is S-phase specific and longer exposures enable more cells to be inhibited during the vulnerable period.

A number of mechanisms have been shown to contribute to the resistance to MTX. These include decreased MTX transport (94), reduced polyglutamation of MTX (101), increased DHFR levels and changes in DHFR affinity for MTX (102).

## **6. Direct linkage of methotrexate to antibodies**

MTX has been conjugated to carriers by a variety of methods. These methods generally make use of the glutamic acid portion of MTX due to the unreactive nature of MTX amino groups (103). One of the earliest methods reported for coupling MTX to IgG was through the diazotization of MTX. DeCarvalho et al. (104) used diazotized benzidine which was reacted first with MTX and then with IgG. It was believed that the major product formed upon reaction of MTX with diazotized benzidine was the 2-substituted derivative of MTX and it was unclear as to which functional groups in the IgG acted to couple the activated MTX. Robinson et al. (103) later attempted to activate MTX directly by diazotization with nitrous acid, but noted the formation of a number of MTX derivatives following the reaction. This method of MTX activation has seen little use in the

conjugation of MTX to proteins due to the comparatively harsh reaction conditions which typically lead to extensive protein precipitation (71).

MTX was reported to have been coupled to an antibody with high incorporations using an anhydride derivative of MTX formed on reaction between MTX and acetic anhydride (105). It was likely that the acylating species in this case was the mixed anhydride, and not a cyclic anhydride formed by cyclization of MTX carboxyls following the activation of one carboxyl. [<sup>14</sup>C]acetic anhydride was used for the reaction with MTX and the resulting antibody conjugates were found to contain an amount of <sup>14</sup>C consistent with the formation of the double mixed anhydride. Using this method, Kulkarni et al. (73) found that incorporation of MTX into IgG was low and neither the conjugate nor the activated MTX product were capable of inhibiting DHFR, indicating that MTX was altered in some way during the activation process, possibly by polymerization of the drug or reaction with the pteridine amino groups.

Watanabe et al. (106) have reported the conjugation of MTX to polyaldehyde dextran, the latter obtained by periodate oxidation of dextran T-40. The reaction was presumably through Schiff base formation between dextran aldehydes and MTX amino groups. The MTX-dextran was then conjugated to a mAb and the product was stabilized by sodium borohydride reduction. The reported conjugate was found to contain a high retention of antibody binding activity, although MTX substitution per mAb was quite low with a maximum of 9 MTX/IgG. These results are surprising for two reasons. The 2- and 4-amino groups of MTX are generally believed to be unreactive, and linkage by these amino groups would be expected to destroy the DHFR inhibitory capacity of MTX as this portion of the molecule must interact intimately with DHFR.

Later, the water-soluble carbodiimide, 1-ethyl-3-(3'-dimethylaminopropyl) carbodiimide (EDCI) was used to activate MTX for coupling with biopolymers such as anti-tumor antibodies (73,107), bovine serum albumin (BSA) (73,108,109), human serum albumin (HSA) (107,110,111), mannosyl BSA (112) and maleyl BSA (113). MTX has

also been linked to a number of synthetic macromolecules including poly(L-lysine) (114,115), poly (D-lysine) (116), and dextran (117) using EDCI. In this method, MTX is activated under aqueous conditions *in situ* in the presence of EDCI and amino group-containing polymer. Activation of MTX carboxyl groups proceeds first by reaction of one or both carboxyls with EDCI producing an O-acylisourea derivative of MTX (70). This derivative undergoes a nucleophilic substitution reaction with an amino group from the polymer, forming an amide bond between polymer and MTX.

In 1981, a method for the activation of MTX by conversion to a succinimidyl ester was described by Kulkarni et al. (73). Since that time, this has become one of the most widely used approaches for the conjugation of MTX to amino-containing polymers. Conjugates prepared with the succinimidyl ester of MTX include antibodies (9,73,79,80,118-127), HSA (120,125), and amino-dextran (117). The succinimidyl ester of MTX, also known as the active ester of MTX (MTX-AE), is prepared by reaction of MTX with dicyclohexylcarbodiimide (DCC) and N-hydroxysuccinimide (NHS) as shown in Figure 3. Reaction of MTX carboxyl groups with DCC results in the formation of the O-acylisourea intermediate which can react with NHS to form the active ester. The active ester is then capable of reaction with protein amino groups resulting in the formation of an amide bond between the glutamate of MTX and the protein amino group. The advantage of this method over the *in situ* carbodiimide method described above is that, by limiting the ratio of DCC over MTX, the amount of carbodiimide introduced into the protein solution can be minimized. In the case of direct carbodiimide activation of MTX in the presence of protein, there is typically a large excess of carbodiimide over protein which can result in protein cross-linking as both amino and carboxyl groups are present (71).

The reactions between MTX and antibodies described above can be considered non-site-specific, in that the attachment of MTX was typically through amino groups which are present at different locations on the antibody. Although linkage of MTX to these sites may not be truly random due to the enhanced reactivity of some amino groups over others,

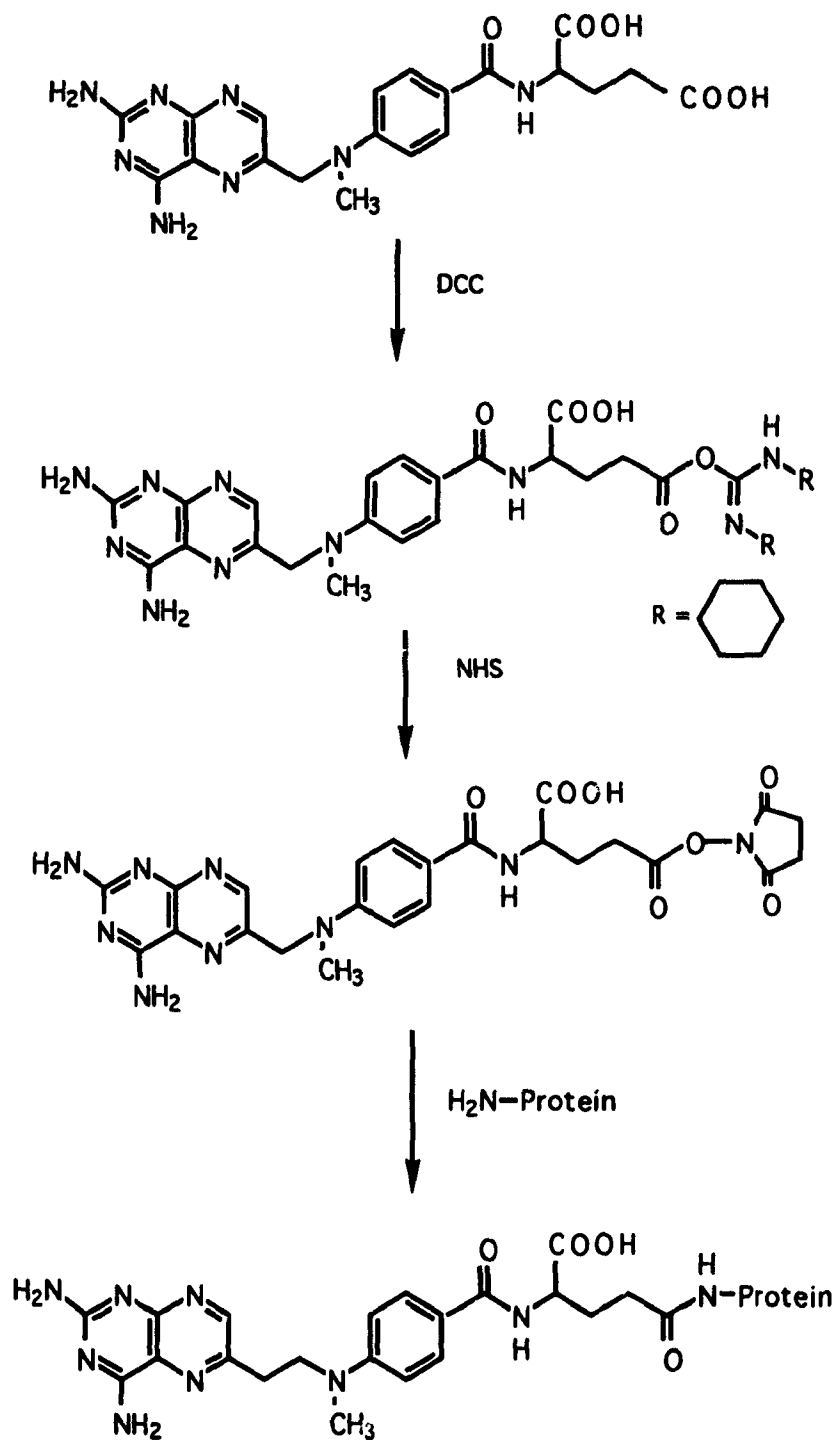


**Figure 3. Synthesis of MTX-AE and its reaction with protein.** MTX carboxyl groups are activated in the presence of dicyclohexylcarbodiimide (DCC) and N-hydroxysuccinimide (NHS) to give an active ester of MTX (MTX-AE). MTX-AE reacts with protein amino groups resulting in an amide linkage between MTX and protein.

conjugates prepared in this manner are considered non-site-specific since the potential for reactivity at different sites exist. A more recent approach of linking MTX to antibodies is a site-specific approach, in which a suitable derivative of MTX is linked to specific sites on the antibody. MTX has been activated by conversion of MTX carboxyl groups to the hydrazide derivatives (128,129). These hydrazides can react with aldehyde groups resulting in the formation of a hydrazone bond. Periodate oxidation of IgG results in the formation of aldehyde groups from IgG carbohydrate residues. Kralovec et al. (128) compared mAb K20 conjugates prepared using the non-site-specific active ester method and the site-specific MTX-hydrazide method with respect to antibody binding activity and cytotoxicity to target Caki-1 cells. Both conjugates contained approximately 6-7 mol MTX/mol IgG and were found to retain full antibody binding activity. The non-site-specific conjugate showed greater *in vitro* cytotoxicity to target cells than the site-specific conjugate. Shih et al. (129) also compared mAb-MTX conjugates prepared using these two methods and found that the site-specific conjugates gave a greater therapeutic effect in treating tumors in mice.

## **7. Linkage of drugs to antibodies through a carrier**

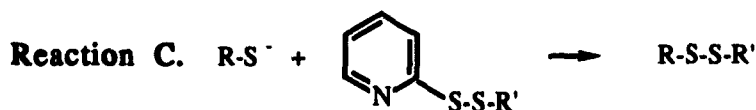
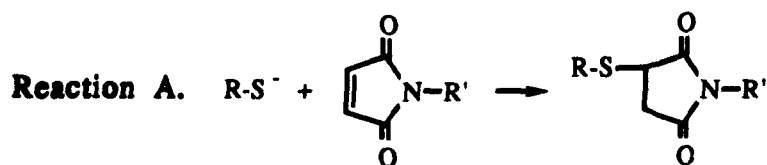
Due to the loss of antigen binding activity seen with some mAbs following conjugation with drugs (1,71), conjugation methods to reduce activity loss while achieving high levels of drug incorporation have been developed. One such method is the use of a drug carrier or intermediary which is first loaded with drug and then linked to the mAb. The rationale behind this type of conjugation is that many more drug molecules can be loaded on the carrier than directly on the mAb. The incorporation of a limited number of these carrier molecules on the mAb would be predicted to maximize the drug load while minimizing damage to mAb activity. This system has been used with a number of mAbs, carriers and types of drugs. A number of physical properties of the polymer to be used as a drug carrier should be considered. The carrier should be homogeneous to facilitate

subsequent separation of conjugates from unbound mAb and carrier, and have a large number of suitable functional groups or be amenable to incorporation of suitable groups for reaction with both mAb and drug. The carrier should also be highly soluble since most anti-cancer drugs have poor water solubility. As with direct MTX-antibody conjugates, conjugates are termed either non-site-specific or site-specific, depending on the location of linkage of the carrier on the mAb. Non-site-specific conjugates contain the carrier linked to functional groups which occur at different locations on the mAb, such as amino groups. Site-specific conjugates contain the carrier linked to a specific location on the mAb. The cystine residues that hold the two heavy chains together, or carbohydrate chains are examples of site-specific modifications since these sites are present only in defined areas of the mAb. For purposes of clarity, another distinction should be made with respect to the nomenclature used for the different types of conjugates. Direct conjugates are those with drug directly bound to the mAb, whereas conjugates in which a carrier is used can be either ternary (drug + carrier + mAb) or binary (carrier/toxin/enzyme + mAb). Intermediaries which have been used as drug carriers in antibody-mediated targeting include serum albumins, dextran and its derivatives, and liposomes. Conjugates prepared with the use of such carriers are described below.

## **8. Chemistry of antibody-protein conjugation**

The field of protein conjugation chemistry has grown considerably and encompasses the cross-linking of proteins with other proteins, drugs, nucleic acids, peptides, and solid particles. The cross-linkers or spacers which are used to achieve conjugation are numerous, with over three hundred having been synthesized up to the present time (130). A number of reviews on this diverse subject have been published (71,130), so an in depth review will not be presented here. Instead, this review will be limited to illustrating the principles involved and the most frequently used methods to achieve the conjugation of antibodies with other proteins.

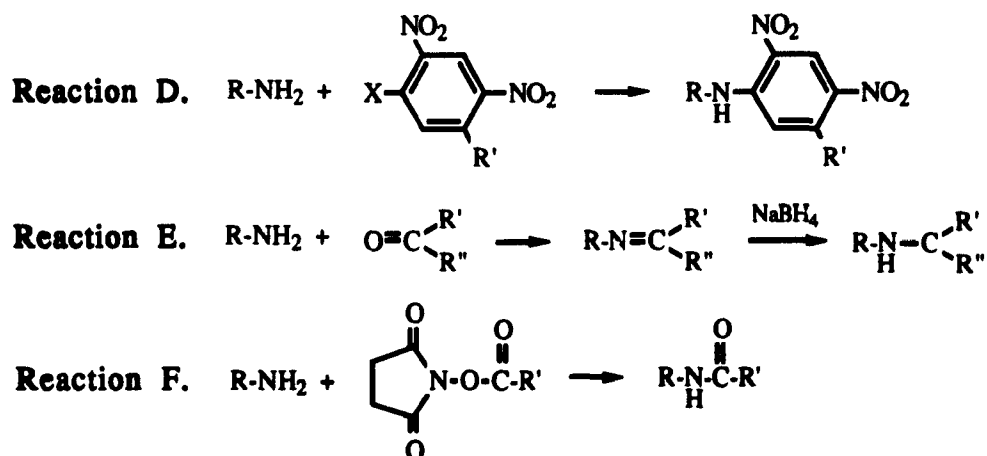
Of the functional groups present in proteins, only a limited number can be considered sufficiently reactive to be useful for conjugation. These include the guanidinyll group of arginine, the side chain carboxyls of glutamic and aspartic acids, the sulfhydryll group of cysteine, the imidazolyl group of histidine, the  $\epsilon$ -amino group of lysine, the thioether moiety of methionine, the indolyl group of tryptophan and the phenolic hydroxyl group of tyrosine (71). Since most protein modification reactions are of the nucleophilic substitution type, the nucleophilicity and hence reactivity of these functional groups increases with increasing pH. The hydroxyl groups of serine and threonine are generally unreactive due to their high pKa values, and methionine and tryptophan are usually buried and therefore not accessible for reaction. Of the remaining reactive groups,  $\epsilon$ -amino groups and sulfhydryll groups have been used most extensively in conjugation reactions and further discussion will be restricted to these two functional groups. The most commonly used reactions of thiol compounds are shown below:



In the above reactions, the thiolate (pKa  $\approx$  8.5) is the reactive species and reactivity therefore increases with increasing pH. Thiols react with maleimides (Reaction A) and  $\alpha$ -haloacetyl compounds (Reaction B, where X = I, Br, Cl) to form stable thioether bonds. Examples of these types of modifications are the blocking of thiol groups by N-ethylmaleimide and carboxymethylation of thiols with iodoacetate, respectively. The

reaction with an activated disulfide such as 2-pyridyldisulfide (Reaction C) results in the formation of a disulfide bond which itself is susceptible to disulfide interchange (reduction) by sulfhydryl reagents. This reaction is also the basis of protein sulfhydryl determination with 5,5'-dithiobis(2-nitrobenzoic acid), (Ellman's reagent) (131). Reaction C can be considered specific for thiols whereas A and B show selectivity towards thiol compounds but also the potential for reaction with amino groups. These minor side-reactions can be reduced considerably by carrying out reactions at neutral to slightly acidic pH.

Amino groups can be alkylated or acylated by a number of reagents as shown below (Reactions D to F). Reaction of amino groups ( $pK_a \approx 9.5$ ) with aryl halides results in alkylation of the amino group (Reaction D,  $X = F, Cl, Br$ ). The product is stable and has been used extensively for protein N-terminal analysis using 1-fluoro-2,4-dinitrobenzene. Other nucleophiles such as thiolates and phenolates also react with aryl halides but only the product formed on reaction with amino groups is stable at alkaline pH. Reaction E represents Schiff base formation following reaction with an aldehyde or ketone. The imine is not stable and requires reduction by reagents such as sodium borohydride. A similar reaction occurs between hydrazides ( $R-CONHNH_2$ ) and carbonyl groups forming a hydrazone bond. Schiff base and hydrazone bonds will be discussed in greater detail in a following section.

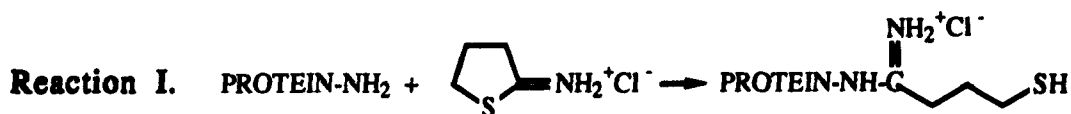
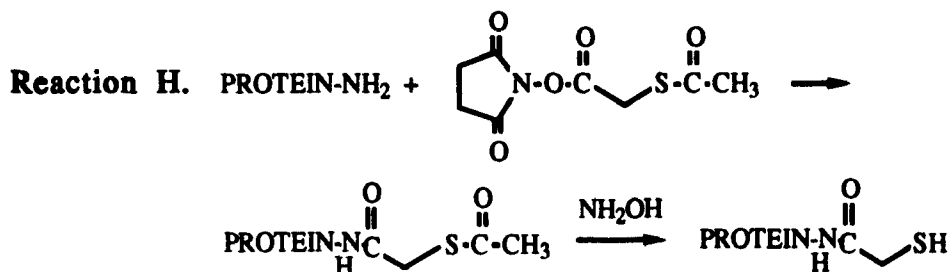
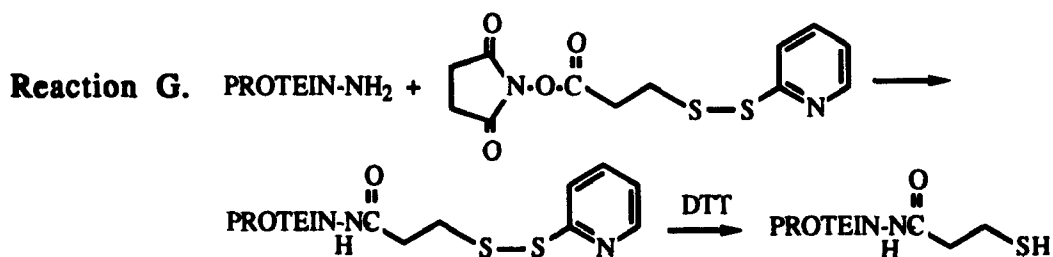


Acylation of amino groups can be achieved by reaction with reagents such as N-succinimidyl esters to form a stable amide bond (Reaction F). Another so called active ester is based on the p-nitrophenyl group which reacts in the same manner as the N-succinimidyl esters. Other reactive groups which have been used to acylate amino groups include isocyanates, isothiocyanates, imidoesters, acyl chlorides and sulfonyl chlorides. As with aryl halides, other nucleophiles react with these acylating species. Many of these other products are not stable and can be hydrolyzed under appropriate conditions. For example, acylated tyrosine can be deacylated with hydroxylamine (118).

It can be envisioned that a compound possessing two reactive functional groups separated by a suitable bridge or backbone would be useful for conjugating two proteins. These compounds are referred to as cross-linkers or spacers. A cross-linker containing two identical reactive groups, or groups, with reactivity toward the same nucleophile, are termed homobifunctional. A cross-linker with specificity for two different functional groups is referred to as heterobifunctional. Many of each type of spacer have been reported in the literature (for a review see reference 132). The backbones of the spacers have been designed to possess desirable characteristics with respect to length, solubility properties, steric properties, and the ability to be cleaved. The use of homobifunctional spacers is generally considered undesirable for the conjugation of two unlike proteins. If each protein possesses the same functional groups, for example amino groups, it is likely that cross-linking with a homobifunctional spacer will result in the formation of homoconjugates i.e. conjugates of two like proteins, as well as heteroconjugates containing both proteins. A more refined approach is possible with heterobifunctional cross-linkers, where one protein (protein-1) is derivatized with the spacer by one of the reactive functions, and then the protein-1-spacer derivative reacted with protein-2 via the second reactive function on the spacer. For example, using a spacer containing amino- and thiol-reactive groups, protein-1 can be modified at amino groups and then reacted with thiol-containing protein-2. In theory, this system eliminates the formation of homoconjugates. Two requirements for the

use of such heterobifunctional spacers are i) that protein-1 not contain any of the functional groups used for conjugation of protein-2 to the spacer (thiol groups), and ii) that protein-2 contains the appropriate functional group for reaction with spacer (thiol groups).

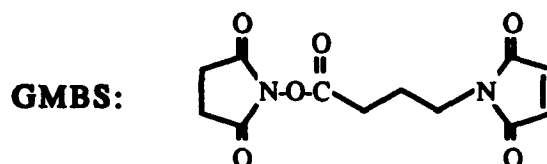
Requirement i) can be met by blocking any thiols on protein-1 prior to reaction with spacer. Since this amino-thiol heterobifunctional approach is widely used in protein conjugation, and few proteins contain free thiols, methods to introduce thiols into proteins have been developed (133-135). The most straightforward method is the reduction of internal disulfide bonds (110,119), but this is not usually desirable since the tertiary structure and/or activity of toxins and enzymes may be altered. Other methods rely on the incorporation of thiols:



The three reagents shown in Reactions G to I above, react with protein amino groups. The cross-linking reagent 3-(2-pyridyldithio)propionic acid succinimidyl ester (SPDP) introduces a blocked thiol (Reaction G) which can be deprotected by reduction with DTT (133). Similarly, N-succinimidyl S-acetylthioacetate (SATA) introduces a blocked thiol

group (Reaction H) which can be deprotected with hydroxylamine (134). 2-Iminothiolane (Reaction I, Traut's reagent) incorporates an unprotected thiol (135). Blocked thiols are useful since spacer-derivatized proteins can be modified with other reagents without the possibility of the thiol participating in the reactions.

Two commonly used cross-linkers for antibody-protein conjugation are SPDP (Reaction G above) and  $\gamma$ -maleimidobutyric acid succinimidyl ester (GMBS):



Variations of these two spacers include those with the same two reactive groups but backbones of different length or steric orientation of functional groups. For example, the presence of a benzene ring within the backbone places the two functional groups at different angles.

## 9. Non-site-specific linkage of carriers to antibodies

A number of carriers containing various drugs have been conjugated to antibodies for the purpose of immunotherapy of cancer. The majority have been constructed using non-site-specific conjugation techniques in which the drug-loaded carrier was linked randomly to functional groups on the antibody.

### Serum albumin

Human serum albumin (HSA) has been used as a carrier for MTX (107,110,111,119). It has a MW of 67,000 and contains 58 lysine residues (136) which could be used for the loading of a substantial amount of MTX, and also has a free thiol at cysteine 34 (136,137) which may be useful for subsequent reaction with the mAb.

Incorporation of MTX into HSA was achieved either through the use of EDCI or the MTX-

AE reactions described above, with incorporations ranging from 24 to 38 mol MTX/mol HSA. Linkage of MTX-loaded HSA to mAbs was achieved in a variety of ways using the specificity of thiol reactions to reduce polymerization of HSA-MTX or mAbs. Garnett et al. (107) incorporated a limited number of blocked thiols into HSA amino groups prior to MTX incorporation using SPDP (133). MTX-HSA-SPDP was then reduced with DTT to deblock the thiols and reacted with iodoacetylated mAb, the latter prepared by reaction of mAb lysine residues with N-succinimidyl iodoacetate. Garnett et al. (110) also used the free cysteine of HSA for conjugation of HSA-MTX with iodoacetylated mAb. Endo et al. (119) prepared mAb-HSA-MTX conjugates in a similar way by reacting DTT-reduced HSA-MTX with a mAb which had been derivatized with maleimide groups using  $\gamma$ -maleimidobutyric acid succinimidyl ester (GMBS). Due to the difficulty in separating specific conjugates from both starting materials and from mAb-HSA-MTX conjugates containing different amounts of HSA-MTX, the conjugates which were isolated by gel filtration were not homogenous and likely contained HSA-MTX of various stoichiometries as well as unreacted mAb. The partially purified preparations were found to retain between 28 and 36% antibody activity relative to native mAb and showed selective cytotoxicity to antigen-positive cell lines. Except for the one conjugate prepared by Garnett et al. (110), these ternary conjugates were less cytotoxic than unconjugated MTX *in vitro*.

Umemoto et al. (138) used bovine serum albumin (BSA) as a carrier for mitomycin C and conjugated mitomycin C-loaded BSA to an IgM monomer fragment (IgMs) derived from IgM by limited reduction and alkylation with iodoacetamide. BSA is similar to HSA in terms of MW, solubility properties, and also contains a free thiol group (139). In these studies, mitomycin C was converted to a succinimidyl ester for reaction with amino groups on IgMs (for direct conjugation), or for reaction with the carrier BSA. The BSA thiol was blocked with 2-pyridyldisulfide prior to reaction with mitomycin C, and then reduced with DTT following drug loading. Conjugation of mitomycin C-BSA to IgMs was through a thioether linkage formed between the carrier and maleimide-derivatized IgMs, the latter

prepared by reaction of IgMs amino groups with N-succinimidyl m-(N-maleimido)benzoate (SMB). Ternary conjugates were isolated by gel filtration but, as with the HSA conjugates discussed above, separation was poor and the isolated conjugate poorly defined. Antibody activity was not reported and, although a direct comparison between the direct and ternary conjugates was not made, both conjugates were less cytotoxic than free mitomycin C against an antigen-positive cell line *in vitro*.

### **Dextran**

Dextran and its derivatives have been used as carriers for a variety of drugs. Arnon and Sela (140) used polyaldehyde dextran (PAD) which was prepared by oxidation of dextran with sodium periodate. PAD was reacted first with daunomycin and then with antibody and Schiff bases reduced with sodium borohydride. The reaction between daunomycin and PAD was believed to produce either Schiff bases with the amino sugar group of daunomycin or an oxazolidine derivative with the sugar amino group and its vicinal hydroxyl group. Attachment of PAD-daunomycin to the antibody was likely through Schiff base formation between unreacted aldehydes on PAD and amino groups on the antibody. These ternary conjugates contained between 25 and 30 mol daunomycin/mol antibody and retained approximately 70% antibody activity, which was comparable to direct conjugates containing from 2 to 6 mol daunomycin/mol antibody. The cytotoxicity of the ternary conjugates was, however, lower than that of direct conjugates, measured on the basis of drug concentration.

PAD was also used as a carrier for cytosine arabinoside (141) as well as for mitomycin C (142) and bleomycin (143). In all cases, an amino group of the drug formed a Schiff base with aldehyde groups on PAD. Linkage of the carrier was either to a polyclonal antibody (141) or a mAb (142,143) and was achieved by Schiff base formation between residual aldehydes present in PAD with amino groups in the IgG. All Schiff bases were stabilized by cyanoborohydride or borohydride reduction. Antibody activity in the

conjugates was claimed to be comparable to native antibody, although examination of the binding data shown for two of these conjugates (142,143) reveals substantial loss of activity. Cytotoxicity to target cells was higher for the mitomycin C and bleomycin conjugates (142,143) and lower for cytosine arabanoside conjugates when compared to free drug.

Hurwitz et al. (144) described a method for preparing a hydrazide derivative of carboxymethyl dextran (CMD). CMD was prepared by the reaction of dextran with chloroacetic acid, and the carboxyl groups of CMD condensed with hydrazine using EDCI. This dextran-hydrazide was used as a carrier for 5-fluorouridine (141). Aldehydes were formed by the periodate oxidation of 5-fluorouridine and reacted with hydrazide groups on the carrier to form hydrazone linkages between drug and carrier. The carrier was then linked to a polyclonal antibody using the dialdehyde cross-linking reagent glutaraldehyde. Glutaraldehyde would theoretically form Schiff bases with proteins; however the cross-linked products have been found to be stable without reduction. The mechanism of this cross-linking remains uncertain, but it appears that glutaraldehyde undergoes polymerization to form  $\alpha,\beta$ -unsaturated aldehyde polymers in solution. Presumably it is the unsaturated polymer which cross-links amino groups (145). Antibody activity was decreased following the linkage of the drug-loaded carrier and was thought to be due to the cross-linking of IgG. The conjugate was found to be less cytotoxic than free drug although it had better activity than the drug linked to carrier without antibody.

### **Polyglutamate**

Rowland et al. (146) used poly-L- $\alpha$ -glutamate (PGA) as a carrier for p-phenylendiamine mustard. The amino group of the drug was linked to PGA carboxyl groups using EDCI. The PGA-drug intermediate was then linked to amino groups of a polyclonal anti-EL4 antibody through unreacted carboxyl groups on PGA with the use of EDCI. The antibody activity of this conjugate was reported as 66% of native antibody, and

the conjugate was shown to dramatically increase survival of EL4 tumor bearing mice relative to untreated control mice.

A more elegant approach was taken by Kato et al. (147) who polymerized  $\gamma$ -benzyl-N-carboxy-L-glutamate anhydride in the presence of a limiting amount of cystamine. The carboxyl groups of N,N'-bis(poly-L-glutamyl)cystamine were deblocked, and the disulfide reduced to allow separation of thiol-containing from non-thiol-containing polymer on thiopropyl-sepharose containing the activated 2-pyridyldithio group. Following elution of the thiol-containing polymer with DTT, the thiol group of the polymer was converted to the 2-pyridyldisulfide and the polymer carboxyl groups reacted with daunomycin in the presence of EDCI. The average MW of polymer obtained by this procedure was 12,000, containing 80 glutamate residues per unit. The substitution with daunomycin was quite low, with only 6.5 mol daunomycin/mol carrier. The daunomycin-containing polymer was then reduced with DTT to deblock the thiol group and reacted with a polyclonal antibody containing maleimide groups introduced into the antibody by reaction of antibody amino groups with N-succinimidyl-4-(N-maleimido)butyrate. Ternary conjugates were purified by preparative PAGE and the isolated material had an average of 1.2 mol carrier/mol antibody. The antibody activity of the ternary conjugate was found to be similar to that of the native mAb and the cytotoxicity of the conjugate was greater than that of free daunomycin against target cells and less than free drug against a non-target cell line. The advantage of this procedure over other carrier-based methods is that a single thiol group was contained in the polymer, thereby reducing the risk of cross-linking antibody molecules to form higher conjugates.

### **Polylysine**

A more recent development in the targeting field is that of antibody-mediated DNA targeting. Although the purpose of this type of targeting is not to cause cell death, gene therapy can be regarded as a form of therapy for the purposes of this review on the use of

drug carriers. In a recent report (148), poly(L-lysine) with an average MW of 3,000 was reacted with SPDP to introduce an activated disulfide at its N-terminal. The pyridyldithio-poly(L-lysine) was reacted with a mAb which had been derivatized at amino groups with iminothiolane to introduce thiol groups. The antibody activity of isolated binary conjugates containing between 2 and 3 poly(L-lysine) units was found to be quite low compared to native mAb (approximately 10% activity). For formation of ternary conjugates, the binary conjugate was complexed with suitable DNA preparations. Target cells, which were incubated with ternary conjugates formed between binary mAb-poly(L-lysine) and plasmids containing the chloramphenicolacetyl transferase marker, were shown to express chloramphenicolacetyl transferase activity at a much higher level than cells which were incubated with a ternary conjugate synthesized with a non-specific mAb.

### **Antibody-bound toxins**

Toxins have been attached to mAbs to achieve directed cytotoxicity. Toxins are complex proteins derived from bacteria or plants which bind to animal cells and deliver an enzymic component into the cytosol that is capable of irreversibly inactivating protein synthesis. Toxins are very potent and only a small number of molecules are required to cause cell death. The toxins most often used in the preparation of immunotoxins are the bacterial *pseudomonas* exotoxin A and diphtheria toxin, and the plant-derived ricin toxin (149). These toxins have been conjugated to antibodies using SPDP, where toxin-SPDP was reacted with thiol-containing antibody (150). Because of their potency, the specificity and non-specific interactions of immunotoxins becomes much more important than in the case of drug conjugates. The lack of specificity of early immunotoxins was due to the presence of recognition sequences within the toxin itself. Apart from the enzymatic activity, toxins possess cell recognition sequences contained either in separate domains or polypeptide chains. More recent immunotoxins have used truncated or mutated versions of the toxins to reduce the non-specific binding caused by these sequences (149,151).

Another recent advance in the preparation of immunotoxins has been the preparation of recombinant chimeric toxins (single chain immunotoxins) where antibody-derived genes for the antigen binding domains (Fv fragments) have been fused with modified toxin genes (152).

### **Antibody-bound liposomes**

Liposomes are microvesicles composed of a continuous bilayer of phospholipid surrounding an aqueous phase. A number of drugs have been encapsulated in liposomes for passive drug delivery or site-avoidance delivery (153). The use of antibody-bound liposomes containing MTX for the purpose of selective drug targeting has been shown effective both *in vitro* (154,155) and in an ascites tumor model *in vivo* (156). In one study, ternary conjugates were shown to be superior to either free drug or direct binary conjugates prepared with the same mAb (155). In these studies pyridyldithio groups were incorporated into the liposomal membrane using N-[3-(2-pyridyldithio)propionyl] stearylamine as a membrane component. MTX entrapment was achieved by allowing liposomes to form in the presence of MTX. The attachment of pyridyldithio-containing liposomes to mAb was achieved by reaction of liposomes with thiol-containing mAb, the latter prepared by reaction of mAb with SPDP followed by reduction with DTT.

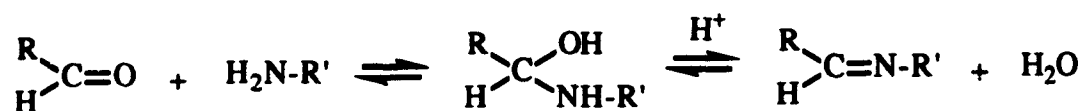
### **10. Site-specific linkage of carriers to antibodies**

The conjugates formed using the linkage procedures described above were non-site-specific in that the carrier was usually attached to amino groups of the antibody. Although these methods allowed increased levels of drug to be incorporated into the antibody, antigen binding activity was still decreased in many cases, presumably due to the modification of amino groups present in the antigen binding site, or by steric hinderance of the carrier due to its proximity to the antigen binding site. Methods to modify antibodies at sites distant from the antigen binding site have been developed. These include the specific modification of thiol groups present in the hinge region of the IgG and the selective

modification of carbohydrate residues contained mostly in the C<sub>H2</sub> domain of IgG (21). The specific modification of hinge region thiols is limited because the selective reduction of only intrachain disulfides is difficult without some reduction of disulfides linking heavy to light chains, and possibly interchain disulfides. Immobilization of IgG fragments through these thiols was found to result in loss of antigen binding capacity (157). Reactions for the selective modification of protein carbohydrate have been known for some time, but it was not until the last decade that such selective reactions were applied to protein labelling and conjugation. As discussed previously, the majority of IgG carbohydrate from all species studied is of the N-linked type attached to Asn 297 in the Fc portion of the molecule. Modifications of IgGs at this site would therefore be expected to have little effect on antigen binding activity. This has been shown to be true for a number of carbohydrate-specific modifications such as immobilization (158-161), incorporation of chelating agents (162-164), incorporation of antitumor drugs (75,83,128,129,165), incorporation of low MW probes such as biotin (166-168), linkage of a dextran-MTX moiety (117), and more recently, the production of a mAb-protein conjugate (169).

The selectivity of carbohydrate-specific reactions arises from the presence of vicinal hydroxyl groups present in the sugar residues of oligosaccharide chains. Aldehyde groups have been generated from these residues both enzymatically and chemically. Galactose oxidase has been used to form a C-6 aldehyde group on terminal galactose or N-acetylglucosamine residues (170). In cases where sialic acid is the terminal residue, it can be removed by neuraminidase to expose the penultimate galactosyl residue. The chemical method involves the periodate oxidation of vicinal diols to aldehydes (171). It has been reported that under suitably mild conditions, the periodate oxidation can be specific for the generation of the exocyclic C-7 aldehyde on sialic acids whereas harsher conditions result in oxidation of other vicinal diols (172).

Aldehydes formed in the carbohydrate chains can react specifically with suitable nitrogen-containing bases. These reactions can be represented as:



R' = NHCO-R'' for a hydrazide compound (pKa  $\cong$  3)  
 = R'' for amino-containing compound (pKa  $\cong$  9.5)

The nucleophilic attack of either a hydrazide or amino group at the carbonyl carbon results in the formation of an intermediate addition compound. The second step is the rate-limiting, acid-catalyzed dehydration of the intermediate to form either a hydrazone bond (R' = NHCO-R'') or a Schiff base (R' = R''), depending on the nucleophile (173). For Schiff base formation, the second step can also be a base-catalyzed dehydration (174), whereas hydrazone formation does not generally appear to occur by this mechanism (175). The pH optima for the two reactions appear to be governed by the opposing effects of general acid catalysis and the decrease in the concentration of attacking free nitrogen base due to conversion to the conjugate acid at low pH (173).

The choice between a hydrazide and amino group for coupling to IgG aldehydes is one based on specificity. Primary amines are present on lysine residues and occur throughout the protein and are therefore available for reaction with aldehyde groups. The reaction with protein amino groups may compete with the desired reaction between amino-containing reagent and result in inter- and intramolecular cross-linking of the IgG, although this might be suppressed through the use of a large excess of amino-containing reagent. Greater specificity can be achieved through the use of a hydrazide-containing reagent. The pKa of the hydrazide and primary amino groups are approximately 3 and 9.5 respectively. Because the unprotonated form of the hydrazide or amino group is the reactive species, the reaction with aldehydes will occur most readily at pH values above the pKa of the functional group. By performing the reaction between a hydrazide-containing reagent and

IgG aldehydes at slightly acidic pH values (typically 4-5.5), Schiff base formation is decreased, resulting in greater specificity for reaction between aldehyde and hydrazide.

It is generally accepted that Schiff bases are unstable and require reduction of the imine by either borohydride or cyanoborohydride for stabilization. However, there is some controversy in the literature regarding the stability of hydrazone bonds. The majority of reports indicate that hydrazone bonds formed between two proteins or between an insoluble matrix and protein are stable (158,169,176,177). King et al. (178) showed that hydrazone bonds formed between model aldehydes and hydrazides were unstable under neutral and acidic conditions and that they could be stabilized by reduction with cyanoborohydride. Others also have reported similar instability (75,83,165) of low molecular weight hydrazides also.

The next logical refinement in the construction of antibody-drug conjugates was the linkage of the carrier site-specifically to the IgG to increase the load of drug and to minimize the effect on antigen binding activity. Such conjugates have been synthesized and are described below.

### **Polyglutamate**

Hurwitz et al. (144) used polyglutamyl hydrazide as a carrier for daunorubicin. Polyglutamyl hydrazide was prepared by reaction of poly- $\gamma$ -benzyl-L-glutamate with hydrazine, and the hydrazide groups of the carrier reacted with IgG aldehydes which were formed by periodate oxidation of IgG carbohydrate. The resulting hydrazone-linked binary conjugate was then reacted with daunorubicin to form further hydrazone linkages between the C13 ketone group of daunorubicin and the hydrazide groups of the carrier. Conjugates formed in this way were found to precipitate following the addition of daunorubicin and were not useful as targeting agents. Precipitation of IgG is a common problem encountered during drug conjugation to IgG. This is likely due to the low water solubility of many anti-

cancer drugs. It has been generally found that the solubility of the IgG, and hence recovery, decreases as the incorporation of drug increases.

### **Dextran**

Shih et al. (117) used dextran as a carrier for MTX and linked dextran-MTX to the carbohydrate moiety of a mAb. Dextran with an average MW of 40,000 was oxidized to PAD, converted to an amino group-containing polymer by reaction with 1,3-diamino-2-hydroxypropane and the Schiff base reduced with borohydride. MTX was coupled to the carrier using EDCI, and the dextran-MTX linked to periodate-oxidized mAb through Schiff base formation between unreacted amino groups on the carrier and aldehyde groups on the mAb. The Schiff bases were stabilized with cyanoborohydride and the conjugates isolated by gel filtration. An average of one carrier unit containing between 30 and 40 MTX was found in the isolated conjugate. Antibody activity in the conjugate approximated that of native mAb, and the conjugate was found to be as effective as free MTX against antigen-positive cells and approximately 100 times less cytotoxic to non-target cells indicating that specificity was conferred by the mAb.

### **Antibody-bound liposomes**

Chua et al. demonstrated that hydrazide groups could be incorporated into liposomal membranes and subsequently used for site-specific attachment to IgM carbohydrate residues (179). They showed that liposomes containing a dye as a marker were attached to IgM with retention of both liposome integrity and IgM antigen binding capacity. Such a system may prove useful for the targeting of drug molecules contained in the liposomes.

### **Antibody-bound toxins**

Vogel et al. (169) recently reported on the synthesis of two site-specific heterobifunctional spacers and used these to conjugate barley toxin to the carbohydrate of IgM. Although the conjugates synthesized were not intended for therapeutic purposes, the procedure illustrates this potential. The spacers which were used were based on the structure of SPDP and contained two different functional groups; a hydrazide and an activated disulfide. (One of the spacers reported by this group was independently synthesized in the present study.) The spacers were incorporated into oxidized IgM carbohydrate through a hydrazone bond to introduce activated disulfides. Barley toxin was modified to contain a thiol group by reaction with SPDP, and the thiol group deblocked and reacted with IgM. Conjugates were purified by gel filtration and contained an average of 3.3 mol barley toxin/mol IgM. Toxin activity was decreased as a result of conjugation to IgM. However, this was found to be due to the acylation of toxin amino groups by SPDP. IgM antigen binding activity was found to be comparable to that of native IgM. This method should prove to be useful for the site-specific linkage of a number of different proteins for the purpose of cancer therapy.

### **11. Project rationale and objectives**

The use of antibodies conjugated to drug-loaded carriers offers the potential to improve the effectiveness of drug-antibody conjugates as cancer treatment agents due to the greater loadings of drug which are possible, compared to direct drug-antibody conjugates. One of the shortcomings of the ternary conjugates which have been synthesized and evaluated for use as targeting agents was the failure to isolate a well characterized homogeneous product. In many cases, conjugates contained free antibody as well as a mixture of different conjugation products, limiting the validity of their evaluation as potential treatment agents.

In order to evaluate the therapeutic potential of these types of conjugates, conjugates constructed with MTX linked directly to a mAb were compared to those in which MTX was linked to a carrier using the same mAb. The carrier-based conjugates were synthesized using both non-site-specific and site-specific conjugation techniques, as the latter offers the further potential for producing conjugates with increased retention of antigen binding activity. Many methods are available for the non-site-specific linkage of the drug-loaded carrier to mAbs, but for the synthesis of site-specific conjugates, appropriate cross-linkers had to be synthesized and conditions for their use established to enable linkage of the carrier to the carbohydrate moiety of the mAb. The three types of conjugates (binary, non-site-specific ternary, and site-specific ternary) were isolated and evaluated with respect to their retention of antigen binding activity as well as cytotoxicity to target and non-target cell lines. Such a comparison between these different linkage methods using the same antibody has not been made in the past, and should prove useful in designing future drug-antibody conjugates.

## **II. Materials and Methods**

### **Materials**

Freund's incomplete adjuvant was from Gibco Laboratories, Grand Island, NY, USA.

Fetal calf serum and horse serum were from Flow Laboratories, McLean, VA, USA.

Bio-Gel P300, desalting columns, Bio-Gel P10, nitrocellulose, acrylamide, bis-acrylamide, ammonium persulfate, Coomassie Blue R-250, Coomassie Blue G-250, sodium dodecyl sulfate, Affi-Gel 102, Bio-Lyte 3/10 carrier ampholytes, goat anti-mouse IgG-peroxidase, isoelectric focusing standards, rabbit anti-HSA, Protein A binding buffer and Protein A elution buffer were from Bio-Rad Laboratories, Richmond, CA, USA.

Caprylic acid, Dulbecco's Modified Eagles Medium, Hank's buffered saline solution, pepsin, papain, chloramine T, sodium metabisulfite, 1-fluoro-2,4-dinitrophenyl benzene, human serum albumin, sodium cyanoborohydride, sodium borohydride, 4-chloro-1-naphthol,  $\gamma$ -maleimidobutyric acid succinimidyl ester, o-phenylenediamine, bovine serum albumin, dithiothreitol, methotrexate, dihydrofolate, dihydrofolate reductase, NADPH, extravidin-peroxidase, penicillin, streptomycin sulfate, thionin chloride, triethylamine, propionaldehyde, crystal violet, Tween 20, N-ethylmaleimide, N,N-di(2,4-dinitrophenyl)-L-cystine,  $\beta$ -mercaptoethanol, and biotin-hydrazide were from Sigma Chemical Co, St. Louis, MO, USA.

Sulfosuccinimidyl 6-(biotinamido)hexanoate was from Pierce, Rockford, IL, USA.

Rabbit serum was from Antibody Incorporated, Davis, CA, USA.

Hydrogen peroxide was from Fischer Scientific, Fairlawn, NJ, USA.

$^{125}\text{I}$  and  $^{131}\text{I}$  supplied as NaI in 0.1 M NaOH at 25 mCi/mL were from ICN, Mississauga, Ont.

Protein A-Sepharose, DEAE-Sepharose, and Pharmalyte 5-8 ampholytes were from Pharmacia Fine Chemicals, Uppsala, Sweden.

**N-hydroxysuccinimide, 11-aminoundecanoic acid, and N,N-dimethylformamide were from Aldrich Chemical Co., Milwaukee, WI, USA.**

**Dicyclohexylcarbodiimide was from Eastman Organic Chemicals, Rochester, NY, USA.**

**96 well Falcon ELISA plates were from Beckton Dickinson, Lincoln Park, NJ.**

**Sodium metaperiodate was from J.T. Baker Chemical Co., Phillipsburg, NJ.**

**<sup>1</sup>H NMR spectra were recorded in CDCl<sub>3</sub> on a Nicolet NT360NB spectrometer with shifts reported relative to tetramethylsilane.**

**TLC was performed on Merck-Kieselgel 60 analytical foil backed silica gel plates containing UV indicator (254nm). EDTA and TLC plates were from BDH, Dartmouth, NS.**

**Melting points were measured with an Electrothermal 9100 melting point apparatus.**

**Buffer A was 0.1 M sodium acetate, pH 4.0.**

## **Methods**

### **1. General Methods**

#### **1.1 Protein assays**

Protein concentration was determined either by the Lowry protein assay (180) or by measurement of absorbance at 280 nm using  $A_{280}$  of a 1.0 mg/mL solution of IgG = 1.4 (133,181), and  $A_{280}$  of a 1.0 mg/mL solution of HSA = 0.49, the latter value determined experimentally. For the Lowry assay, 10 to 30  $\mu$ g of protein in 0.2 mL was mixed with 1.0 mL of a solution containing 0.02% (w/v)  $\text{CuSO}_4$ , 0.04% (w/v) potassium tartrate, 2% (w/v)  $\text{Na}_2\text{CO}_3$  in 0.1 M NaOH. After 10 min, 0.1 mL of Folin-Ciocalteu phenol reagent diluted 1:2 in  $\text{dH}_2\text{O}$  was added while mixing and samples incubated at RT for 30 min, at which time the absorbance at 700 nm was measured. Standards used for determining unknown HSA and IgG concentrations were HSA and NRG, respectively, since these proteins are known to give different responses in the Lowry assay (181).

#### **1.2 Polyacrylamide gel electrophoresis**

The procedure of Laemmli (182) was followed for sodium dodecylsulfate polyacrylamide gel electrophoresis (SDS PAGE) using the Bio-Rad Mini-Protean II apparatus. Stacking gels were 3% (w/v) acrylamide and running gels varied from 6% (w/v) to 12% (w/v) acrylamide, depending on the sample to be analyzed. The thickness of the gels was 0.75 mm. Electrophoresis was carried out using a constant voltage of 200 V until the tracking dye reached the bottom of the gel. Native PAGE was carried out essentially by the same method as SDS PAGE, with the exception that SDS was omitted from samples, gels and running buffer. One to 2  $\mu$ g of protein were typically loaded per lane. Gels were stained with 0.1% (w/v) Coomassie Blue R-250 in 10% (v/v) acetic acid and 10% (v/v) isopropanol, and destained in the acetic acid/isopropanol solution.

### 1.3 Desalting

Low MW components were separated from proteins by gel filtration. For small volumes, prepacked columns (10 mL) were equilibrated with 20 mL of desired buffer and up to 1.5 mL of sample applied, followed by buffer. After collecting 1.5 mL of eluate, protein was collected in the following 2.5 mL fraction. For larger volumes, columns were packed with Bio-Gel P10 and samples desalted as with prepacked columns with the exception that the column effluent was monitored at 280 nm for collection of protein.

### 1.4 Iodination of proteins

Proteins were radiolabelled using the chloramine-T method (183). Proteins to be radiolabelled with  $^{131}\text{I}$  or  $^{125}\text{I}$  were equilibrated with 0.3 M sodium phosphate buffer, pH 7.3, to give a protein concentration of 1 to 2 mg/mL. Radioactive iodine, supplied as NaI in 0.1 M NaOH (typically at 25 mCi/mL), was neutralized with an equal volume of 0.1 M HCl. Using the experimentally observed iodination efficiencies of 30% for  $^{125}\text{I}$  and 50% for  $^{131}\text{I}$ , an amount of neutralized radioiodine calculated to give the desired specific activity, was added to the protein solution while stirring. Chloramine T, freshly dissolved in dH<sub>2</sub>O at 1 to 5 mg/mL, was added to the protein/iodine solution to give a final concentration of 100  $\mu\text{g}$  of chloramine T per mg protein. After 3 min, sodium metabisulfite, freshly dissolved in dH<sub>2</sub>O at 1 to 5 mg/mL, was added to give a concentration of 100  $\mu\text{g}$  sodium metabisulfite/mg protein and the protein solution desalted into PBS after 5 min. The protein concentration was determined either by the Lowry assay or by measurement of A<sub>280</sub> and radioactivity measured in a Beckman Gamma 4000 counter. Iodine incorporation was determined by comparison to a standard containing a known amount of radioiodine prepared at the time of protein iodination. Specific activities were calculated on the basis of these two measurements.

## **2. Cell lines**

The human renal cell carcinoma cell line Caki-1(184) was maintained in Dulbecco's Modified Eagles Medium (DME) containing 10% (v/v) fetal calf serum (FCS), 200 units/mL penicillin, 0.2 mg/100 mL streptomycin sulfate and 0.11% (w/v) sodium pyruvate. For propagation, cells attached to glass flasks were treated with 2 mL of 0.25% (w/v) trypsin in HBSS for 30 sec to release cells from glass, collected in 14 mL of PBS in plastic conical tubes, centrifuged at a setting of 3 on an IEC model CL clinical centrifuge (approximately 500 x g), and PBS decanted. Cells were dislodged from the bottom of tubes by gentle agitation, and taken up in growth medium. Cell clumps were broken up by repeated passage through a 1.5 inch x 22 gauge needle attached to a 3 mL syringe, and an aliquot counted in a Coulter model Zf cell counter. For routine subculturing of Caki-1 cells,  $1.5 \times 10^6$  cells were seeded in glass flasks containing 25 mL of growth medium and incubated at 37 °C in an atmosphere of 5% CO<sub>2</sub>.

The cell line D10-1, a human B-cell lymphoma, was maintained in culture as a suspension. D10-1 cells were subcultured in the same manner as Caki-1 cells described above with the exception that trypsin treatment was not required.

## **3. Production and isolation of IgG**

### **3.1 Hybridoma growth and ascites formation**

mAb K20, an IgG<sub>1</sub> mAb directed against a cell surface antigen on the renal cell carcinoma cell line, Caki-1, was obtained from hybridoma K20 (185). The K20 hybridoma was grown as a suspension in 96 mm plastic petri dishes in DME containing 10% (v/v) horse serum, collected by centrifugation (500 x g, 10 min) and resuspended in DPBS. The cells were washed twice and resuspended in DPBS at a density of  $30 \times 10^6$  cells/mL.

Balb/c mice were primed by injection (i.p.) with 0.1 mL of Freund's incomplete adjuvant 7 days prior to hybridoma injection. The K20 hybridoma was injected as a

suspension in DPBS ( $15 \times 10^6$  cells/mouse in 0.5 mL). After 7 to 10 days following hybridoma injection, ascites fluid was obtained from mice by insertion of a needle (25 gauge x 1.5 inch) into the peritoneal cavity and fluid collected by gravity into 15 mL glass screwcap tubes. Tubes were centrifuged in the IEC tabletop centrifuge at a setting of 6 for 20 min, supernatants pooled, heated at 56 °C for 40 min to inactivate complement, and frozen.

### **3.2 Purification of antibodies**

**Fractionation with caprylic acid.** IgG from ascites fluid and normal rabbit serum was isolated using the caprylic acid precipitation method described by McKinney and Parkinson (186), with minor modifications. Serum or ascites fluid was diluted with four volumes of 0.1 M sodium acetate buffer, pH 4.5, and caprylic acid (25  $\mu$ L/mL of diluted sample) was added dropwise while stirring at RT. After 30 min, the precipitate was removed by centrifugation (10,000 x g, 30 min), the supernatant diluted with 0.1 volume of 10 times concentrated PBS, adjusted to pH 7.4 with 1.0 M NaOH, and cooled to 4 °C. IgG was then precipitated by the addition of ammonium sulfate (60% saturation) while stirring for 30 min, and collected by centrifugation (10,000 x g, 15 min). The pellet was redissolved in a small volume of PBS and dialyzed against PBS at 4 °C for 3 days with 6 changes of buffer.

**Chromatography using Protein A-Sepharose.** Ascites fluid was diluted with two volumes of Protein A binding buffer and passed through a column of Protein A-Sepharose previously equilibrated with binding buffer. The column was washed with binding buffer until the absorbance at 280 nm returned to the baseline value, and the IgG fraction eluted with Protein A elution buffer. The eluted fraction was neutralized immediately with a small volume of 2.0 M Tris/HCl pH 9.0 and dialyzed against PBS at 4 °C for 3 days with 6 changes of buffer.

## **4. Characterization of mAb K20**

### **4.1 Determination of the immunoreactive fraction**

The immunoreactive fraction (IRF) of mAb K20 was measured using the method of Lindmo and Bunn (45) with some modifications. mAb K20 was radiolabelled with  $^{125}\text{I}$  as described in Section 1.4 to a specific activity of  $0.27 \mu\text{Ci}/\mu\text{g}$ . A non-specific monoclonal IgG<sub>1</sub> antibody (mAb IgG<sub>1</sub>) of unknown specificity was also labelled with  $^{125}\text{I}$  to approximately the same specific activity as mAb K20. Caki-1 cells were removed from flasks by treatment with 0.02% (w/v) EDTA in HBSS, washed twice with PBS, and resuspended in a small volume of growth medium. Two parallel serial 1:2 dilutions of Caki-1 cells were made with DME containing 10% FCS, and 0.2 mL of each diluted cell suspension added to glass 5 mL test tubes previously coated with 1% (w/v) BSA in PBS. An aliquot of cell suspension was counted in the cell counter to determine the number of cells in each dilution. To the first series of tubes was added 0.1 mL of radiolabelled mAb K20 (0.18  $\mu\text{g}$ , 0.049  $\mu\text{Ci}$ ) in PBS containing 1% BSA, and an equivalent amount of mAb IgG<sub>1</sub> in 0.1 mL was added to the second series. The amount of radioactivity added per tube was determined by counting 0.1 mL of both the mAb K20 and mAb IgG<sub>1</sub> solutions. Tubes were incubated for 1 h at 4 °C with shaking after which time tubes were centrifuged, the supernatant removed and cells resuspended in 2.0 mL of PBS containing 0.1% (w/v) BSA. The wash procedure was repeated twice and tubes were counted to determine cell-associated radioactivity. Non-specific binding as determined with the non-specific mAb IgG<sub>1</sub> preparation was subtracted from mAb K20 counts at each cell concentration, and the specific binding expressed as a fraction of total mAb K20 counts added. The IRF was determined by extrapolation to the ordinate from a plot of the inverse of the fraction bound against the inverse of cell concentration.

## **4.2 Determination of the number of binding sites per cell and the apparent affinity constant**

Caki-1 cells were removed from flasks by treatment with 0.02% (w/v) EDTA in HBSS, washed twice with PBS, and resuspended in DME containing 10% FCS at a density of  $4.56 \times 10^6$  cells/mL. A series of dilutions of  $^{125}\text{I}$ -mAb K20 (3.38  $\mu\text{Ci}/\mu\text{g}$ ) were made in PBS containing 0.2% (w/v) BSA (PBS/BSA) starting at an mAb K20 concentration of 2.56  $\mu\text{g}/\text{mL}$ . In glass test tubes previously coated with 2% (w/v) BSA in PBS was added 0.1 mL of Caki-1 cell suspension and 0.3 mL of an mAb K20 dilution. Assay tubes were incubated at 4 °C for 1 h with shaking, at which time cells were washed 3 times with PBS/BSA and cell-associated radioactivity measured in the gamma counter. The number of binding sites and the apparent affinity constant were determined by Scatchard analysis after correction for the IRF of mAb K20. The ratio of the amount of bound to free mAb K20 in each dilution was plotted against the amount of bound mAb K20. From the plot, the apparent  $K_a$  was determined from the negative slope, and the estimated extent of maximal binding determined by extrapolation to the abscissa.

## **4.3 Isoelectric focusing**

mAb K20 was analyzed by isoelectric focusing (IEF) under both native and urea-denatured conditions. For IEF in the presence of urea, the Bio-Rad Mini Protein cell was used and all urea-containing solutions were freshly prepared. Samples were dissolved in sample buffer containing 20 mM Tris/HCl, pH 8.2, and 8 M urea, and loaded on 5% (w/v) acrylamide gels cast to contain 7% (w/v) urea, 5% (v/v) Bio-Lyte 3/10 carrier ampholytes, and 10% (v/v) glycerol. Gels were prefocused for 30 min at 110 V, samples loaded and focused for 6 h at 200 V using 0.02 M NaOH and 0.01 M  $\text{H}_3\text{PO}_4$  as catholyte and anolyte respectively. Gels were stained using Coomassie Brilliant Blue G-250 (0.027% (w/v) in 3.5% (v/v) perchloric acid) and destained with 10% (v/v) acetic acid. For IEF under native conditions, gels were cast using the Bio-Rad Mini Protein system, but were run using an

LKB Multiphor horizontal system. Native IEF gels contained 5% (w/v) acrylamide, 6% (v/v) Pharmalyte 5-8, and 10% (v/v) glycerol, and were poured so as not to contain sample wells. Once polymerized, one plate from the sandwich was removed and the gel placed on the cooling stage of the LKB 2117 Multiphor apparatus previously cooled to 4 °C. Samples were applied directly to the gel by absorption through Whatman 3 MM filter paper, and gels were focused for 4 h at 500 V and 4 °C using 1.0 M NaOH as catholyte and 0.04 M glutamic acid as anolyte. Gels were fixed in 4% (w/v) sulfosalicylic acid and 12% (w/v) TCA for 1 h, then stained with a solution containing 0.5% (v/v) CuSO<sub>4</sub>, 0.04% (w/v) Coomassie Blue R-250, 7% (v/v) ethanol, and 10% (v/v) acetic acid for 2 h and destained in the same solution without Coomassie Blue.

## **5. Coupling of MTX to HSA**

### **5.1 Synthesis of MTX-AE**

Stock solutions of MTX (25 mM), DCC (200 mM) and NHS (200 mM) were prepared in DMF and appropriate volumes of each mixed to give the desired reactant ratios and a final MTX concentration of 12.5 mM. The reaction mixtures were stirred at RT for 16 h, cooled to -20 °C, filtered through glass wool to remove precipitated dicyclohexylurea, and the MTX concentration determined spectrophotometrically using  $\epsilon = 7000 \text{ cm}^{-1}\text{M}^{-1}$  at 370 nm for free MTX (71). An aliquot of each MTX-AE preparation was diluted in PBS (approximately 0.15  $\mu\text{mol}$  in 0.5 mL), passed slowly through a column containing 1 mL of Affi-Gel 102 previously equilibrated with PBS, and the column washed with 5.0 mL of PBS to remove unbound MTX. The amount of MTX eluted from the column was determined spectrophotometrically, and the percentage bound taken to be the amount of activated MTX in the preparation. Affi-Gel 102 contains 15  $\mu\text{mol}$  of amino groups per mL of gel, and typically 0.15  $\mu\text{mol}$  of MTX was passed through the column to ensure an excess of amino groups over MTX.

MTX reaction mixtures prepared using different ratios of MTX:NHS:DCC were also analyzed by TLC. Samples of reaction mixtures after 1 h and 24 h were mixed with an equal volume of methanol before application to TLC plates, and plates developed using a 3:2 CHCl<sub>3</sub>/DMSO system.

The MTX-AE was isolated from some reaction mixtures as follows. The cooled reaction mixture was filtered through glass wool, and the MTX-AE in a small volume of DMF precipitated by the slow addition of 25 mL of diethyl ether while stirring. The precipitate was collected by centrifugation (12,000 x g, 10 min) and redissolved in a small volume of DMF. The procedure was repeated and the ether in the final pellet removed with a stream of nitrogen and the MTX-AE dissolved in DMF.

## 5.2 Incorporation of MTX-AE into HSA

**Effect of molar ratio of MTX-AE over HSA.** MTX-AE was prepared by mixing MTX, DCC, and NHS in a molar ratio of 1:3:3 in DMF (90  $\mu$ mol of MTX in 2.0 mL) and the reaction mixture stirred at RT for 16 h, after which the solution was cooled to -20 °C and the precipitate removed by filtration. The amount of activated MTX in the preparation was determined using Affi-Gel 102 as described in Section 5.1, and was found to be 82%. The MTX-AE in DMF was added dropwise to HSA (10 mg, 1.0 mL PBS) while stirring to give a molar excess of MTX-AE over HSA between 8- and 80-fold, and a final concentration of HSA of 8.1 mg/mL. The solutions were stirred slowly at 4 °C for 4 h, centrifuged to remove precipitate (12,000 x g, 15 min), and dialyzed against PBS. The molar incorporation of MTX into HSA was determined using  $\epsilon = 6500 \text{ cm}^{-1}\text{M}^{-1}$  for protein bound MTX (117) at 370 nm, and HSA concentration determined using the Lowry assay with HSA as the standard.

**Effect of pH .** The effect of pH on MTX incorporation into HSA was determined between pH 7.2 and 9.0. The MTX-AE preparation was obtained by reacting

MTX, NHS, and DCC in a molar ratio of 1:3:3 as follows. MTX (14.1 mg, 31  $\mu\text{mol}$ ), DCC (19.1 mg, 93  $\mu\text{mol}$ ), and NHS (10.7 mg, 93  $\mu\text{mol}$ ) were added to 1.0 mL of DMF and stirred at RT for 18 h, the mixture cooled at  $-20\text{ }^{\circ}\text{C}$ , and the precipitate removed by filtration. The percentage of activated MTX in the preparation was found to be 83% using Affi-Gel 102 (Section 5.1). To HSA (3.6 mg/mL, 1.0 mL) in either PBS or 0.5 M Tris/HCl in the pH range of 7.2 to 9.0, was added an 80-fold molar excess of MTX-AE in 132  $\mu\text{L}$  of DMF while stirring. The solutions were stirred for 4 h at  $4\text{ }^{\circ}\text{C}$ , dialyzed against PBS, and centrifuged to remove any precipitate. The molar incorporation of MTX in HSA at each pH was determined as described in Section 5.2.

**Routine synthesis of HSA-MTX.** For the routine synthesis of HSA-MTX, MTX-AE was prepared by reacting MTX with DCC and NHS in a 1:3:3 molar ratio (MTX/DCC/NHS), and the MTX-AE partially purified from the reaction mixture as described in Section 5.1. To a solution of HSA (10 to 20 mg/mL) in 0.15 M Tris/HCl, pH 9.0, was added DMF to a concentration of 20% (v/v) followed by an 80-fold molar excess of MTX-AE in DMF while stirring to give a final DMF concentration of 35% (v/v). The pH was adjusted to 9.0 with 0.1 M NaOH and the solution left at RT for 2 to 3 h with occasional stirring. HSA-MTX was then desalted into the appropriate buffer.

### 5.3 Incorporation of MTX into HSA using EDCI

MTX was coupled to HSA using EDCI to activate MTX for reaction with protein amino groups(107,108). To 1.0 mL of HSA (6.5 mg/mL, 97 nmol) in PBS was added MTX (4.4 mg, 9.7  $\mu\text{mol}$ ) followed by EDCI (2.8 mg, 14.5  $\mu\text{mol}$ ) giving a molar ratio of 1:100:150 (HSA:MTX:EDCI). The mixture was stirred at  $4\text{ }^{\circ}\text{C}$  for 4 h, centrifuged at  $12,000 \times g$  for 30 min, dialyzed against PBS to remove unreacted EDCI and MTX, and centrifuged to remove any precipitate. The molar incorporation of MTX into HSA was determined as described in Section 5.2.

## **6. Direct incorporation of MTX into IgG**

MTX was coupled to mAb K20 using the same active ester method with the exception that MTX was activated using a 1:1:1 ratio of MTX:DCC:NHS instead of a 1:3:3 ratio which was used for HSA coupling. The 1:1:1 ratio was used in direct coupling because high incorporations of MTX were not desired unlike the case of MTX reaction with HSA. The molar excess of MTX over IgG varied and was dependent on the molar incorporation desired. To mAb K20 in PBS at 5 to 10 mg/mL, was added DMF dropwise to a concentration of 10% (v/v) followed by an excess of filtered MTX-AE in DMF ranging from 5- to 50-fold over IgG while stirring to give a final DMF concentration of 20%. The solution was left at RT for 2 h after which time it was desalted into PBS.

## **7. Activation of HSA for conjugation to IgG**

### **7.1 Direct reduction of HSA with DTT.**

Direct reduction of HSA was accomplished by the addition of an excess of DTT. To HSA at 10 mg/mL in PBS, was added DTT in dH<sub>2</sub>O while stirring to give a range of molar excess from zero to 20. Samples were left at RT for 30 min, desalted into PBS, and the thiol content determined. The thiol content of HSA was measured using DTNB as follows. To 1.0 mL of 0.1 M sodium phosphate, pH 7.3, containing 1 mM EDTA, in a 1.0 mL cuvette was added 100  $\mu$ L of a stock DTNB solution (10 mM in 0.1 M phosphate, pH 7.3, 1 mM EDTA) and either 100  $\mu$ L of sample to be assayed in PBS or 100  $\mu$ L of PBS, and the contents of the cuvette mixed by inversion. After 15 min, the absorbance of the sample cuvette was measured relative to the reference at 412 nm and the thiol concentration in the sample determined using  $\epsilon = 14,150 \text{ cm}^{-1}\text{M}^{-1}$  (131,187). The protein concentration was measured by the Lowry assay and the number of moles of thiol per mole of HSA calculated for the sample.

## **7.2 Incorporation of thiols into HSA using SPDP.**

To react HSA with SPDP, SPDP dissolved in a small volume of DMF was added to HSA at a concentration of 5 to 10 mg/mL in PBS while stirring to give a 5- to 10-fold molar excess of SPDP over HSA. After 30 min, the solution was desalted into 0.1 M sodium acetate, pH 4.5, 0.15 M NaCl and DTT added to a concentration of 50 mM. The solution was desalted into 0.1 M phosphate, pH 7.3, 1 mM EDTA after 20 min. SPDP incorporation was determined by measuring the absorbance at 343 nm of an aliquot of HSA-SPDP in the presence of 100 mM DTT using  $\epsilon = 8080 \text{ cm}^{-1}\text{M}^{-1}$  for pyridine-2-thione (133) and the HSA concentration measured using the Lowry assay with HSA as standard or by measurement of A<sub>280</sub> using the following correction for pyridyldithio group contribution to A<sub>280</sub>:  $A_{280} \text{ actual} = A_{280} \text{ measured} - 5100 \times [\text{pyridine-2-thione}]$ , where the pyridine-2-thione concentration is the molar concentration determined in the presence of 100 mM DTT.

## **8. Synthesis of MTX-HSA-SPDP for conjugation to IgG**

To HSA (200 mg, 3.0  $\mu\text{mol}$ ) in 20 mL of PBS was added SPDP (9.6 mg, 30  $\mu\text{mol}$ ) in 2.0 mL of DMF while stirring at RT. After 30 min, DMF was added to a concentration of 20% (v/v), followed by 2.0 M Tris/HCl, pH 9.0, and a 75-fold molar excess of partially purified MTX-AE in DMF to give final concentrations of 0.1 M Tris/HCl, 35% DMF and 6.8 mM MTX. The pH was adjusted to pH 9.0 with 0.1 M NaOH and the solution left at RT for 2.5 h with occasional stirring. While stirring, 35 mL of PBS was then added, followed by the dropwise addition of a sufficient volume of 2.0 M sodium acetate, pH 4.0, to lower the pH of the reaction mixture to 4.5. The precipitated MTX-HSA-SPDP was collected by centrifugation (10,000 x g, 15 min), the pellet redissolved in 0.5 M Tris/HCl, pH 9.0, and MTX-HSA-SPDP equilibrated with PBS. The MTX-HSA-SPDP monomer was purified from MTX-HSA-SPDP polymers by gel filtration chromatography on Bio Gel P-300 (2.5 cm x 90 cm, 7.5 mL/h). The monomer

was concentrated by precipitation at pH 4.5 as described above, and equilibrated with 0.1 M sodium phosphate, pH 7.3, 1 mM EDTA.

## **9. Synthesis of non-site-specific IgG-HSA and IgG-HSA-MTX conjugates**

### **9.1 Incorporation of SPDP and GMBS spacers into IgG**

mAb IgG<sub>1</sub> and mAb K20 were reacted with SPDP as described in Section 7.2 using a 5- to 10-fold molar excess of SPDP over IgG. Maleimide groups were introduced into IgG by reaction of IgG with GMBS under the same conditions as for reaction with SPDP.

The number of maleimide groups introduced into IgG by reaction with GMBS was determined with N-(2,4-dinitrophenyl)-L-cysteine (DNP-cys). DNP-cys was prepared by the addition of mercaptoethanol (100  $\mu$ L, 1.5 mmol) to N,N-di-(2,4-DNP)-L-cystine (4.0 mg, 7.0  $\mu$ mol) dissolved in 1.7 mL of acetone and 0.2 mL dH<sub>2</sub>O. The solution was stirred at RT for 2 h, mercaptoethanol removed by evaporation with nitrogen, aliquoted, and DNP-cys stored at -20 °C covered in foil. To assay for protein maleimide groups, a 100-fold molar excess of DNP-cys over IgG was dissolved in a small volume of DMF and added to protein in PBS while stirring. After 30 min at RT, the solution was desalted into PBS and the incorporation of DNP-cys determined spectrophotometrically using  $\epsilon = 17\ 000\ \text{cm}^{-1}\text{M}^{-1}$  (138) at 360 nm for DNP-cys. The protein concentration was measured using the Lowry assay with NRG as standard.

### **9.2 Non-site-specific conjugation of spacer-derivatized IgG to HSA and HSA-MTX**

For synthesis of non-site-specific IgG-HSA-MTX ternary conjugates, IgG-SPDP was equilibrated with 0.1 M sodium acetate, pH 4.5, 0.15 M NaCl following reaction of IgG with SPDP, and DTT added to a concentration of 20 mM. After 20 min at RT, the solution was desalted into 0.1 M sodium phosphate, pH 7.3, 1 mM EDTA, and MTX-

HSA-SPDP (Section 8) added to give a two-fold molar excess of HSA over IgG. After 16 h at RT, a 100-fold molar excess of N-ethylmaleimide over IgG was added in a small volume of DMF to block free thiols.

For the synthesis of non-site-specific IgG-HSA binary conjugates, IgG-SPDP or IgG-GMBS were equilibrated with 0.1 M sodium phosphate, pH 7.3, 1 mM EDTA and reacted with HSA-SPDP-SH (Section 7.2). HSA-SPDP-SH was added at a ratio of 2 HSA/IgG. After 16 h at RT, a 100-fold molar excess of N-ethylmaleimide over HSA was added to block free thiols.

## **10. Synthesis of heterobifunctional site-specific spacers**

### **10.1 Synthesis of SPDP**

SPDP (N-Succinimidyl 3-[2-pyridyldithio]-propionate) was synthesized using the method of Carlsson(133) with minor modifications. The TLC system used in all the following procedures was 9:1 chloroform:methanol unless stated otherwise. To 2,2'-dipyridyldisulfide (3.75 g, 17 mmol) dissolved in 15 mL ethanol containing 0.4 mL glacial acetic acid was added 3-mercaptopropionic acid (0.9 g, 0.74 mL, 8.5 mmol) dropwise in 5 mL ethanol. The reaction mixture was stirred vigorously for 10 h at RT after which time the ethanol was removed by evaporation and the pale oil taken up in dichloromethane/ethanol (3:2) and added to ca. 50 g of alumina in suspension in dichloromethane/ethanol (3:2) in a beaker while stirring. The solvent was removed by filtration and the alumina washed with dichloromethane/ethanol (3:2). The washing was repeated until TLC showed no starting material remaining in the wash. The product, 2-carboxyethyl 2-pyridyl disulfide, was then eluted from the alumina using 4 mL acetic acid in 100 mL of dichloromethane/ethanol (3:2). The solvent was evaporated and the acetic acid removed under vacuum to give 1.30 g (6.0 mmol, yield 71%) of oil. N-hydroxysuccinimide (0.76 g, 6.6 mmol) and dicyclohexylcarbodiimide (1.36 g, 6.6 mmol) were added to the oil which was dissolved in 5 mL of dichloromethane, and the reaction

mixture stirred for 2 h at RT. The mixture was cooled to -20 °C, the precipitate removed by filtration and the dichloromethane washed with saturated sodium bicarbonate, then water, dried with sodium sulfate, dichloromethane evaporated and SPDP crystallized from ethanol at 4 °C. The crystals were collected by filtration and dried under vacuum. Yield 1.5 g, 56%; Rf 0.84. <sup>1</sup>H NMR δ 2.83 (s, 4H), 3.13 (m, 4H), 7.13 (m, 1H), 7.69 (m, 2H), 8.50 (m, 1H).

## 10.2 Synthesis of HPDP

To SPDP (1.0 g, 3.2 mmol) dissolved in 20 mL of methanol was added 160 μL of hydrazine (4.8 mmol) in 5 mL of methanol. The reaction mixture was stirred at RT for 15 min, methanol removed under reduced pressure, the oil taken up in methylene chloride and extracted first with saturated sodium bicarbonate followed by water, dried with sodium sulfate and the methylene chloride evaporated. The product was crystallized from diethyl ether to give a fine white powder. The product reacted with both acetone and DTT as followed by TLC, confirming the presence of the hydrazide and disulfide functions. Yield 0.20 g, 27%; mp 91.5-92.5 °C; Rf 0.41. <sup>1</sup>H NMR δ 2.62 (t, 2H), 3.10 (t, 2H), 3.98 (s, 2H), 7.14 (m, 1H), 7.62 (m, 2H), 8.24 (s, 1H), 8.52 (m, 1H).

## 10.3 Synthesis of AUPDP

**11-[3-(2-pyridyldithio)propionyl]aminoundecanoic acid.** To 11-aminoundecanoic acid (129 mg, 0.64 mmol) and sodium bicarbonate (108 mg, 1.28 mmol) dissolved in 2 mL of a 2:1 water-ethanol mixture, was added SPDP (200 mg, 0.64 mmol) in 4 mL of ethanol. The solution was stirred at RT for 1 h, adjusted to pH 7.0 with 1 M HCl, and the solvent removed under reduced pressure, the residue distributed between water and chloroform, extracted with water, and dried over sodium sulfate. Chloroform was evaporated to give a white powder. Hydrolysis of the product with 7 M HCl at 50 °C for 16 h confirmed the presence of 11-aminoundecanoic acid in the product as

determined by TLC of the hydrolyzate (4:1:1 n-butanol/acetic acid/ H<sub>2</sub>O). Yield 232 mg, 91%; R<sub>f</sub> 0.46.

#### **11-[3-(2-pyridyldithio)propionyl]aminoundecanoic acid hydrazide.**

To 11-[3-(2-pyridyldithio)propionyl]aminoundecanoic acid (232 mg, 0.58 mmol) dissolved in 5 mL of methylene chloride was added NHS (73 mg, 0.64 mmol) and DCC (131 mg, 0.64 mmol). The mixture was stirred for 2 h at RT, cooled to -20 °C, dicyclohexylurea removed by filtration, and methylene chloride evaporated. To 11-[3-(2-pyridyldithio)propionyl]aminoundecanoic acid succinimidyl ester (284 mg, 0.58 mmol, R<sub>f</sub> 0.64) dissolved in 5 mL of methanol was added hydrazine (37  $\mu$ L, 1.16 mmol) dissolved in a small amount of methanol and the solution stirred for 1 h at RT. Methanol was removed by evaporation, the residue taken up in methylene chloride and extracted with saturated sodium bicarbonate then with saturated NaCl, dried over sodium sulfate, evaporated, and the solid washed with ether to give a white powder. The product reacted with both acetone and DTT, indicating the presence of both hydrazide and disulfide functions. Yield 160 mg, 61%; mp 105 °C; R<sub>f</sub> 0.32. <sup>1</sup>H NMR  $\delta$  1.22 (s, 18H), 1.51 (p, 2H), 1.62 (p, 2H), 2.50 (t, 2H), 2.60 (t, 2H), 3.08 (t, 2H), 3.26 (q, 2H), 3.96 (bs, 2H), 6.50 (s, 1H), 7.13 (q, 1H), 7.20 (s, 1H), 7.66 (m, 2H), 8.45 (m, 1H).

#### **10.4 Synthesis of DNP-AU-hydrazide**

**11-aminoundecanoic acid methyl ester.** To 4 mL of methanol at -10 °C (ethanol/ice bath) with stirring was added thionyl chloride (1.04 mL, 14 mmol) followed by the slow addition of 11-aminoundecanoic acid (800 mg, 4 mmol). After addition, the solution was stirred at RT for 1 h after which time two volumes of diethyl ether were added and the white precipitate isolated by filtration.

**11-(2,4-dinitrophenyl)aminoundecanoic acid methyl ester.** To 11-aminoundecanoic acid methyl ester hydrochloride (150 mg, 600  $\mu\text{mol}$ ) and triethylamine (167  $\mu\text{L}$ , 1.2 mmol) in 10 mL of DMF was added 1-fluoro-2,4-dinitrobenzene (68  $\mu\text{L}$ , 540  $\mu\text{mol}$ ) and the reaction mixture stirred at RT for 1 h. The DMF was removed by evaporation, the residue taken up in chloroform, extracted with 0.1 M HCl, washed with saturated NaCl, dried with sodium sulfate and evaporated. The product was dried with ether to give a yellow powder. Yield 155 mg, 75%; Rf 0.96 in 19:1  $\text{CHCl}_3$ /methanol.  $^1\text{H}$  NMR  $\delta$  1.29 (s, 10H), 1.46 (m, 2H), 1.60 (m, 2H), 1.78 (p, 2H), 2.33 (t, 2H), 3.44 (q, 2H), 3.68 (s, 3H), 6.94 (d, 1H), 8.28 (d, 1H), 8.58 (bs, 1H), 9.15 (t, 1H).

**11-(2,4-dinitrophenyl)aminoundecanoic acid hydrazide.** To 11-(2,4-dinitrophenyl)aminoundecanoic acid methyl ester (130 mg, 341  $\mu\text{mol}$ ) in 50 mL of methanol was added hydrazine (5.2 mL, 166 mmol) and the reaction mixture stirred for 16 h at RT at which time TLC showed complete conversion to product. The methanol was removed by evaporation, the residue taken up in chloroform, extracted with saturated sodium bicarbonate, dried with sodium sulfate and evaporated to give a yellow powder. Yield 117 mg, 90%; mp 119-121  $^\circ\text{C}$ ; Rf 0.17 in 19:1  $\text{CHCl}_3$ /methanol;  $\lambda_{\text{max}} = 360 \text{ nm}$ ;  $\epsilon = 17,000 \text{ M}^{-1}\text{cm}^{-1}$  (138).  $^1\text{H}$  NMR  $\delta$  1.30 (s, 10H), 1.43 (p, 2H), 1.63 (m, 2H), 1.77 (p, 2H), 2.15 (t, 2H), 3.41 (q, 2H), 3.90 (bs, 2H), 6.66 (bs, 1H), 6.92 (d, 1H), 8.28 (dd, 1H), 8.56 (bs, 1H), 9.16 (t, 1H).

## **11. Synthesis of site-specific IgG-HSA and IgG-HSA-MTX conjugates**

### **11.1 Oxidation of IgG with sodium periodate**

IgG was oxidized with sodium periodate using 100 to 150 mM periodate for conjugation of IgG with HSA or HSA-MTX, and 0.26 to 260 mM periodate for spacer incorporation studies. To IgG (5 to 10 mg/mL) in 0.1 M sodium acetate, pH 5.5, 0.15 M NaCl at 0  $^\circ\text{C}$  was added a suitable excess of sodium meta-periodate (100 mg/mL in  $\text{dH}_2\text{O}$ )

while stirring. The solution was left for 20 min in the dark at 0 °C after which it was desalted into 0.1 M sodium acetate, pH 4.0.

### **11.2 Incorporation of HPDP and AUPDP spacers into oxidized IgG**

To oxidized IgG in 0.1 M sodium acetate, pH 4.0 was added DMF while stirring to a concentration of 15% (v/v), followed by the addition of either HPDP or AUPDP dissolved in DMF to give a final DMF concentration of 25% and a 50-fold molar excess of spacer over IgG. After 3 h at RT the solution was either desalted into 0.1 M sodium phosphate, pH 7.3, 1 mM EDTA for conjugation, or 0.1 M sodium acetate, pH 4.0 for stabilization with sodium cyanoborohydride. The number of spacers introduced into IgG were determined as described for SPDP incorporation in Section 7.2.

### **11.3 Site-specific conjugation of spacer-derivatized IgG to HSA and HSA-MTX**

For comparison of conjugation efficiency between IgG-HPDP and IgG-AUPDP with various derivatives of HSA, IgG-HPDP or IgG-AUPDP in 0.1 M sodium phosphate, pH 7.3, 1 mM EDTA were reacted with a four-fold molar excess of either HSA-SH, HSA-SPDP-SH (Section 7), MTX-HSA-SH (Section 5.2), or MTX-HSA-SPDP-SH (Section 8). The latter derivatives of HSA were prepared by direct reduction of the parent compound in PBS (20-fold excess DTT, 20 min). After 16 h free thiols were blocked by the addition of a 100-fold molar excess of N-ethylmaleimide over HSA and reaction mixtures analyzed by native PAGE.

For the synthesis of stable ternary conjugates, IgG-AUPDP was stabilized by reduction with sodium cyanoborohydride. To IgG-AUPDP (Section 11.2) in 0.1 M sodium acetate, pH 4.0 was added sodium cyanoborohydride in dH<sub>2</sub>O to a concentration of 15 mM. After 90 min at RT, DTT in dH<sub>2</sub>O was added to a concentration of 15 mM, the solution desalted into 0.1 M sodium phosphate, pH 7.3, 1 mM EDTA after 15 min and

HSA-SPDP-MTX added at a ratio of 2 mol HSA/mol IgG. After 16 h a 100-fold molar excess of N-ethylmaleimide over IgG was added to block unreacted thiols.

For synthesis of stabilized binary mAb K20-HSA conjugates, mAb K20-AUPDP in 0.1 M sodium phosphate, pH 7.3, 1 mM EDTA was mixed with HSA-SPDP-SH (Section 7.2) at a ratio of 2 mol HSA/mol IgG. After 16 h at RT, N-ethylmaleimide was added as above, followed by sodium cyanoborohydride to a concentration of 15 mM. After 90 min at RT, the solution was desalted into PBS.

## **12. Stability of site-specific conjugates**

### **12.1 Native PAGE and elution of conjugates from the gels**

Conjugation mixtures were prepared using mAb K20 modified with either HPDP or AUPDP (Section 11.2), and GMBS or SPDP (Section 9.2) by reaction of mAb K20-spacer with HSA-SPDP-SH as described in Section 11.3. Reaction mixtures were separated by native PAGE on 5% gels using a preparative comb in a Bio Rad Mini-Protean II apparatus with gels of 0.75 mm thickness. Samples containing between 150 and 260  $\mu$ g of mAb K20 were mixed with an equal volume of sample buffer and loaded onto gels. After electrophoresis, a narrow strip from the edge of the gel was cut out, stained, and used as a reference to cut out the remaining conjugate-containing band from the gel. The electroelution apparatus consisted of two reservoirs connected by dialysis bags in each reservoir and a bridge between the two bags. The reservoir, dialysis bags and bridge were filled with 50 mM Tris/HCl, pH 8.6, with the gel-containing bag in the cathode compartment. Elution conditions were 100 V for 7 h, after which the collection bags were removed, and eluted conjugates dialyzed against 50 mM  $\text{NH}_4\text{CO}_3$ , lyophilized, and analyzed by SDS PAGE.

## **12.2 Dialysis of IgG containing DNP-AU-hydrazide as a reporter group**

Site-specific IgG-DNP-AU-hydrazide was prepared as follows: to NRG (25 mg, 167 nmol) in 2.1 mL of 0.1 M sodium acetate buffer, pH 5.5, containing 0.15 M NaCl at 0 °C was added sodium periodate dissolved in 0.8 mL dH<sub>2</sub>O (100 mg, 334 μmol) while stirring. The reaction mixture was kept in the dark for 20 min at 0 °C after which time it was desalted into 0.1 M sodium acetate buffer, pH 4.0 (Buffer A). To 4 mL of oxidized NRG was added 706 μL of DMF while stirring followed by DNP-AU-hydrazide (6.4 mg, 16.7 μmol) in 627 μL DMF to give a final DMF concentration of 25% (v/v). The reaction mixture was kept in the dark for 4 h after which it was desalted into Buffer A. Reporter group-containing NRG was either treated with 15 mM sodium cyanoborohydride, 15 mM sodium borohydride, or not treated. After 48 h at RT, solutions were desalted into Buffer A, dialyzed at 37 °C, samples taken over a period of 11 days and the number of DNP-AU-hydrazide groups/NRG determined. Protein concentration was measured by the Lowry assay using NRG as the standard and the DNP-reporter group measured at 360 nm using  $\epsilon = 17,000 \text{ cm}^{-1}\text{M}^{-1}$  (138). Control reactions were carried out in which i) a 100-fold molar excess of DNP-AU-OMe was added to oxidized NRG in Buffer A, and ii) a 100-fold molar excess of DNP-AU-hydrazide was added to non-oxidized NRG in Buffer A. After 4 h at RT the mixtures were desalted into Buffer A and the number of reporter groups/NRG determined as above.

To determine the effect of cyanoborohydride treatment prior to reaction with DNP-AU-hydrazide, oxidized NRG in Buffer A was treated with a molar excess of sodium cyanoborohydride ranging from 0 to 4,000 (0 to 110 mM). The reaction mixtures were left at RT for 48 h after which time they were desalted into Buffer A, reacted with DNP-AU-hydrazide (100-fold molar excess) for 4 h, desalted into Buffer A and the incorporation of DNP-AU-hydrazide determined.

### **12.3 Competitive release of DNP-AU-hydrazide with propanal**

Oxidized NRG containing DNP-AU-hydrazide prepared as described in Section 12.2 was either treated with 15 mM sodium cyanoborohydride or sodium borohydride for 48 h, or not treated. Each reaction mixture was desalted into Buffer A and a 10,000-fold molar excess of propanal over IgG added (80 mM) in a small volume of DMF. After 48 h at RT, reaction mixtures were desalted into Buffer A and the incorporation of reporter groups determined.

### **12.4 Time required for hydrazone stabilization by cyanoborohydride**

NRG containing hydrazone-linked reporter groups was prepared as in Section 12.2 and treated with 15 mM sodium cyanoborohydride. Samples were taken over a 26 h period, desalted into Buffer A and propanal added as above. After 24 h, each solution was desalted into Buffer A and the incorporation of DNP groups/NRG determined.

## **13. Purification of conjugates**

### **13.1 Binary mAb K20-HSA conjugates**

mAb K20-HSA binary conjugates were purified from the conjugation mixtures by gel filtration chromatography on Bio Gel P300 (2.5 cm x 90 cm) equilibrated with PBS using an upward flow system with a flow rate of 7.5 mL/h. Fractions collected were either 3.75 mL or 7.5 mL and were analyzed by SDS PAGE for purity of conjugates. Conjugation mixtures were concentrated prior to gel filtration by ammonium sulfate precipitation (60% saturation), centrifuged (10,000 x g, 20 min), the precipitate redissolved in a small aliquot of PBS and desalted into PBS.

### **13.2 Ternary mAb K20-HSA-MTX conjugates**

mAb K20-HSA-MTX ternary conjugates were purified by the same method as the binary conjugates with the exception of an initial step using DEAE-Sepharose.

Conjugation reaction mixtures were passed through a column containing DEAE-Sepharose previously equilibrated with PBS and washed with PBS containing 0.15 M NaCl until the absorbance at 280 nm returned to baseline. MTX-containing species were eluted from the column using PBS containing 1.0 M NaCl and concentrated by the addition of a volume of 2.0 M sodium acetate pH 4.0 sufficient to lower the pH to 4.5. The precipitate was centrifuged (12,000 x g, 10 min) redissolved in a small volume of 0.5 M Tris/HCl, pH 9.0, equilibrated with PBS, and separated on Bio Gel P300 as described for binary conjugates above.

#### **14. Characterization of conjugates**

##### **14.1 Measurements of antibody activity**

**Antibody activity by ELISA.** Caki-1 cells in DME containing 10% (v/v) FCS were plated in 96 well ELISA plates 96 h before use (5000 cells/well in 0.2 mL). Cells were fixed with 0.5% (v/v) glutaraldehyde in PBS for 1 min and washed 3 times with PBS. All subsequent washes were 3 times with PBS containing 0.1% BSA (PBS/BSA). Serial 1:2 dilutions of native mAb K20 or modified mAb K20 in PBS/BSA were added to wells in a volume of 100  $\mu$ L in triplicate, incubated with cells for 1 h, washed, and 100  $\mu$ L of goat anti-mouse IgG-peroxidase conjugate (1:3000 in PBS/BSA) added for 1 h. Plates were then washed, and 100  $\mu$ L of o-phenylenediamine at 0.4 mg/mL in 50 mM citrate/25 mM phosphate buffer pH 5.0, containing 0.015% (v/v) H<sub>2</sub>O<sub>2</sub> added per well. After 5-15 min the reaction was stopped by the addition of 100  $\mu$ L of 2.5 M H<sub>2</sub>SO<sub>4</sub> and the absorbance at 490 nm measured using a Bio Rad model 3550 ELISA Plate Reader. Native mAb K20 binding was compared to modified mAb K20 by plotting A<sub>490</sub> against the concentration of mAb K20 added. Percent binding activity was determined using the following formula:  $IC_{50} \text{ native mAb K20} / IC_{50} \text{ test mAb K20} \times 100$ , where  $IC_{50}$  is the concentration of antibody required to give half the saturation A<sub>490</sub>.

**Antibody activity by competition with  $^{125}\text{I}$ -mAb K20.**  $^{125}\text{I}$ -mAb K20 (3.38  $\mu\text{Ci}/\mu\text{g}$ , 0.52  $\mu\text{g}$ ) in PBS containing 0.1% (w/v) BSA (PBS/BSA) was mixed in duplicate with dilutions (in PBS/BSA) of either native mAb K20, site-specific mAb K20-HSA conjugate, or non-site-specific mAb K20-HSA conjugate in a volume of 0.3 mL to give a range of unlabelled mAb K20 between 0.20  $\mu\text{g}$  to 4.0  $\mu\text{g}$  per tube. Control tubes containing no competing unlabelled antibody were also prepared. Tubes were previously blocked with PBS containing 1% BSA and cooled to 4 °C prior to addition of cells. Caki-1 cells were removed from flasks by treatment with 0.02% (w/v) EDTA in HBSS, washed with PBS, resuspended in PBS/BSA and  $5.0 \times 10^5$  cells in 0.1 mL added to each tube. Cells were incubated at 4 °C with occasional shaking, and after 2 h tubes centrifuged, the supernatant removed and cells resuspended in 2.0 mL PBS containing 1% BSA. The wash procedure was repeated twice and tubes counted for radioactivity in the gamma counter. Conjugates of mAb K20 were compared to native mAb K20 by plotting the percentage of label bound against the amount of unlabelled mAb K20 added. The percent inhibition of  $^{125}\text{I}$ -mAb K20 binding was determined using the formula:  $(1 - \text{cpm bound in presence of noniodinated mAb K20} / \text{cpm bound in absence of noniodinated mAb K20}) \times 100$ . Percent activity of mAb K20 conjugates was determined using the formula:  $\text{IC}_{50} \text{ native mAb K20} / \text{IC}_{50} \text{ conjugated mAb K20} \times 100$ , where  $\text{IC}_{50}$  is the concentration of noniodinated mAb K20 required to give 50% inhibition of iodinated mAb K20 binding.

**Antibody activity by competition with mAb K20-biotin.** Caki-1 cells in DME containing 10% (v/v) FCS were plated in 96 well ELISA plates 96 h before use (5000 cells/well in 0.2 mL). Cells were fixed with 0.5% (v/v) glutaraldehyde in PBS for 1 min and washed 3 times with PBS. A non-site-specific mAb K20-biotin competition mAb was prepared by reaction of mAb K20 (4 mg/mL, 0.6 mL) in PBS with a 10-fold molar excess of sulfosuccinimidyl 6-(biotinamido)hexanoate (90  $\mu\text{g}$  in 25  $\mu\text{L}$  DMF) and the solution desalted into PBS after 1 h. Equal volumes of mAb K20-biotin and serial 1:2

dilutions of either native mAb K20 or modified mAb K20 were mixed and 100  $\mu\text{L}$  added per well in triplicate. All samples were diluted with PBS containing 1% BSA (PBS/BSA) and the final concentration of mAb K20-biotin was 5  $\mu\text{g}/\text{mL}$  and that of competing mAb K20, either native or modified, was typically in the range of 0.1  $\mu\text{g}/\text{mL}$  to 80  $\mu\text{g}/\text{mL}$ . Samples were incubated for 1 h, plates washed 3 times with PBS/BSA, and 100  $\mu\text{L}$  of extravidin-peroxidase (2  $\mu\text{g}/\text{mL}$  in PBS/BSA) added. After 1 h, plates were washed 3 times with PBS/BSA, and 100  $\mu\text{L}$  of o-phenylenediamine substrate solution prepared as described above, added. Colour development proceeded for 5 to 10 min, was quenched by the addition of 100  $\mu\text{L}$  of 2.5 M  $\text{H}_2\text{SO}_4$  and absorbance at 490nm was measured using the ELISA plate reader. Inhibition of mAb K20-biotin binding by native and modified mAb K20 was determined as described above for  $^{125}\text{I}$ -mAb K20 binding inhibition with the exception that  $A_{490}$  was substituted for cpm.

#### 14.2 Measurement of cytotoxicity of conjugates

Caki-1 cells were plated in 96 well plates at a density of 1000 cells/well in 0.1 mL of growth medium. After 48 h, medium was removed and serial dilutions of MTX or conjugates containing MTX were added in HBSS containing 10% (v/v) growth medium in triplicate. Concentrations were typically in the range of 0.01  $\mu\text{M}$  to 4  $\mu\text{M}$  for free MTX, 0.1  $\mu\text{M}$  to 100  $\mu\text{M}$  for mAb K20-MTX conjugates, and 10  $\mu\text{M}$  to 120  $\mu\text{M}$  for HSA-MTX. Cells were exposed to MTX or conjugates for 6 h after which time the cytotoxic agent was removed, 200  $\mu\text{L}$  of medium added, and cells incubated for 72 h (37  $^\circ\text{C}$ , 5%  $\text{CO}_2$ ). Following incubation, 100  $\mu\text{L}$  of medium was removed by aspiration and cells were fixed by the addition of 100  $\mu\text{L}$  of 2% (v/v) glutaraldehyde in PBS. Cells were quantitated using a crystal violet staining method (188) in which plates were washed four times with  $\text{dH}_2\text{O}$ , 100  $\mu\text{L}$  of 0.1% (w/v) crystal violet in 0.1 M sodium acetate, pH 5.0 added, and plates incubated for 15 min. The crystal violet solution was removed, plates washed four times with  $\text{dH}_2\text{O}$ , dried overnight, 200  $\mu\text{L}$  of 10% acetic acid added to solubilize the dye, and

absorbance at 590 nm was measured in the ELISA plate reader. The  $IC_{50}$  of conjugates relative to untreated Caki-1 cells was determined from plots of  $\lambda_{590}$  against MTX concentration, where  $IC_{50}$  is the concentration of MTX required to inhibit growth by 50%. Standardization experiments showed that crystal violet staining was directly proportional to cell number.

D10-1 cells were plated in 96 well plates at a density of 40,000 cells/well in 0.1 mL of growth medium. After 24 h, plates were centrifuged (500 x g, 10 min), medium removed, and either MTX or MTX-containing conjugates added in triplicate as described above for Caki-1 cells. After 6 h, plates were centrifuged (500 x g, 10 min), test agents removed, and 200  $\mu$ l of growth medium added. Cells were incubated for 5 days (37 °C, 5%  $CO_2$ ), and cells counted in the Coulter counter. The  $IC_{50}$  for each conjugate was determined as described for Caki-1 cells above.

### 14.3 DHFR inhibition assay

MTX and MTX-containing conjugates were assayed for their ability to inhibit DHFR using the method of Peterson (189) with the exception that 0.1 M Tris/HCl, pH 7.5 was used instead of 0.5 M sodium acetate, pH 6.0. Assay mixtures contained 0.1 M Tris/HCl, pH 7.5, 0.6 M KCl, 50  $\mu$ M NADPH, 33 mM dihydrofolate, 0.015 units DHFR/mL, and MTX concentrations in free or conjugated form ranging from 0 to 500 nM. All components of the assay mixture were added with the exception of DHF, the mixture incubated for 30 sec and the rate of NADPH oxidation monitored at 340 nm for 2 min following the addition of DHF. The  $IC_{50}$  was determined for samples relative to the uninhibited rate from plots of reaction rate against MTX concentration.

### 14.4 Establishment of conjugate composition

**Native PAGE and Western blot analysis of conjugates.** A conjugate mixture obtained by reaction of mAb K20-HPDP with HSA-SPDP-SH (Section 11.3) as

well as both mAb K20-HPDP and HSA-SPDP-SH were separated on native PAGE under non-reducing conditions in duplicate, and the proteins transferred to nitrocellulose. The transfer buffer contained 25 mM Tris, 192 mM glycine, and 20% (v/v) methanol, pH 8.3, and the transfer conditions were 100 V (constant) for 1 h at 4 °C and nitrocellulose was blocked for 1 h with PBS containing 0.05% Tween 20 (PBS/Tween). One membrane was probed for mAb K20, and the other for HSA. To demonstrate the presence of mAb K20, nitrocellulose was incubated with goat anti-mouse IgG-peroxidase (1 in 3000 in PBS/Tween) for 1 h, nitrocellulose washed 6 times with PBS/Tween, and peroxidase detected with 100 mL of substrate solution consisting of 7 mg/mL 4-chloro-1-naphthol in PBS containing 20% methanol and 0.03% (v/v) H<sub>2</sub>O<sub>2</sub>. To show the presence of HSA, the nitrocellulose was first incubated with rabbit anti-HSA (1 in 1000 in PBS/Tween) for 1 h, washed 3 times with PBS/Tween, incubated with goat anti-rabbit whole serum-peroxidase (1 in 3000 in PBS/Tween) for 1 h, washed 6 times with PBS/Tween, and peroxidase detected as above.

**Dual labelling experiments to determine conjugate composition.** NRG was labelled with <sup>131</sup>I and HSA with <sup>125</sup>I to specific activities of 6.2 μCi/mg and 2.9 μCi/mg respectively, as described in Section 1.1. NRG-GMBS was prepared as in Section 9.1 and MTX-HSA-SH as in Section 11.3, and the two mixed at a ratio of 4 HSA/IgG. After 16 h at RT, an aliquot of the conjugation mixture was analyzed by SDS PAGE under non-reducing conditions. The gel was stained with Coomassie Blue and the band migrating directly above NRG was cut out and counted for both <sup>125</sup>I and <sup>131</sup>I with correction for spillover of <sup>131</sup>I into the <sup>125</sup>I channel. A total of eleven conjugate bands were cut out and counted in this manner. The ratio of HSA to IgG in the conjugate band was calculated on the basis of the known specific activities.

#### **14.5 Evidence for site-specificity in site-specific conjugates**

**Labelling of mAb K20 with biotin.** mAb K20 was labelled with either sulfosuccinimidyl 6-(biotinamido)hexanoate or biotin-hydrazide. Non-site-specific mAb K20-biotin was prepared as described in Section 14.1. To prepare site-specifically modified mAb K20, mAb K20 (4 mg/mL, 0.3 mL) in pH 5.5 sodium acetate buffer containing 0.15 M NaCl, was treated with sodium periodate (6.8 mg in 68  $\mu$ L dH<sub>2</sub>O) while stirring at 0 °C and then left for 20 min in the dark at 0 °C. Oxidized mAb K20 was desalted into sodium acetate pH 4.0 and a 100-fold molar excess of biotin-hydrazide (0.18 mg in 50  $\mu$ L DMF) was added while stirring. The solution was left for 4 h at RT, after which time sodium cyanoborohydride (1.0 mg in 100  $\mu$ L dH<sub>2</sub>O) was added while stirring. After 1 h at RT the mixture was desalted into PBS.

**Digestion with papain.** To 10  $\mu$ L (25  $\mu$ g in PBS) of mAb K20, modified either site-specifically with biotin hydrazide, or non-site-specifically with sulfosuccinimidyl 6-(biotinamido)hexanoate, was added 30  $\mu$ L of 0.1 M sodium acetate buffer, pH 5.5, 2  $\mu$ L of 1 M cysteine in dH<sub>2</sub>O, 2  $\mu$ L of 20 mM EDTA in dH<sub>2</sub>O, and 5  $\mu$ L (0.5  $\mu$ g) of papain in sodium acetate buffe.. Final incubation conditions were 70 mM sodium acetate, pH 5.5, 50 mM cysteine, 1 mM EDTA, and 20  $\mu$ g papain/mg mAb K20. The digestion mixtures were incubated at 37 °C for 2 h, at which time 1.5  $\mu$ L of 1.7 M Tris/HCl, pH 6.9 was added and an aliquot mixed with an equal volume of reducing SDS PAGE sample buffer. Samples were analyzed by SDS PAGE on 12% gels.

**Digestion with pepsin.** To 10  $\mu$ L (25 $\mu$ g in PBS) of mAb K20 modified either site-specifically with biotin hydrazide, or non-site-specifically with sulfosuccinimidyl 6-(biotinamido)hexanoate, was added 30  $\mu$ L of 0.1 M citrate, pH 3.5, and 5  $\mu$ L of pepsin (0.25  $\mu$ g, 10  $\mu$ g/mg mAb K20) in citrate buffer. The digestion mixture was incubated at 37 °C for 30 min, at which time 4  $\mu$ L of 2.0 M Tris/HCl, pH 9.0 was added and aliquots

mixed with equal volumes of either reducing SDS PAGE sample buffer or non-reducing SDS PAGE sample buffer. Samples were analyzed by SDS PAGE on 7% gels (non-reduced samples) or on 12% gels (reduced samples).

**Western blot analysis of digested mAb K20-biotin.** Site-specific mAb K20-biotin, non-site-specific mAb K20-biotin and their pepsin and papain digests prepared as above were separated on SDS PAGE in duplicate. Both gels were transferred to nitrocellulose and either stained for total protein using India ink or probed for biotin using extravidin-peroxidase. The composition of the transfer buffer was 50 mM Tris, 380 mM glycine, 0.1% SDS, and 20% methanol, and the transfer conditions were 85 V (constant) for 1.5 h at 4 °C. For total protein staining, blots were washed in PBS containing 0.4% (v/v) Tween 20 with two changes of 5 min each, stained with 0.1% (v/v) India ink in PBS/Tween for 30 min and destained in PBS. For biotin-specific staining, blots were rinsed with PBS, blocked with 2% BSA in PBS (PBS/BSA) for 1 h, and treated with extravidin-peroxidase diluted to 1 µg/mL in PBS/BSA for 1 h. Blots were then washed with PBS/BSA four times (10 min each wash) and peroxidase activity detected with 100 mL of substrate solution consisting of 7 mg/mL 4-chloro-1-naphthol in PBS containing 20% methanol and 0.03% (v/v) H<sub>2</sub>O<sub>2</sub>.

#### **14.5 Long term stability of mAb K20-HSA binary conjugates**

Purified mAb K20-HSA binary conjugates prepared as described in Sections 9.2 and 11.3, were analyzed by SDS PAGE under non-reducing conditions after storage for 16 months at 4 °C in PBS containing 0.02% (w/v) sodium azide.

### **III. Results**

#### **1. Rationale for IgG-HSA-MTX conjugate construction**

Methotrexate has been conjugated directly to amino groups on monoclonal antibodies (123,124,127) in spite of the fact that derivatization of some antibodies at their lysine  $\epsilon$ -amino groups with methotrexate results in a decrease in antigen binding activity (72,73,190). This loss of activity is presumably due to modification of residues in and around the antigen binding site. In order to maximize the amount of methotrexate loaded per antibody molecule while minimizing damage to antibody activity, HSA has been used as a carrier for methotrexate, and methotrexate-loaded HSA bound to antibodies (110,119). While the use of HSA as a carrier enabled greater loading of methotrexate, antibody activity was still reduced since HSA was linked via lysine  $\epsilon$ -amino groups of the antibody.

The use of carbohydrate-directed conjugation techniques for the synthesis of immunoconjugates has become popular in recent years. The majority of the carbohydrate present on IgG is located in the hinge region of the molecule, well away from the antigen binding site (23,24,191,192). Modifications to the carbohydrate moiety would therefore be predicted to result in minimal damage to antigen binding activity. Indeed, antibodies have been modified at their carbohydrate residues with low MW drugs (75,83,128,165), liposomes (179), toxin molecules (169), and radionuclides (163) with full retention of antibody activity reported in many cases. The specific modification of carbohydrate residues involves the oxidation of IgG carbohydrates with sodium periodate to generate aldehyde groups, followed by reaction with a suitable hydrazide-containing compound, resulting in the formation of a hydrazone bond between IgG carbohydrate and the hydrazide compound. In this report, modifications to IgG carbohydrate are termed site-specific, whereas amino group-modifications are termed non-site-specific.

Based on the findings that HSA can effectively serve as an intermediary for MTX conjugation to antibodies, and that site-specific modifications of antibodies result in minimal damage to antibody activity, the feasibility of conjugating MTX-loaded HSA to the carbohydrate moiety of mAb K20 was investigated in this thesis. Conjugates synthesized in this manner were compared with similar non-site-specific conjugates in which HSA-MTX was linked to amino groups on IgG. The preparation of site-specific conjugates entailed the synthesis of suitable hydrazide-containing cross-linkers, as none were available at the outset, followed by the development of the methodology to first link the spacers site-specifically to IgG, and then to link a suitably activated form of HSA-MTX to the spacers on IgG.

HSA contains a thiol group (136,137) which can be used as the site for linkage with IgG. However, this sulfur is typically found in a disulfide bond with cysteine or glutathione (137,139) and therefore must be reduced to liberate the free thiol. Alternatively, a protected thiol can be introduced into HSA using the heterobifunctional cross-linking reagent SPDP. This reagent contains a succinimidyl ester which reacts with protein amino groups, and a pyridyldithio group which can either react with thiols, or be reduced with DTT to generate thiol groups (133) (see Figure 4). By reacting SPDP with HSA prior to reaction with MTX, a number of protected thiols can be introduced into HSA which can be used for reaction with appropriately activated IgG.

For the non-site-specific conjugation of HSA-MTX to IgG, IgG can be activated for reaction with thiol groups on HSA either by the introduction of maleimide- or pyridyldithio-containing heterobifunctional spacers into the IgG using the reagents GMBS and SPDP, respectively. Both these spacers contain a succinimidyl ester which, upon reaction with protein amino groups, results in an amide linkage between the spacer and protein (Figure 4). These cross-linkers are termed non-site-specific in that both modify amino groups which are distributed throughout the IgG molecule and their incorporation is therefore not restricted to a single site on IgG.

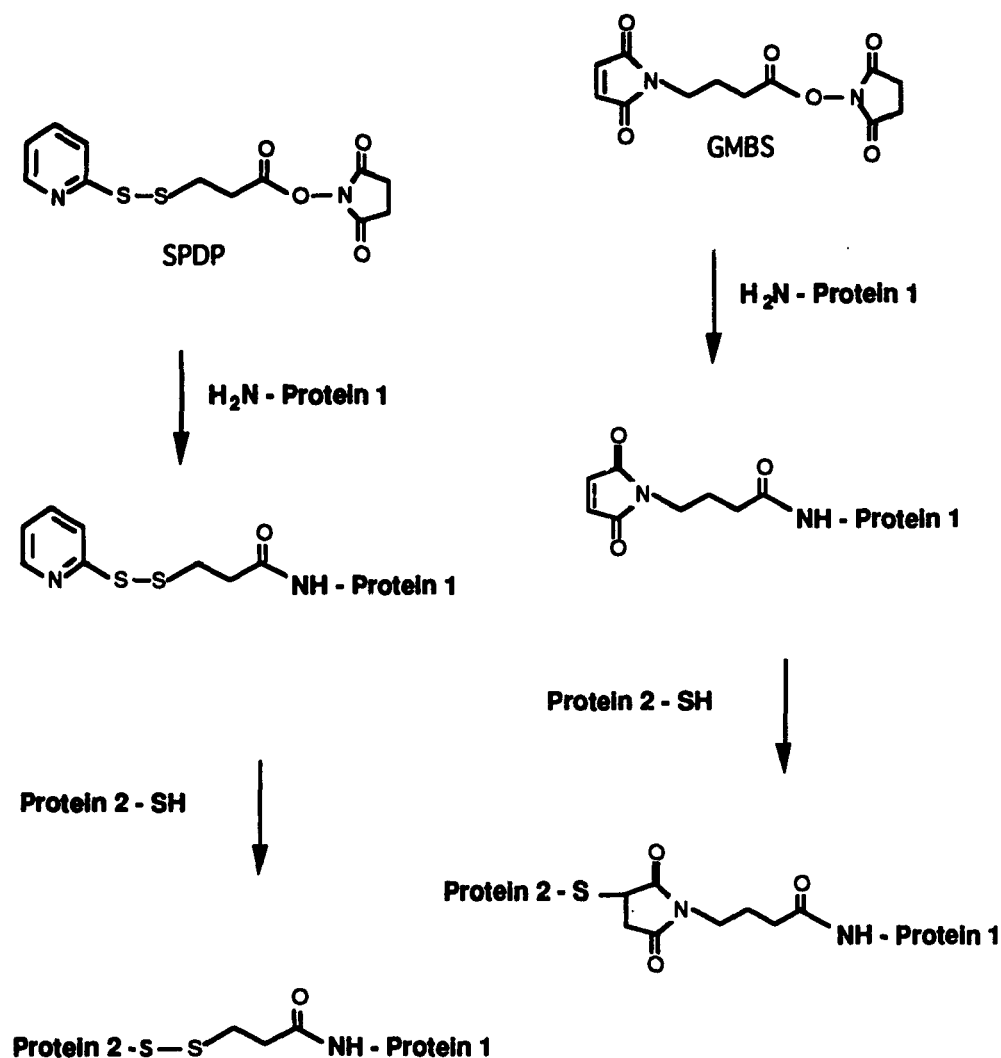


**Figure 4. Reactions of SPDP and GMBS with proteins.**

SPDP (left) and GMBS (right) are heterobifunctional cross-linkers which react with amino groups and thiol groups. In both cases an amide bond is formed between spacer and protein upon reaction of the succinimidyl group with protein amino groups. On reaction with protein thiols, SPDP gives a disulfide linkage whereas GMBS gives a thioether linkage.

The presence of MTX on HSA complicated the conjugation reactions owing to its low solubility as well as to steric factors imposed by the presence of MTX itself. For these reasons, conjugates were first synthesized using HSA without MTX in order to define the conditions for the synthesis of stable, well-defined conjugates. These IgG-HSA conjugates without MTX are termed binary conjugates in this thesis. Once procedures were established, conjugates containing MTX (ternary conjugates) were synthesized for evaluation of their targeting potential.

## **2. Activation of MTX**

### **2.1 Formation of MTX-AE**

MTX was activated for reaction with proteins by conversion to its active ester form (MTX-AE) by reacting MTX with N-hydroxysuccinimide (NHS) and dicyclohexylcarbodiimide (DCC) under anhydrous conditions (73,190). The conversion of MTX to MTX-AE was evaluated using the analytical method described by Kulkarni et al. (73), where activated MTX was reacted with Affi-Gel 102, an agarose-based gel substituted with amino groups. From the amounts of MTX which were bound to the gel, it was possible to estimate the proportion of activated MTX in any given preparation without the need to isolate the active ester from the reaction mixture. To determine the influence of the molar ratios of MTX, NHS and DCC during the preparation of MTX-AE, products from reaction mixtures containing different ratios of MTX, NHS, and DCC were tested for their reactivity towards Affi-Gel 102. Known amounts of MTX from each reaction mixture were passed through a column containing Affi-Gel 102 and the proportion of MTX which reacted with the resin, and was therefore in an active form, determined by subtracting the amount that passed through the column (Table 1). Using a ratio of MTX/DCC/NHS of 1:1:1, it was found that 51% of the MTX was activated. The amount of activated MTX increased to 82% with a 1:3:3 ratio and 91% with a 1:5:5 molar ratio of MTX/DCC/NHS.

<b>MTX:DCC:NHS ratio</b>	<b>% MTX activated</b>
1:1:1	51
1:3:3	82
1:5:5	91
1:5:0	40
1:3:1	72
1:5:1	71
1:1:0	9

**Table 1. Effect of reactant ratio on activation of MTX.** MTX was activated in the presence of DCC and NHS in the ratios indicated and the amount of activated MTX formed determined by reaction with Affi-Gel 102.

In another experiment, MTX, DCC and NHS were mixed in different molar ratios and reaction products analyzed by TLC after 1 and 24 h. MTX has an Rf of approximately 0.4 in this solvent system. After 1 h, all reaction mixtures except that with a 1:4:0 ratio showed a new product with an Rf of 0.5, as well as a second product with an Rf of 0.8, and all contained unreacted MTX. After 24 h, no unreacted MTX was seen in 1:2:2, 1:4:4, 1:4:1, and 1:4:0 mixtures, and the intermediate product with Rf 0.5 was no longer present. The 1:1:1, 1:2:1, and 1:1:2 mixtures all contained unreacted MTX and the product with Rf 0.5, as well as the product with Rf 0.8. It would appear that the product with Rf 0.5 is an intermediate in the formation of the final product with Rf 0.8 since the Rf 0.5 product is formed first and not present after 24 h under conditions of excess DCC and NHS. The product with Rf 0.8 appears to be the major active ester product as long as both DCC and NHS are present in excess over MTX. This assumption is based on the finding that the product activated under these conditions has high acylating activity (Table 1). When NHS was left out altogether, a new product with Rf 0.9 was the major product with some material of Rf 0.8. This higher mobility product also appears to have acylating ability as seen in Table 1 where a similar ratio of 1:5:0 showed 40% activity.

A ratio of 1:3:3 (MTX/DCC/NHS) was chosen for the synthesis of MTX-AE for use in coupling MTX to HSA since the product contained a reasonably high proportion of

activated MTX, and for limiting the amount of excess reactants in the final preparation of MTX-AE which would be added to HSA.

## 2.2 Isolation of MTX-AE

A method to isolate MTX-AE from reaction mixtures before addition to HSA was developed. MTX-AE is not soluble in diethyl ether whereas NHS and DCC, the two reactants present in excess, and the urea product are. By precipitating MTX-AE from the reaction mixture with ether, the excess reactants and products were removed from the MTX-AE preparation, resulting in less precipitation of MTX and HSA during coupling reactions. Using MTX-AE isolated by this method, consistently high loadings of MTX into HSA were achieved.

## 3. Coupling of MTX to HSA

### 3.1 Effect of coupling conditions on MTX-AE incorporation into HSA

In order to establish conditions to achieve high loadings of MTX into HSA, the effect of MTX-AE excess over HSA and of pH during coupling were studied. In the first case, HSA dissolved in PBS was reacted with a molar excess of MTX-AE over HSA between 8- and 80-fold for 4 h and the amount of MTX incorporated into HSA determined after removal of unreacted MTX (Table 2).

MTX-AE excess	MTX Incorporation <sup>a</sup>
8	2
16	5
32	8
48	9
64	15
80	18

**Table 2. Effect of MTX-AE excess on incorporation into HSA**  
 MTX-AE was prepared using a 1:3:3 molar ratio (MTX:DCC:NHS) and reacted with HSA in PBS using the excess of MTX-AE over HSA indicated.  
<sup>a</sup> mol MTX/mol HSA

It can be seen that there was a linear relationship between the excess of MTX-AE used and the molar incorporation of MTX into HSA, with incorporations ranging from 2 mol MTX/mol HSA at an 8-fold molar excess, to 18 mol MTX/mol HSA when an 80-fold excess of MTX-AE was used.

The reaction of MTX-AE with proteins is believed to occur primarily at amino groups in a nucleophilic substitution type reaction (73,110). It was anticipated that the incorporation of MTX into HSA could be increased by raising the pH, as the unprotonated  $\epsilon$ -amino group of HSA lysine residues is thought to be the reactive species. HSA was reacted with a fixed excess of MTX-AE, in this case an 80-fold molar excess, at different pH values and the incorporation of MTX determined after removal of unreacted MTX. These incorporation studies were carried out in Tris/HCl buffer over a pH range of 7.2 to 9.0 (Table 3). It was found that the molar incorporation could be doubled from 20 to 40 MTX/HSA by increasing the pH from 7.2 to 9.0 and that there was an approximately linear relationship between pH and incorporation in this pH range.

pH	MTX incorporation <sup>a</sup>
7.2 (PBS)	20
7.2	20
7.6	24
8.0	30
8.2	34
8.6	37
9.0	40

**Table 3. Effect of pH on MTX-AE incorporation into HSA.** MTX-AE prepared using a 1:3:3 molar ratio (MTX:DCC:NHS) was reacted with HSA in PBS or in Tris/HCl at the pH values indicated using an 80-fold molar excess of MTX-AE over HSA.  
<sup>a</sup> mol MTX/mol HSA.

There was progressively more yellow precipitate seen in reaction mixtures as the pH decreased. However, the precipitated material would appear to be MTX, since recovery of HSA in the form of HSA-MTX was 80% in all cases. It is interesting to note that the buffer itself can theoretically react with the active ester since it also contains an amino

group. This reaction does not appear to occur to an appreciable extent since high loadings of MTX into HSA were achieved.

HSA-MTX to be used for subsequent conjugation to IgG was synthesized using the most favorable conditions which were determined from the preceding experiments: activation of MTX with a 1:3:3 molar ratio (MTX:NHS:DCC); isolation of MTX-AE by ether precipitation; the use of an 80-fold molar excess of MTX-AE over HSA, with coupling carried out at pH 9.0. Under these conditions, molar incorporations of between 30 and 35 mol MTX/mol HSA were consistently achieved.

### **3.2 Coupling of MTX to HSA using EDCI**

The use of the water soluble carbodiimide, EDCI, was also evaluated for the coupling of MTX to HSA. Because EDCI is soluble in aqueous solutions, MTX was activated *in situ* with this reagent in the presence of HSA amino groups. Using a molar ratio of 1:100:150 (HSA:MTX:EDCI), an incorporation of 11 MTX/HSA was obtained. By subjecting this conjugate to a second cycle of MTX and EDCI treatment, the incorporation was increased to 18 MTX/HSA. Yields were considered quantitative since there was no loss due to precipitation during the reactions. The advantage of this method over the MTX-AE method is that fewer steps are involved. The disadvantages are that the efficiency of MTX incorporation is low, although this might have been increased at a higher pH, and that there is an increased potential of crosslinking HSA by activation of HSA carboxyl groups with EDCI. This method for coupling of MTX to HSA was not investigated further since high incorporations of MTX into HSA and acceptable yields of HSA-MTX were achieved using the MTX-AE method.

### **3.3 Purification of HSA-MTX monomer**

It was found that dimers and trimers of HSA were formed during the reaction of MTX-AE with HSA. Although HSA preparations themselves contained small amounts of

dimer prior to coupling with MTX, these were disulfide linked since they were reducible as demonstrated by SDS PAGE under reducing conditions. The dimers and trimers of HSA formed during MTX incorporation on the other hand were not reducible with mercaptoethanol, indicating that the cross-linking was not through disulfide bonds. The basis of this cross-linking is not readily apparent since it occurred whether or not excess DCC and NHS were removed by purification of MTX-AE. In order to facilitate the subsequent separation of IgG-HSA-MTX conjugates by gel filtration chromatography, the HSA-MTX monomer was separated from dimers and trimers by gel filtration. Recovery of HSA as the HSA-MTX monomer was typically 50%.

#### **4. Activation of HSA and HSA-MTX for conjugation with IgG**

##### **4.1 Introduction of thiols using SPDP**

Protected thiols were introduced into HSA by reacting HSA with SPDP, an N-succinimidyl derivative of pyridyldithiopropionic acid. This reagent is known to react with protein amino groups at neutral pH to form an amide linkage between protein and cross-linker (133) as shown in Figure 4. The molar excess of SPDP over HSA used was varied depending on the age of the SPDP preparation, since older preparations showed some hydrolysis of the N-succinimidyl ester as monitored by TLC. Typically, with a fresh preparation of SPDP, a 5-fold molar excess of SPDP over HSA resulted in the incorporation of 2.5 pyridyldithio groups per HSA. HSA was reacted with SPDP prior to MTX loading since both SPDP and MTX-AE react with amino groups, and prior reaction with a large excess of MTX-AE would inhibit the subsequent incorporation of SPDP into HSA. For the synthesis of ternary IgG-HSA-MTX conjugates, pyridyldithio groups in MTX-HSA-SPDP were reacted with free thiol groups introduced into IgG, whereas for the synthesis of binary IgG-HSA conjugates, pyridyldithio groups in HSA-SPDP were reduced with DTT to produce free thiols (HSA-SPDP-SH), and these reacted with pyridyldithio groups introduced into IgG.

## 4.2 Introduction of thiols by direct reduction of HSA with DTT

A different approach was taken in testing the effect of spacer length on conjugation, where thiols were derived from HSA itself. HSA contains 35 cysteine residues forming 17 disulfide bonds leaving one free thiol group (136,137). It has been shown however that the majority of these "free" thiols are in fact disulfide bonded to low MW sulfur-containing compounds such as cysteine and glutathione (137,139). Measurement of the thiol content of unreduced HSA with DTNB confirmed that only 30% of the cysteine residues existed in the thiol form, with the remainder presumably blocked (Table 4).

excess of DTT over HSA	extent of HSA reduction <sup>a</sup>
0	0.3
2.5	1.0
5	1.1
10	1.5
20	2.7

**Table 4. Reduction of HSA disulfides with DTT.**

HSA dissolved in PBS was treated with the molar excess of DTT indicated for 30 min and the solution desalted into PBS. The number of thiols generated were determined using DTNB.

<sup>a</sup> mol SH/mol HSA

It was found that the extent of HSA reduction by DTT could be controlled to a large degree by the excess of the reducing agent over HSA. Treatment of HSA with a 2.5-fold to 5-fold molar excess of DTT generated a total of one thiol group per HSA, this most likely being the blocked "free" thiol. An excess of DTT of 10-fold or greater resulted in the production of more than one thiol per HSA, indicating that under these conditions internal disulfides were reduced. These reduction studies were performed using HSA not containing MTX. It was assumed that HSA and HSA-MTX would be reduced to similar extents.

## **5. Site-specific IgG-HSA-MTX conjugates**

In an effort to produce mAb K20-HSA-MTX conjugates with high retention of antibody binding activity, a site-specific conjugation approach was taken. Methods for the site-specific immobilization or conjugation of antibodies have been based on the specific reactivity of IgG aldehydes generated by the oxidation of IgG carbohydrate by periodate. These aldehydes have been reacted with either hydrazide-containing spacers resulting in the formation of a hydrazone bond between spacer and antibody (167), or with amino groups present on carriers resulting in the formation of a Schiff base between antibody and carrier (117). All hydrazide spacers commercially available at the beginning of this study were homobifunctional in nature, i.e. contained two hydrazide groups. The use of a homobifunctional spacer for the conjugation of HSA to IgG was unsuitable since the formation of antibody homoconjugates was possible. The use of a Schiff base to link IgG with HSA-MTX was also undesirable because the formation of IgG homoconjugates during the conjugation was likely. For this reason, two hydrazide-containing heterobifunctional spacers were synthesized. These were derived from the non-site-specific cross-linker SPDP (Figure 5) and were designed to contain two different functional groups. Both contained a hydrazide group for reaction with IgG aldehydes, and a pyridyldisulfide group for reaction with thiols, but differed in the distance between the two functional groups.

### **5.1 Synthesis of the site-specific spacers HPDP and AUPDP**

The two heterobifunctional spacers, HPDP (1b) and AUPDP (2c) were synthesized from SPDP (1a) as shown in Figure 5. HPDP was prepared directly from SPDP by reaction with hydrazine to yield the corresponding hydrazide. The influence of both solvent composition and molar excess of hydrazine over SPDP were investigated in the preparation of this derivative. DMF, n-butanol and methanol were compared as solvents to find that giving the greatest conversion to the hydrazide. All gave comparable conversion

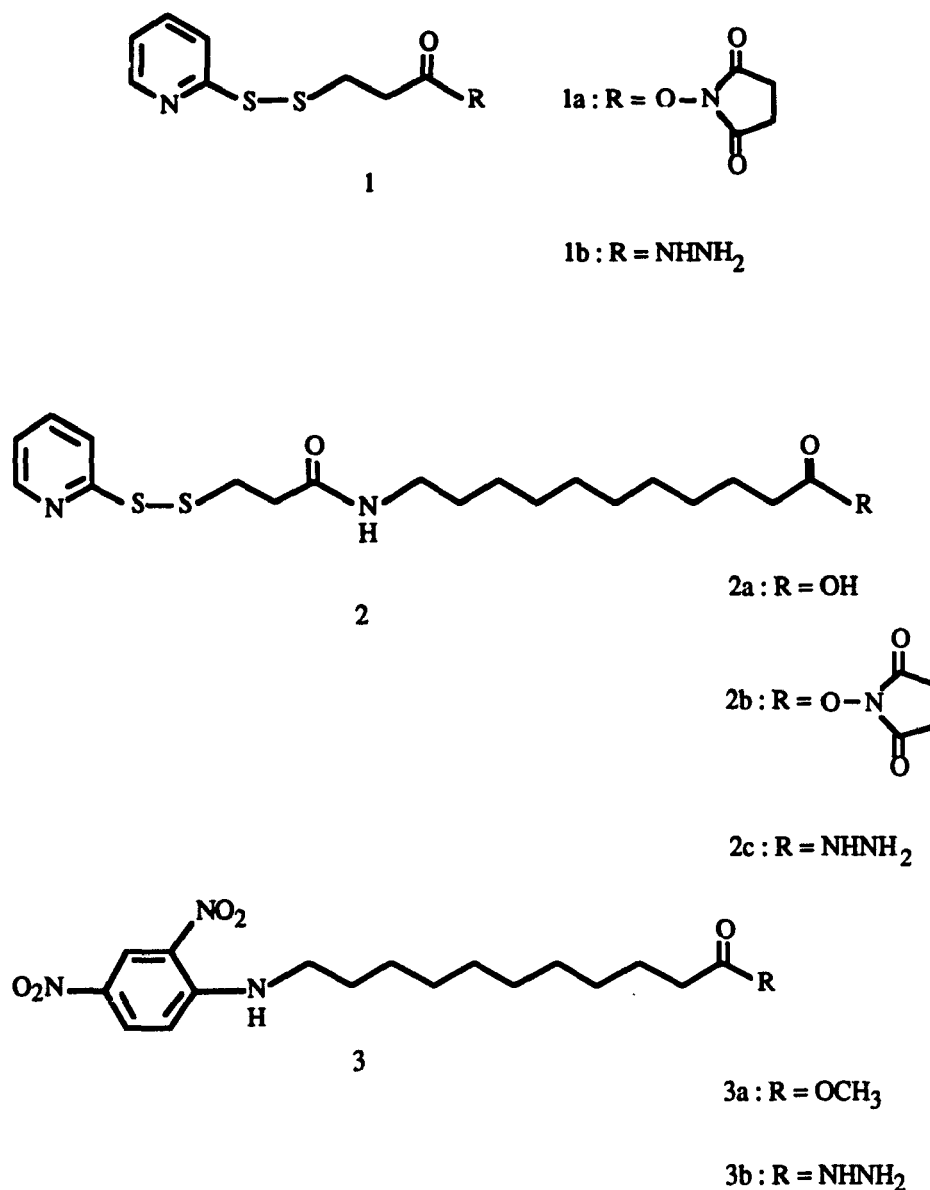


**Figure 5. Structures of site-specific cross-linkers and a site-specific stability probe.**

HPDP (1b) was derived from SPDP (1a) by treatment with an excess of hydrazine. For the synthesis of AUPDP (2c), SPDP was reacted with 11-aminoundecanoic acid and the product of this reaction, 11-[3-(2-pyridyldithio)propionyl]aminoundecanoic acid (2a), converted to the succinimidyl ester (2b) by reaction with NHS and DCC. Treatment of 2b with hydrazine resulted in the formation of AUPDP (2c). The site-specific stability probe, DNP-AU-hydrazide (3b) was obtained by reaction of 11-aminoundecanoic acid methyl ester with 1-fluoro-2,4-dinitrobenzene. The product of this reaction, 11-(2,4-dinitrobenzene)aminoundecanoic acid methyl ester (3a), was then treated with an excess of hydrazine to give DNP-AU-hydrazide (3b).

to the hydrazide, but methanol was found to be the most convenient solvent. In testing the excess of hydrazine required for complete conversion of SPDP to HPDP, it was found that using either a one-fold or more than a two-fold molar excess resulted in the formation of side products, whereas a 1.5 to 2.0-fold excess gave the desired product in greatest yield. Following extraction and crystallization, the product was judged to be of high purity on the basis of lack of contaminants as seen by TLC and its narrow melting point range. Reaction of HPDP with either acetone or DTT confirmed the presence of the hydrazide and disulfide functions and NMR spectroscopy confirmed the structure as HPDP.

In the first attempt to synthesize AUPDP, the methyl ester of 11-aminoundecanoic acid was prepared and reacted with SPDP to give 11-[3-(2-pyridyldithio)propionyl]amino undecanoic acid methyl ester in good yield. The product was then treated with hydrazine to convert the methyl ester to the hydrazide, but the high excess required also resulted in cleavage of the disulfide bond and release of pyridine-2-thione. The second synthetic approach was similar to that used in the preparation of HPDP. SPDP was reacted with 11-aminoundecanoic acid, and the resulting acid (2a) converted to the succinimidyl ester (2b) which, upon treatment with hydrazine, gave the hydrazide derivative (2c). It was found necessary to carry out the reaction between SPDP and aminoundecanoic acid in aqueous ethanol containing sodium bicarbonate in order for any appreciable reaction to occur. The conversion to the succinimidyl ester was carried out using a slight excess of NHS and DCC, and as with HPDP, it was found that the use of a 1.5- to 2.0-fold molar excess of hydrazine was important in preventing the formation of unwanted side products. Hydrolysis of the product with 6 M HCl confirmed the presence of aminoundecanoic acid, and reaction with acetone and reduction with DTT showed the presence of the hydrazide and disulfide functionalities, respectively. Purity was judged to be high on the basis of the lack of contaminants TLC and its narrow melting point range. NMR data also supported the structure as that of AUPDP.

## **5.2 Site-specific modification of IgG with HPDP and AUPDP**

HPDP and AUPDP were incorporated into the oxidized carbohydrate of IgG for subsequent conjugation with HSA-MTX (or HSA). Preliminary experiments using NRG were performed to define the oxidation conditions required to incorporate sufficient spacers into the carbohydrate moiety. NRG was oxidized with an excess of periodate at pH 5.5 for 20 min at 0 °C, and then reacted with a fixed excess of AUPDP following removal of excess periodate. As shown in Figure 6, the incorporation of AUPDP into NRG was dependent on the excess of periodate used. Incorporations ranged from 0.4 spacers/IgG with 0.26 mM periodate and 5 spacers/IgG with 260 mM periodate, corresponding to molar excesses of 10- and 10,000-fold over IgG, respectively. The low solubility of both HPDP and AUPDP in aqueous solution required that these spacers be added to IgG solutions containing 15% DMF to prevent precipitation of HPDP and AUPDP during the coupling reaction.

For the site-specific incorporation of HPDP and AUPDP into mAb K20, oxidation was carried out for 20 min at pH 5.5 and 0 °C using a 4,000-fold molar excess of periodate (100-200 mM). Incorporations of approximately 4 spacers/mAb K20 were consistently achieved under these conditions.

## **5.3 Site-specific conjugation of HSA and HSA-MTX to IgG**

**Conjugation of mAb K20 with HSA.** In order to evaluate HPDP and AUPDP for use in conjugation, spacer-containing IgG was reacted with various forms of HSA and HSA-MTX. mAb K20, modified with either HPDP (3.8 HPDP/mAb K20) or AUPDP (4.6 AUPDP/mAb K20), was reacted with either HSA which had been reduced directly with DTT (HSA-SH, 2 thiols/HSA) or with HSA which had been modified with SPDP and then reduced with DTT (HSA-SPDP-SH, 2.5 thiols/HSA). Where HSA was reduced directly, the thiol was generated from HSA itself, whereas in the case of SPDP-modified HSA, the thiol was derived from the spacer. Conjugate formation was monitored

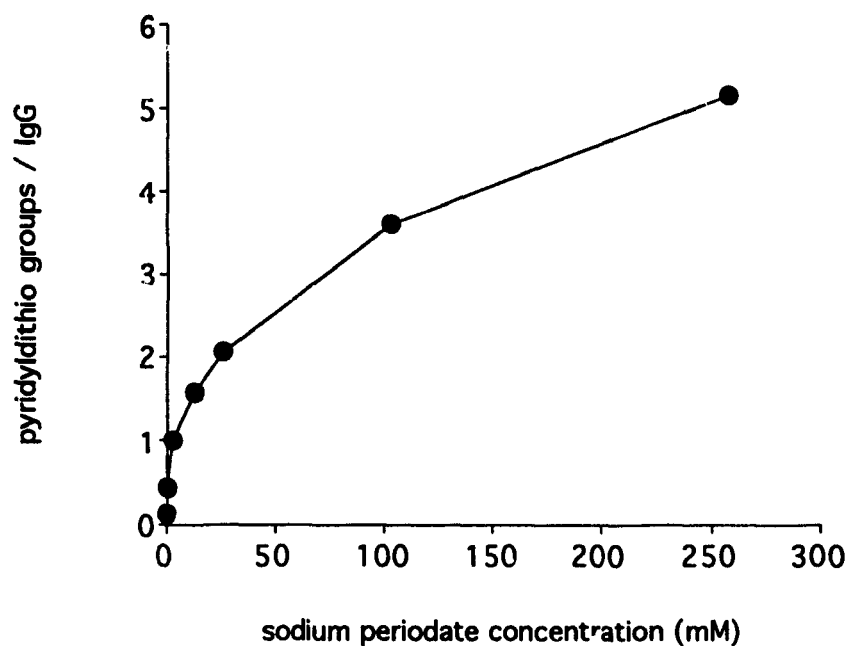


**Figure 6. Effect of oxidation level on incorporation of AUPDP into NRG.** NRG at a concentration of 8.7 mg/mL in 0.1 M sodium acetate, pH 5.5, containing 0.15 M NaCl, was oxidized with sodium periodate at the concentrations indicated. After 20 min at 0 °C in the dark, samples were desalted into 0.1 M sodium acetate, pH 4.0, DMF added to a concentration of 15%, and a 50-fold molar excess of AUPDP dissolved in DMF added to give a final DMF concentration of 25%. Samples were desalted into 0.1 M sodium acetate, pH 4.0, after 3 h and the incorporation of AUPDP into NRG determined. NRG concentration was measured by the Lowry assay with NRG as standard, and the spacer concentration determined spectrophotometrically in the presence of 100 mM DTT using  $\epsilon = 8080 \text{ cm}^{-1}\text{M}^{-1}$  at 343 nm.

by native PAGE as shown in Figure 7A. Lanes 4 and 6 show the products of reaction between directly reduced HSA and HPDP- and AUPDP-derivatized mAb K20 respectively. The band migrating directly below mAb K20 itself on native PAGE was shown to contain both HSA and mAb K20 by Western blotting. It is apparent that the use of the longer AUPDP resulted in a much higher yield of conjugate compared to HPDP. When HSA was first modified with SPDP and then reduced, a similar pattern was seen in which AUPDP-derivatized mAb K20 (lane 5) gave greater conversion than HPDP-derivatized mAb K20 (lane 3). These data suggest that the ability to link HSA to the carbohydrate of mAb K20 is dependent on the length of spacer or spacers between the two proteins. The finding that the extent of conversion to conjugates using AUPDP can be further increased when SPDP is present on HSA (lanes 5 and 6) indicates that there is still some degree of steric hindrance present when AUPDP is used alone, and suggests that a longer spacer may be more appropriate for synthesis of site-specific mAb K20-protein conjugates.

**Conjugation of mAb K20 with HSA-MTX.** Figure 7B shows a similar experiment in which HSA or HSA-SPDP were reacted first with MTX and then reduced with DTT prior to conjugation with HPDP- or AUPDP-derivatized mAb K20. In this case, no conjugates were formed when mAb K20-HPDP was reacted with MTX-HSA-SH or MTX-HSA-SPDP-SH (lanes 3 and 4). In contrast, mAb K20-AUPDP did show conversion to conjugates with both MTX-HSA-SH and MTX-HSA-SPDP-SH (lanes 5 and 6), although the difference between HSA with and HSA without SPDP was not as large as seen in Figure 7A. These findings indicate that, while HPDP may be useful for the synthesis of mAb K20-HSA binary conjugates, the presence of MTX on HSA appears to create a further steric barrier to conjugation making it necessary to use the longer crosslinker AUPDP for synthesis of site-specific ternary conjugates. Site-specific conjugates between HSA or HSA-MTX and mAb K20 which were synthesized for



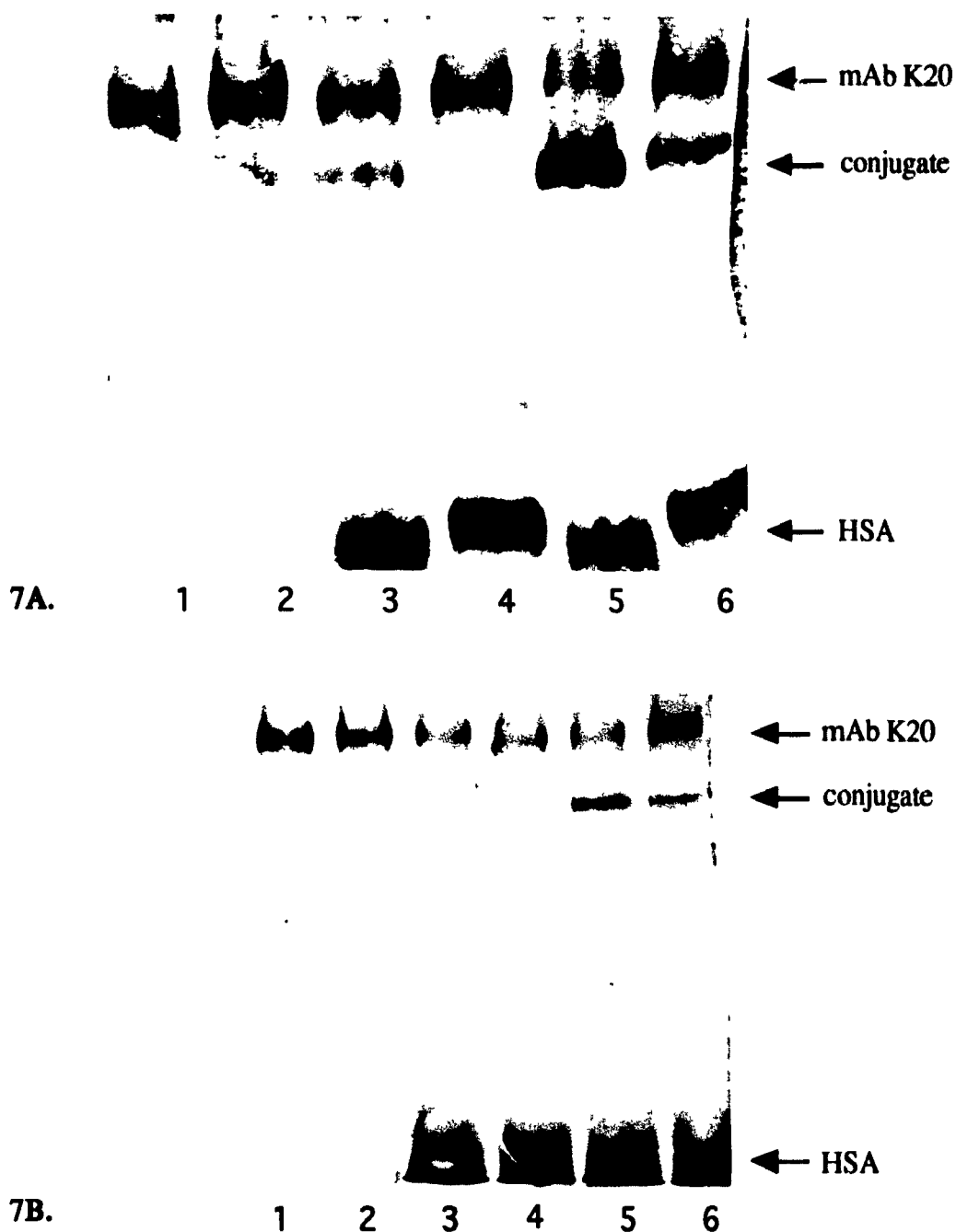


**Figure 7. Analysis of site-specific conjugation yield by native PAGE.** HSA or HSA-SPDP (Figure 7A) and HSA-MTX or MTX-HSA-SPDP (Figure 7B) were reduced with DTT and reacted with mAb K20 derivatized with either HPDP or AUPDP and reaction mixtures separated by native PAGE as described in Section 11.3 of Materials and Methods.

**Figure 7A:** lane 1, mAb K20-HPDP; lane 2, mAb K20-AUPDP; lane 3, mAb K20-HPDP + HSA-SPDP-SH; lane 4, mAb K20-HPDP + HSA-SH; lane 5, mAb K20-AUPDP + HSA-SPDP-SH; lane 6, mAb K20-AUPDP + HSA-SH.

**Figure 7B:** lane 1, mAb K20-HPDP; lane 2, mAb K20-AUPDP; lane 3, mAb K20-HPDP + MTX-HSA-SPDP-SH; lane 4, mAb K20-HPDP + MTX-HSA-SH; lane 5, mAb K20-AUPDP + MTX-HSA-SPDP-SH; lane 6, mAb K20-AUPDP + MTX-HSA-SH.

evaluation of antibody activity and conjugate cytotoxicity were therefore synthesized using AUPDP as the cross-linker to maximize the yield of conjugates obtained.

**Conjugation of NRG with HSA.** Unlike mAb K20, the conjugation of HSA to NRG did not show the same steric restrictions. Conjugation was found to proceed to a similar extent whether NRG was derivatized with HPDP or AUPDP. Furthermore, the presence of SPDP on HSA made little difference in the yield of conjugates.

#### **5.4 Evaluation of hydrazone bond stability and stabilization with cyanoborohydride**

**Elution of conjugates from native PAGE gels.** The first indication that the hydrazone bond between mAb K20 and HSA had limited stability arose from the inability to isolate these site-specific conjugates in pure form by gel filtration chromatography. Following chromatography, the conjugate-containing fractions were found to contain both unconjugated HSA and mAb K20 as well as the conjugate. In order to investigate the apparent instability further, site-specific conjugates contained in reaction mixtures were separated from unreacted HSA and mAb K20 by native PAGE on a preparative scale, and conjugate bands eluted from the gels. The eluates were analyzed by SDS PAGE as shown in Figure 8. As seen in lanes 2 and 3, respectively, both HPDP- and AUPDP-linked conjugates showed the presence of free mAb K20 and HSA as well as the conjugates. For comparison, conjugates between HSA and mAb K20 were also synthesized non-site-specifically, and were treated under the same conditions (the synthesis of non-site-specific conjugates is described in Section 6.2). Both non-site-specific conjugates, either disulfide-linked using mAb K20-SPDP (lane 5), or thioether-linked using mAb K20-GMBS (lane 6), showed very little free HSA or free mAb K20 in the isolated conjugates. The linkage between mAb K20 and spacer was an amide bond in the case of non-site-specific conjugates, and a hydrazone bond in the site-specific conjugates.

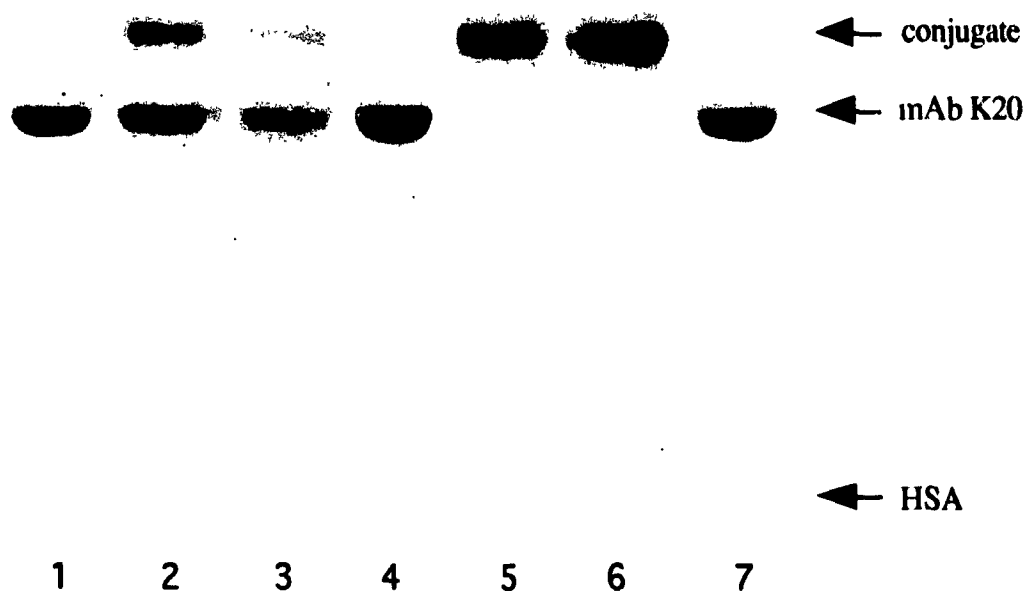


**Figure 8. SDS PAGE analysis of conjugates eluted from native gels.** Binary mAb K20-HSA conjugates were prepared as described in Sections 11.3 and 9.2 under Materials and Methods. Site-specific conjugates were prepared with either HPDP or AUPDP, and non-site-specific conjugates were prepared with SPDP or GMBS. Each conjugate-containing reaction mixture was subjected to preparative native PAGE, and the band containing the conjugate cut out and material from the band eluted from the gel as described in Section 12.1 under Materials and Methods. Eluted material was lyophilized and analyzed by SDS PAGE.

Lanes 1, 4 and 7, mAb K20; lane 2, AUPDP conjugate; lane 3, HPDP conjugate; lane 5, SPDP conjugate; lane 6, GMBS conjugate.

The inability to isolate the site-specific conjugates in pure form indicated that the site of instability was most likely the hydrazone linkage between mAb K20 and spacer. The disulfide bond was not the site of instability because non-site-specific conjugates synthesized with mAb K20-SPDP contained the same disulfide linkage present in the site-specific conjugates, and the disulfide-linked non-site-specific conjugates were of comparable stability to thioether-linked conjugates synthesized using GMBS.

**Model studies with DNP-AU-hydrazide.** King et al. (178) showed that hydrazone bonds could be stabilized by cyanoborohydride reduction. A chromophoric DNP hydrazide was used to assist in defining conditions for stabilization of site-specific conjugates. Retention of DNP groups in the protein could be used to monitor hydrazone stability whereas pyridyldithio groups from AUPDP were found to be susceptible to disulfide reduction by cyanoborohydride with accompanying loss of pyridyldithio reporter function. DNP-AU-hydrazide was synthesized by reaction of fluoro-2,4-dinitrobenzene with 11-aminoundecanoic acid methyl ester, and the methyl ester (3a, Figure 5) converted to the hydrazide (3b, Figure 5) by reaction with an excess of hydrazine. As expected on the basis of the similarity in structure in the region of the hydrazide group, it was found to display similar reactivity toward oxidized IgG as AUPDP. DNP-AU-hydrazide was incorporated into NRG following IgG oxidation with periodate using conditions similar to those for reaction with AUPDP. Control reactions in which oxidized NRG was treated with the methyl ester derivative of DNP-AU-hydrazide, or where non-oxidized NRG was treated with DNP-AU-hydrazide showed no incorporation of the DNP label into NRG, indicating the specificity of the reaction between oxidized NRG and hydrazide.

It was first determined whether the incorporation of DNP-AU-hydrazide into oxidized NRG could be prevented by prior reduction of NRG aldehyde groups with cyanoborohydride. Table 5 shows that NRG which had been oxidized and reacted with DNP-AU-hydrazide incorporated 6.2 DNP groups/NRG. However, NRG which was

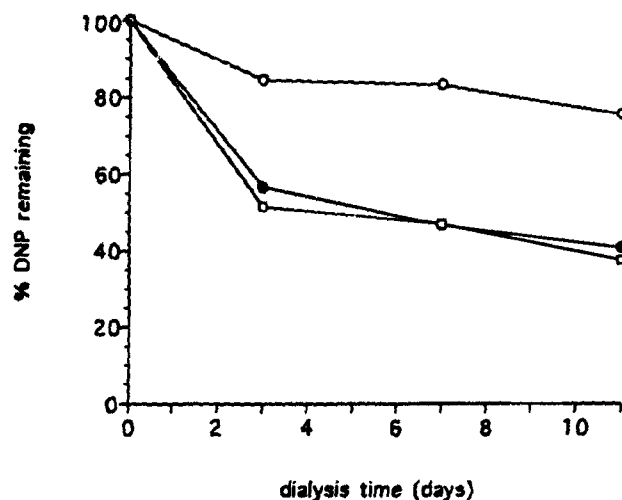
treated with cyanoborohydride prior to reaction with the probe showed that approximately 1 DNP group/NRG was introduced, demonstrating that the majority of aldehyde groups generated by periodate oxidation of NRG carbohydrate were also sterically accessible to reduction by cyanoborohydride.

<b>molar excess of cyanoborohydride</b>	<b>number of DNP groups/NRG</b>
0	6.2
500	1.0
1000	1.0
2000	0.8
4000	1.2

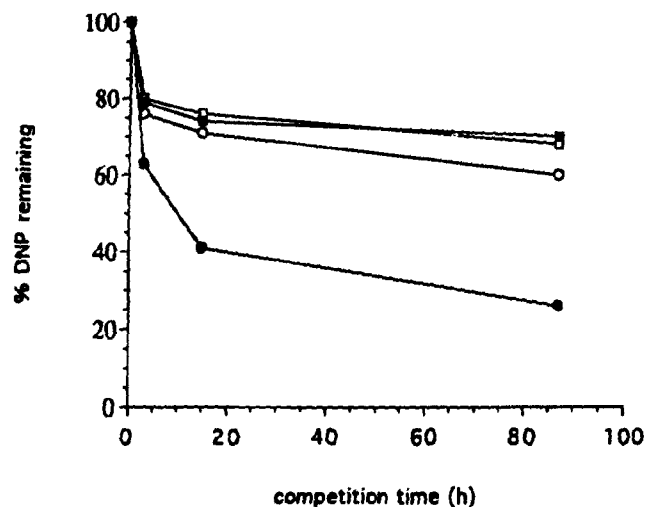
**Table 5. Reduction of NRG aldehyde groups by cyanoborohydride.** NRG was oxidized with sodium periodate and treated with the molar excess of cyanoborohydride indicated (0 to 110 mM) for 48 h. Samples were desalted and reacted with DNP-AU-hydrazide for 4 h and the incorporation of DNP groups into NRG determined as described in Section 12.2 of Materials and Methods.

In order to evaluate the stability of the hydrazone bond formed by reaction of NRG aldehyde groups with the hydrazide probe, probe modified-NRG (DNP-NRG) was dialyzed over a period of 11 days at 37 °C. Figure 9A shows that approximately 60% of probe is lost from both the non-reduced control and the sodium borohydride treated samples after this period of time. In contrast, DNP-NRG which had been treated with sodium cyanoborohydride in order to reduce the hydrazone bonds prior to dialysis, showed retention of approximately 75% of the DNP-probe after 11 days, indicating that a proportion of the hydrazone bonds had been reduced and stabilized.

King et al. (178) also showed that hydrazone-linked protein-protein conjugates could be dissociated by an exchange reaction with an excess of acetyl hydrazide. Extending this displacement approach to the DNP-NRG system, it was found that release of the DNP-probe from NRG could be achieved by treatment with an excess of propionaldehyde. As seen in Table 6, NRG which contained 7.9 DNP groups initially and was treated with an excess of propanal for 48 h showed retention of only 1.5 DNP



9A.



9B.

**Figure 9. Stabilization of the hydrazone linkage between DNP reporter groups and NRG with cyanoborohydride.**

**Figure 9A:** NRG was oxidized with sodium periodate, reacted with an excess of DNP-AU-hydrazide and either treated with 15 mM sodium borohydride (open squares), 15 mM sodium cyanoborohydride (open circles) or not treated (filled circles) and dialyzed at 37 °C. Samples were taken at the times indicated and the percentage of DNP groups remaining associated with NRG determined.

**Figure 9B:** To study the effect of sodium cyanoborohydride reduction time on DNP-hydrazone stability, DNP-IgG was either not treated (filled circles) or treated with 15 mM sodium cyanoborohydride for 1.5 h (open circles), 18.5 h (open squares), or 26 h (filled squares). Samples were then incubated with a 10,000-fold molar excess of propanal in 0.1 M sodium acetate, pH 4.0, at RT, aliquots desalted at the times indicated, and the percentage of DNP groups remaining associated with NRG determined.

groups/NRG (23%). However, DNP-NRG which had been reduced with cyanoborohydride prior to aldehyde treatment retained substantially more DNP i.e. 4.5 DNP groups/NRG (57%) after reaction with propanal.

Sample	Treatment	number of DNPa groups/NRG	% DNP/NRG remaining
	start	7.9	100
1	after NaCNBH <sub>3</sub>	5.1	65
2	after NaBH <sub>4</sub>	6.3	80
3	control	7.0	89
1	NaCNBH <sub>3</sub> + aldehyde	4.5	57
2	NaBH <sub>4</sub> + aldehyde	1.7	22
3	control + aldehyde	1.8	23

**Table 6. Stabilization of DNP-NRG hydrazone bonds with sodium cyanoborohydride.**

Oxidized NRG was reacted with an excess of DNP-AU-hydrazide for 4 h, desalted, and samples treated with 15 mM sodium borohydride (NaBH<sub>4</sub>), 15 mM sodium cyanoborohydride (NaCNBH<sub>3</sub>), or untreated (control). After 48 h samples were desalted and treated with an excess of propanal for 48 h and the number of DNP groups remaining bound to NRG determined.

<sup>a</sup> mol DNP/molNRG

This competition study essentially showed the same result as the dialysis study, indicating that untreated hydrazones and those treated with sodium borohydride at pH 4.0 showed very limited stability, with approximately 20% of hydrazone bonds remaining intact following removal of unstable linkages by propanal. Sodium cyanoborohydride treatment on the other hand, resulted in the stabilization of approximately 60% of the hydrazone bonds. Competition with propanal also showed that treatment of DNP-NRG with 15 mM cyanoborohydride for 1.5 h was sufficient to reduce the majority of hydrazone bonds, with little more stabilization being achieved after this time (Figure 9B).

### 5.5 Synthesis of stabilized site-specific conjugates

**mAb K20-HSA conjugates.** Site-specific conjugates were first synthesized with HSA not containing MTX in order to test whether the stabilization conditions

determined for the DNP-AU-hydrazide probe would result in sufficient stabilization of the hydrazone bond to allow the isolation of conjugates. Site-specific mAb K20-HSA binary conjugates were constructed using the scheme shown in Figure 10. mAb K20 was first oxidized with sodium periodate and then reacted with AUPDP to incorporate pyridyldithio groups into the carbohydrate moiety of the IgG. mAb K20-AUPDP was then reacted with HSA-SPDP-SH and the resulting conjugate was treated with cyanoborohydride for 90 min. The 1:1 HSA:mAb K20 conjugate was separated from the conjugation mixture by gel filtration chromatography as shown in Figure 11. Collected fractions were analyzed by SDS PAGE to determine which fractions contained purified conjugate, and fractions 38 to 43 from Figure 11 were pooled. Lane 3 of Figure 12A shows the pooled conjugate analyzed by non-reducing SDS PAGE where it can be seen that the conjugate was isolated without contamination by unbound mAb K20 or HSA. Lane 3 in Figure 12B shows the same site-specific conjugate analyzed under reducing conditions where it is seen to break down to the expected components under these conditions: HSA, IgG heavy, and IgG light chains. The recovery of mAb K20 in the binary conjugate was 15%. The ability to isolate the site-specific binary conjugate indicated that the cyanoborohydride treatment had stabilized a proportion of hydrazone bonds.

**mAb K20-HSA-MTX conjugates.** Site-specific mAb K20-HSA-MTX ternary conjugates were prepared using the scheme shown in Figure 13 where IgG was oxidized and reacted with AUPDP. Stabilization of the hydrazone bond was achieved by reduction of mAb K20-AUPDP with cyanoborohydride, following which spacer pyridyldithio groups were reduced with DTT to give the free thiol. mAb K20-AUPDP-SH was then reacted with MTX-HSA-SPDP (28 MTX/HSA) resulting in the formation of stabilized site-specific ternary conjugates. The conjugation reaction mixture as analyzed by SDS PAGE is shown in lane 1 of Figure 14. Purification of the conjugate was achieved by a two step procedure involving ion exchange chromatography on DEAE-Sepaharose

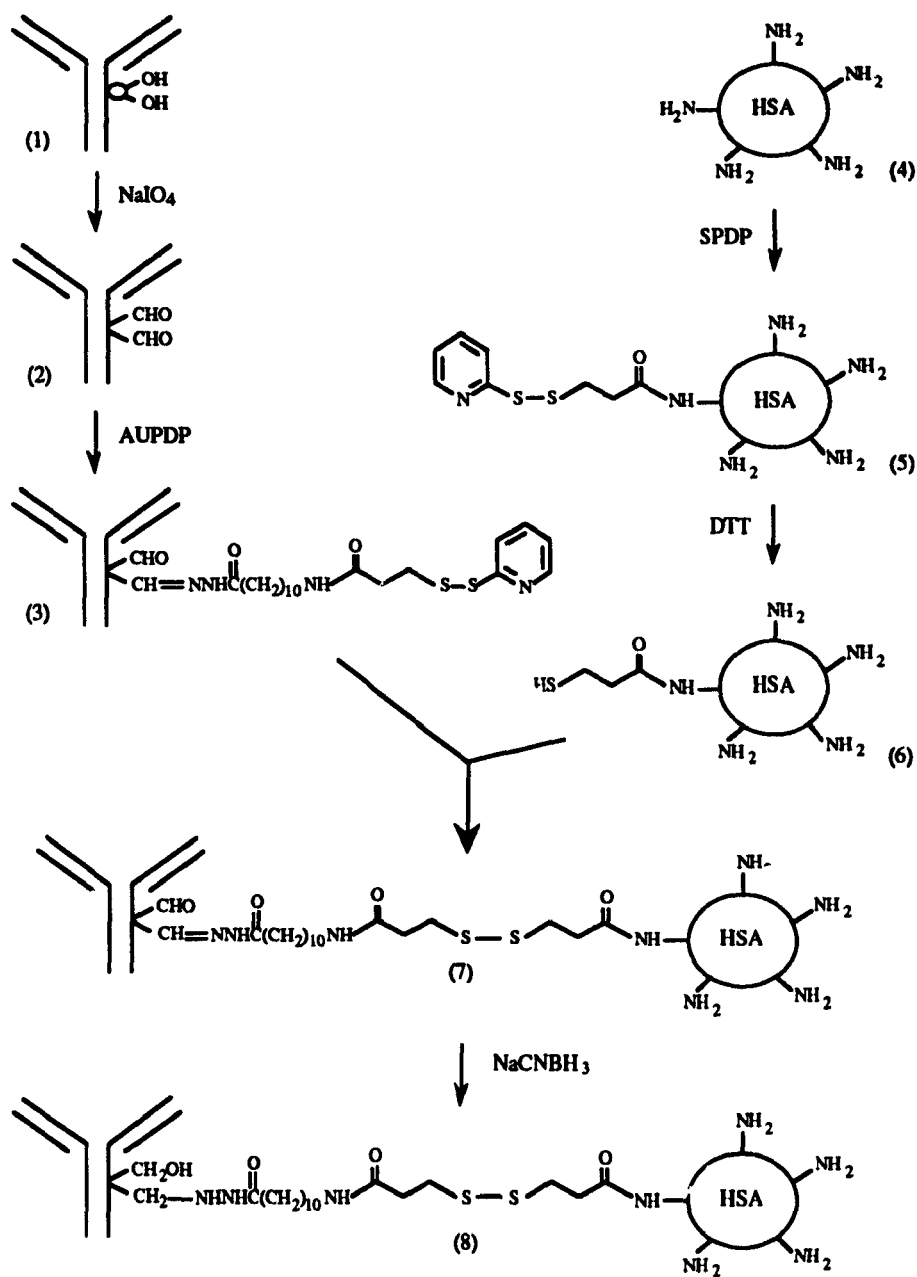


**Figure 10. Scheme for the synthesis of site-specific mAb K20-HSA binary conjugates.** mAb K20 (1) carbohydrate was oxidized with sodium periodate and oxidized mAb K20 (2) reacted with the site-specific cross-linkers AUPDP or HPDP (AUPDP shown). HSA (4) amino groups were derivatized with pyridyldithio groups using SPDP and HSA-SPDP (5) then treated with DTT to generate thiol groups from protected disulfides. HSA-SPDP-SH (6) was then reacted with mAb K20-AUPDP (3) resulting in the formation of the binary mAb K20-HSA conjugate (7). The hydrazone bond between IgG and HSA was reduced with sodium cyanoborohydride giving the stabilized site-specific binary mAb K20-HSA conjugate (8).

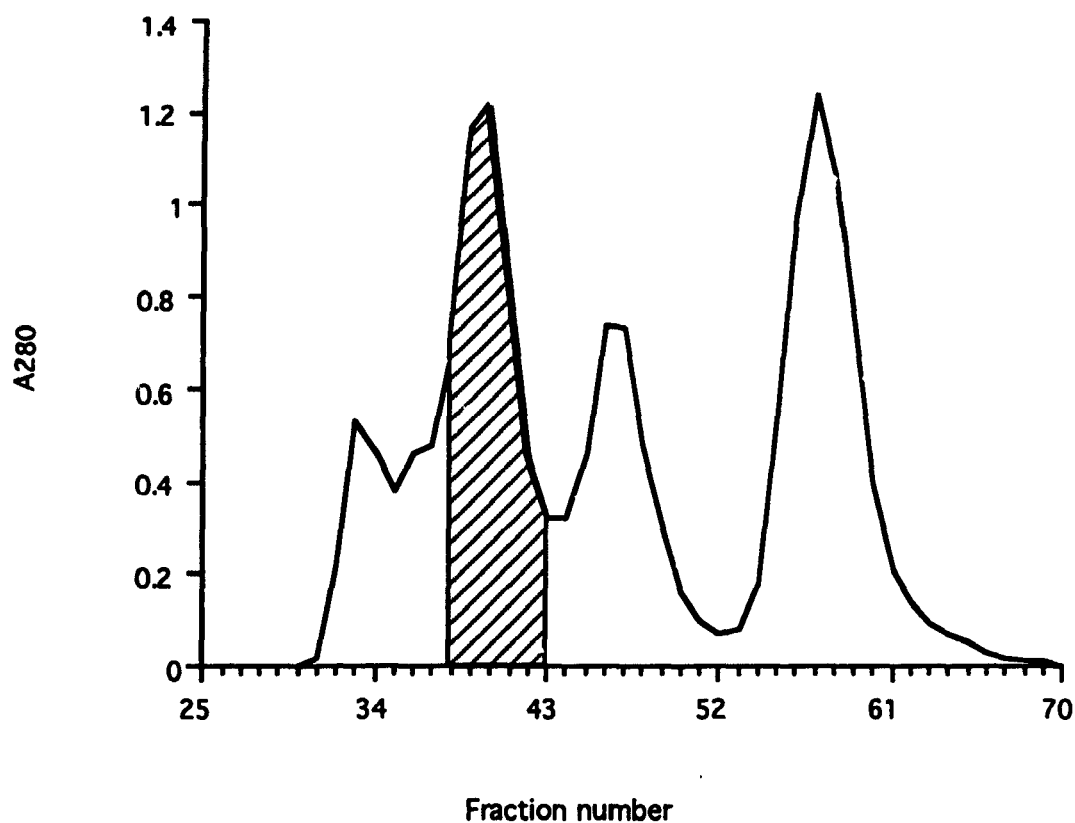


**Figure 11. Purification of a site-specific mAb K20-HSA binary conjugate by gel filtration chromatography.**

A site-specific binary conjugate was synthesized with mAb K20 and HSA using the scheme shown in Figure 10. The conjugation mixture was separated by gel filtration chromatography on Bio Gel P300 (2.5 cm x 90 cm) using an upward flow system with PBS as eluant and a flow rate of 7.5 mL/h. Fractions of 3.75 mL were collected. The shaded area represents the fractions containing purified conjugate as determined by SDS PAGE. SDS PAGE analysis of the pooled fractions is shown in Figure 12.

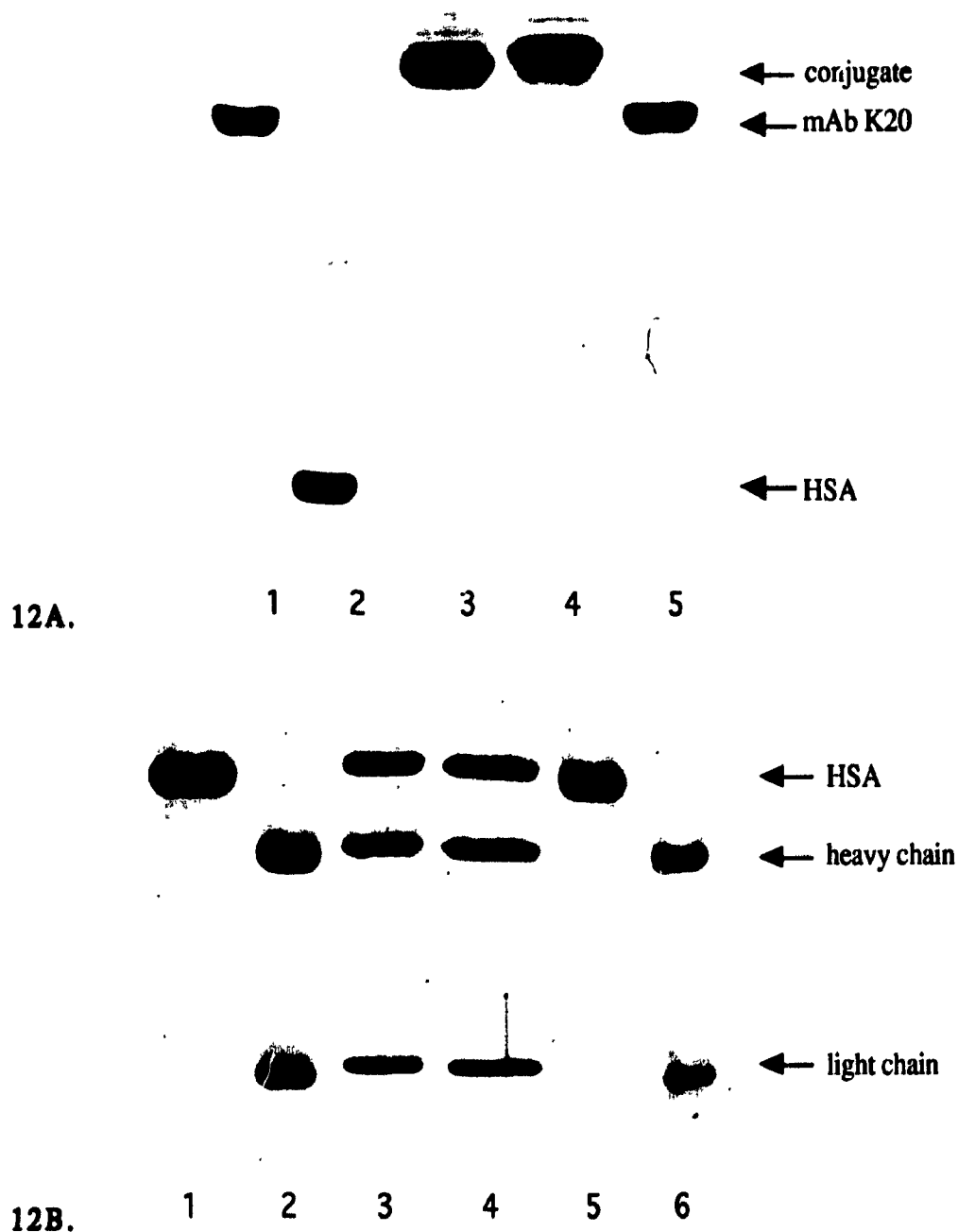


**Figure 12. Comparison of purified mAb K20-HSA site-specific and non-site-specific binary conjugates by SDS PAGE.**

Binary mAb K20-HSA conjugates were synthesized either by using the non-site-specific method as shown in Figure 16, or by the site-specific approach using mAb K20-AUPDP as shown in Figure 10 and conjugates purified by gel filtration chromatography. Purified conjugates were analyzed either under non-reducing conditions (12A) or under reducing conditions (12B).

**Figure 12A:** lanes 1 and 5, mAb K20; lane 2, HSA; lane 3, purified site-specific mAb K20-HSA conjugate; lane 4, purified non-site-specific mAb K20-HSA conjugate.

**Figure 12B:** lanes 1 and 5, HSA; lanes 2 and 6, mAb K20; lane 3, purified mAb K20-HSA site-specific conjugate; lane 4, purified mAb K20-HSA non-site-specific conjugate.

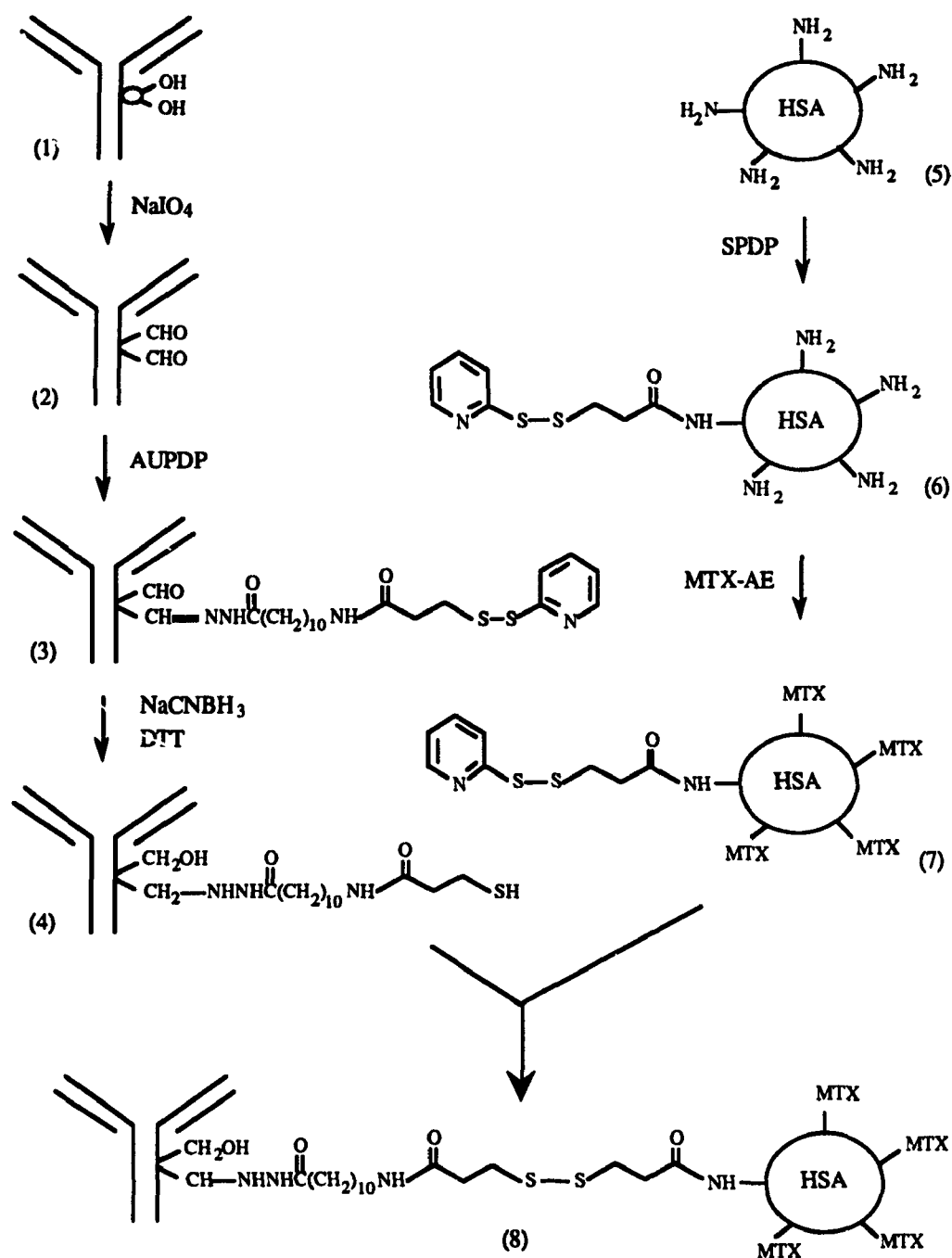


**Figure 13. Scheme for the synthesis of site-specific mAb K20-HSA-MTX ternary conjugates.**

IgG (1) carbohydrate was oxidized with sodium periodate and oxidized IgG (2) reacted with the heterobifunctional site-specific cross-linkers AUPDP or HPDP (AUPDP shown). IgG-AUPDP (3) was then treated with sodium cyanoborohydride and cross-linker disulfides reduced with DTT. HSA (5) was first derivatized with SPDP, and HSA-SPDP (6) reacted with MTX-AE to give MTX-HSA-SPDP (7). Reaction of IgG-AUPDP-SH (4) with MTX-HSA-SPDP (7) resulted in the formation of stable site-specific ternary conjugates (8).

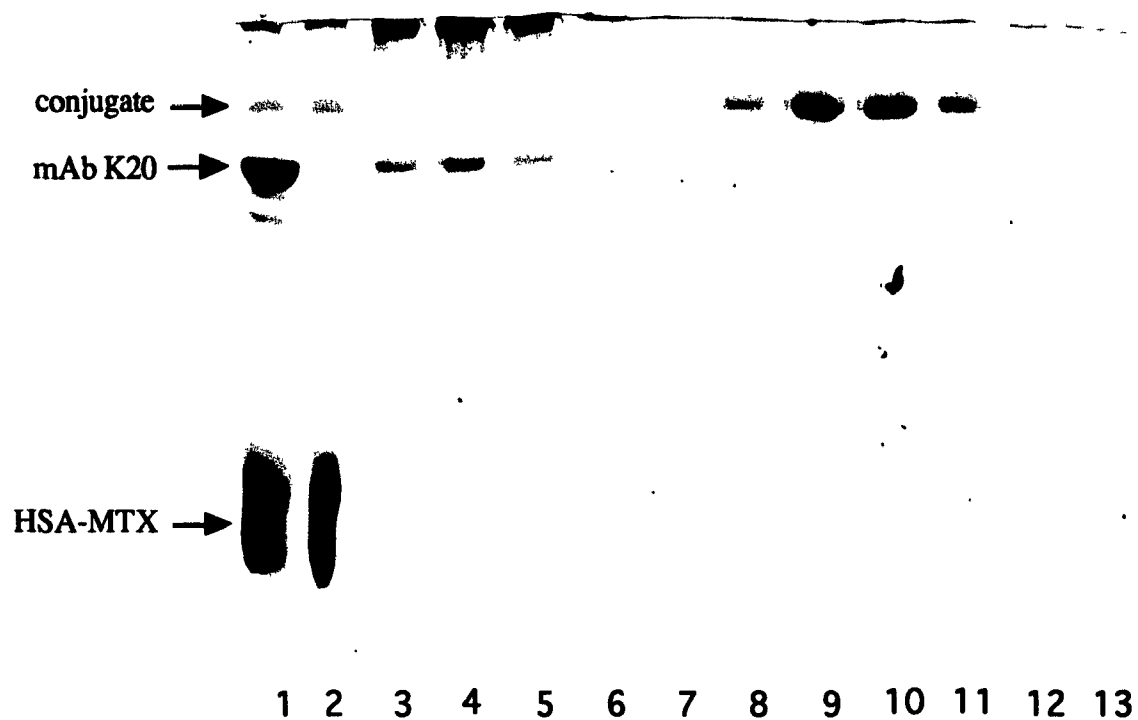


**Figure 14. SDS PAGE analysis of a site-specific mAb K20-HSA-MTX conjugation mixture and conjugate purification.**

A site-specific mAb K20 conjugate was prepared as shown in Figure 13 . The conjugate was purified by ion exchange chromatography on DEAE-Sepharose followed by gel filtration on Bio Gel P300 and collected fractions analyzed by SDS PAGE.

Lane 1, mAb K20 site-specific conjugation mixture; lane 2, mAb K20 conjugation mixture after ion exchange chromatography; lanes 3 to 13, fractions collected by gel filtration.

followed by gel filtration. Only MTX-containing species bound to the ion exchange column when the conjugation mixture was applied in PBS, with unreacted mAb K20 passing through the column. MTX-containing species were then eluted from the column using PBS containing 1.0 M NaCl. As seen in lane 2 of Figure 14, the majority of unreacted mAb K20 was removed by this method. The eluted conjugate mixture was then separated by gel filtration chromatography. Figure 14, lanes 3 to 13 show the SDS PAGE analysis of these collected fractions, and the fractions shown in lanes 8 to 11 were pooled as purified conjugate. Figure 15, lane 5 shows the pooled purified conjugate. The recovery of mAb K20 in the purified 1:1 conjugate form was 2.5% in one experiment and 1.2% in a second experiment (Table 7). These yields were substantially lower than that obtained with the binary conjugates, where 15% recovery of mAb K20 in conjugate form was achieved. The reason for these low yields may in part be related to the solubility of mAb K20-AUPDP and the final conjugates. Solutions of mAb K20-AUPDP were typically cloudy, likely due to the presence of the hydrophobic cross-linker. Following reaction with HSA however, solutions were clear, this most likely due to a solubilizing effect of HSA. HSA-MTX on the other hand, being less soluble than HSA, most likely did not contribute to the solubility of conjugates to the same degree. Another reason for the lower yields of ternary conjugates may be related to the increased steric hinderance imposed by MTX. As shown previously, the presence of MTX on HSA reduced the yield of conjugate.

It was found necessary to stabilize the hydrazone bond between mAb K20 and AUPDP prior to reaction with HSA-MTX because HSA-MTX or conjugates containing HSA-MTX precipitate at pH values below 6. Cyanoborohydride reduction at a pH above 6 was found to be inefficient, and reduction with sodium borohydride at pH 6 was found to alter the absorption spectrum of MTX, suggesting that MTX itself was reduced under these conditions. These problems were avoided by stabilizing the hydrazone bond prior to conjugation with HSA-MTX.

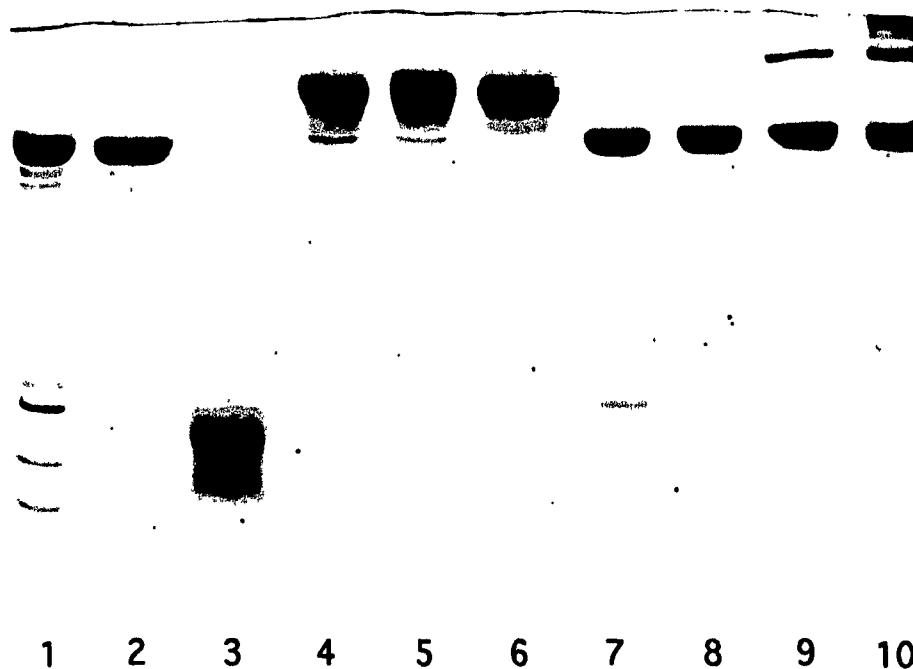


**Figure 15. SDS PAGE analysis of purified mAb K20-HSA-MTX conjugates.**

Fractions containing purified site-specific and non-site-specific mAb K20-HSA-MTX conjugates shown in Figures 14 and 17, respectively, were pooled and analyzed by SDS PAGE. Shown also are direct mAb K20 and mAb IgG1 conjugates.

Lane 1, mAb IgG<sub>1</sub>; lane 2, mAb K20; lane 3, HSA-SPDP-MTX; lane 4, purified mAb IgG<sub>1</sub>-HSA-MTX non-site-specific conjugate; lane 5, purified mAb K20-HSA-MTX site-specific conjugate; lane 6, purified mAb K20-HSA-MTX non-site-specific conjugate; lane 7, mAb IgG<sub>1</sub>-MTX (2.6)\*; lane 8, mAb IgG<sub>1</sub>-MTX (4.6); lane 9, mAb K20-MTX (4.2); lane 10, mAb K20-MTX (8.4).

\* the number in ( ) indicates the molar incorporation of MTX in direct IgG-MTX conjugates

Type of conjugate	Incorporation of MTX <sup>a</sup>	% yield of IgG in conjugate form <sup>b</sup>
<b>Direct IgG-MTX conjugates</b>		
mAb K20-MTX	4.2	77
	8.4	29
mAb IgG <sub>1</sub> -MTX	2.6	100
	4.6	99
<b>Binary conjugates</b>		
mAb K20-HSA site-specific	-	15
mAb K20-HSA non-site-specific	-	19
<b>Ternary conjugates</b>		
mAb K20 site-specific	28	2.5
mAb K20 site-specific	35	1.2
mAb IgG <sub>1</sub> non-site-specific	28	6.4
mAb K20 non-site-specific	28	11.2
mAb K20 non-site-specific	35	6.2

**Table 7. Recovery of IgG in conjugates.**

<sup>a</sup> mol MTX/mol conjugate

<sup>b</sup> amount of IgG recovered in conjugate form relative to starting amount of IgG

## **6. Non-site-specific IgG-HSA-MTX conjugates**

Conjugates between mAb K20 and HSA-MTX were also prepared using a non-site-specific approach in which the antibody was activated for conjugation with heterobifunctional cross-linkers in a random manner. These conjugates were synthesized to allow comparison with the site-specific conjugates with respect to retention of antibody binding activity and cytotoxicity toward target and non-target cell lines. A non-site-specific mAb IgG<sub>1</sub>-HSA-MTX ternary conjugate was also prepared as a control conjugate for cytotoxicity testing.

The non-site-specific heterobifunctional spacers SPDP and GMBS were used to activate mAb K20 for subsequent conjugation with thiol-containing HSA or HSA-MTX. Both spacers contain an N-succinimidyl ester which reacts with protein amino groups,

resulting in an amide linkage between spacer and IgG, and a thiol-reactive function as shown in Figure 4. SPDP contains an activated disulfide which reacts with protein thiols to form a disulfide linkage between the protein and spacer, whereas GMBS contains a maleimide group, which, upon reaction with a thiol, results in a thioether bond between the thiol-containing protein and spacer. Non-site-specific conjugates synthesized for comparison with site-specific conjugates were constructed using SPDP so as to contain the same disulfide linkage present in the site-specific conjugates. The stability of disulfide and thioether bonds is known to differ, the former being susceptible to disulfide exchange with thiol-containing compounds. To minimize the differences between the two types of conjugates, the same type of linkage within the spacers between the two proteins was used.

### **6.1 Incorporation of SPDP and GMBS spacers into IgG**

The reaction between SPDP and IgG was carried out under conditions similar to that between SPDP and HSA, where a five-fold molar excess of fresh SPDP resulted in the incorporation of two to three pyridyldithio groups per IgG. The reaction of GMBS with IgG showed a similar pattern of incorporation.

### **6.2 Non-site-specific conjugation of IgG with HSA**

Non-site-specific conjugates without MTX were prepared to allow comparison with binary site-specific conjugates. These two types of binary conjugates were compared with respect to yield and retention of antibody binding activity. The conjugation procedure used for the synthesis of non-site-specific conjugates between mAb K20 and HSA was similar to that shown in Figure 16. mAb K20 was first derivatized with SPDP to introduce pyridyldithio groups into IgG, and then reacted with HSA which had also been derivatized with SPDP and treated with DTT to release the free thiol from the pyridyldithio group. As with the site-specific binary conjugate, purification of the 1:1 binary mAb K20-HSA conjugate was achieved by gel filtration. The yield of mAb K20 in the mAb K20-HSA

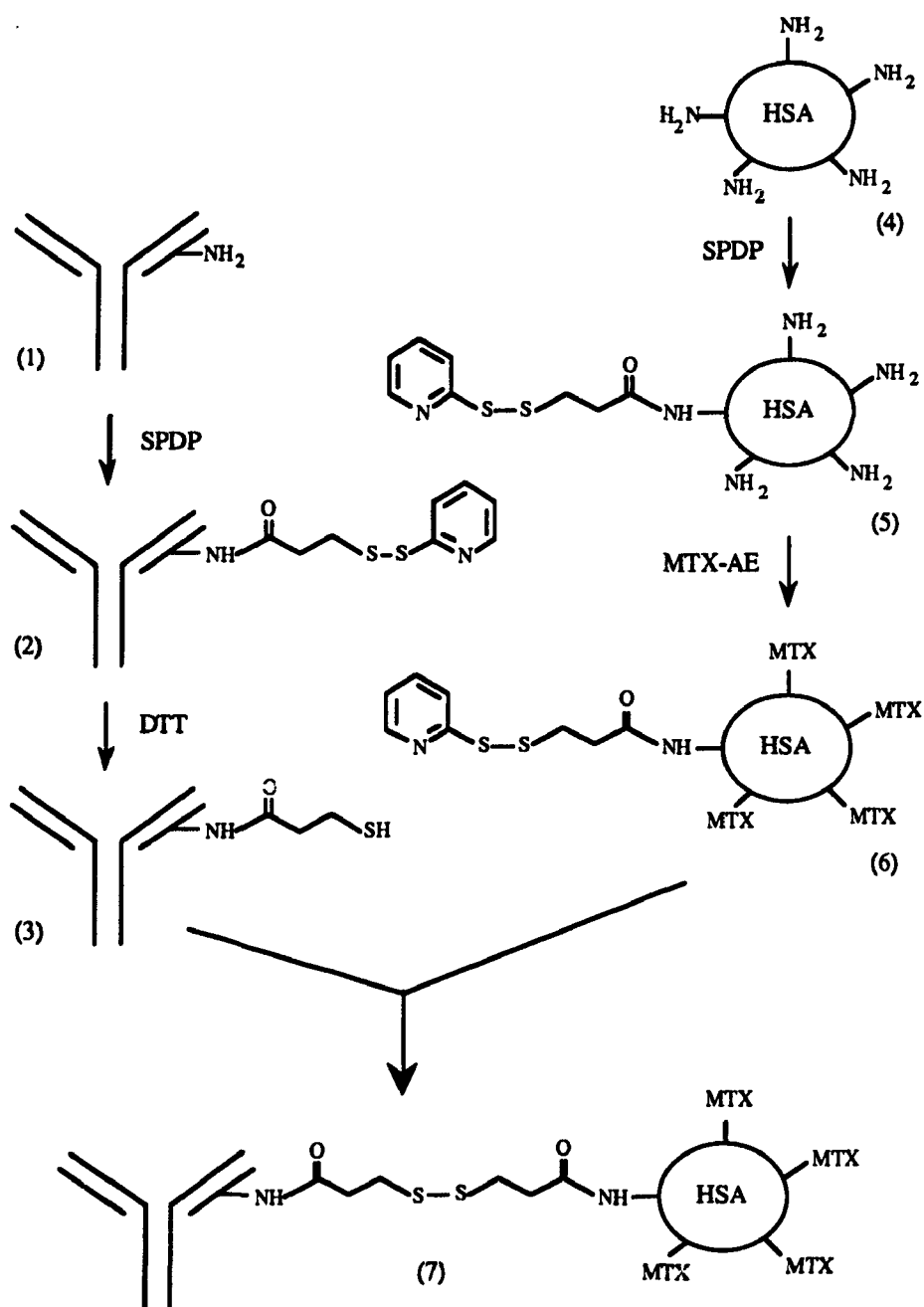


**Figure 16. Scheme for the synthesis of non-site-specific IgG-HSA-MTX ternary conjugates.**

IgG (1) and HSA (4) were both reacted with the non-site-specific cross-linker SPDP to introduce protected thiol groups. IgG-SPDP (2) was reduced with DTT to give the spacer-derived thiol group, and HSA-SPDP (5) reacted with MTX-AE to give MTX-HSA-SPDP (6). MTX-HSA-SPDP (6) was then reacted with IgG-SPDP-SH (3) resulting in the formation of non-site-specific ternary conjugates (7).

binary conjugate was 19%, this being comparable with the 15% yield obtained for the site-specific binary conjugate (Table 7). Figure 12A, lane 4 shows the high degree of purity of the conjugate isolated as seen by SDS PAGE under non-reducing conditions. In Figure 12B the conjugate was analyzed by SDS PAGE under reducing conditions where it can be seen that the conjugate breaks down into three bands (lane 4), these corresponding to the mobility of HSA and mAb K20 heavy and light chains. This was the expected pattern for a disulfide linked conjugate since the HSA-IgG disulfide bond as well as IgG interchain disulfides are reduced under these conditions.

### **6.3 Non-site-specific conjugation of IgG with HSA-MTX**

mAb K20-SPDP and mAb IgG<sub>1</sub>-SPDP were conjugated to HSA-SPDP-MTX (28 MTX/HSA) using the reaction scheme shown in Figure 16. HSA was first reacted with SPDP to introduce activated disulfides into HSA, followed by reaction with MTX-AE. IgG was also reacted with SPDP and the free thiol released from the pyridyldithio group by treatment with DTT. Thiol-containing IgG was then mixed with MTX-HSA-SPDP for conjugation of the two proteins. As with the site-specific ternary conjugates, the non-site-specific ternary conjugates were purified by a combination of ion exchange and gel filtration chromatography to isolate the 1:1 IgG:HSA ternary conjugate as shown in Figure 17 for the mAb K20 conjugate. The ion exchange step was found to be very efficient for removing unreacted IgG from the reaction mixture as can be seen by comparison of lanes 1 and 2 in Figure 17. Following ion exchange chromatography, the conjugate was separated by gel filtration as shown in lanes 3 to 11 in Figure 17. Both conjugates isolated following gel filtration were considered pure as shown in Figure 15, lanes 4 and 6 for mAb IgG<sub>1</sub> and mAb K20 conjugates respectively. Recovery of IgG in the conjugates was 6.4% for mAb IgG<sub>1</sub> and 11% for mAb K20. In a second experiment, the yield of mAb K20 in ternary conjugate form was 6.2% (Table 7). The recoveries of mAb K20 in site-specific and non-

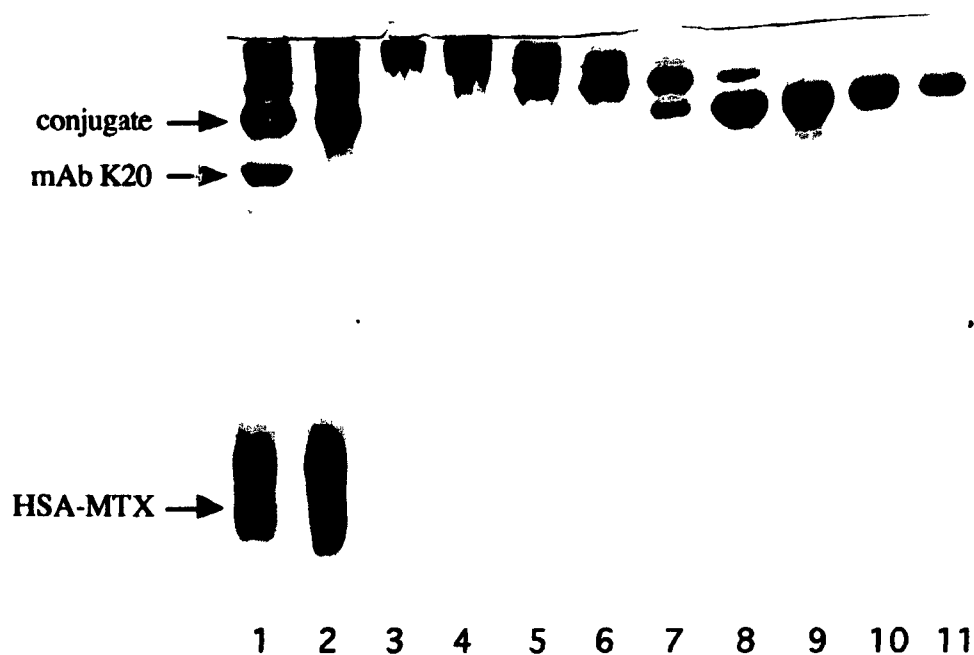


**Figure 17. SDS PAGE analysis of a non-site-specific mAb K20-HSA-MTX conjugation mixture and conjugate purification.**

A non-site-specific mAb K20 conjugate was prepared as shown in Figure 16. Conjugates were purified by ion exchange chromatography on DEAE-Sepharose followed by gel filtration on Bio Gel P-300 and fractions analyzed by SDS PAGE.

Lane 1, mAb K20 non-site-specific conjugation mixture; lane 2, mAb K20 conjugation mixture after ion exchange chromatography; lanes 3 to 11, fractions collected by gel filtration.

site-specific ternary conjugates were quite different, with yields approximately four to five times greater for non-site-specific conjugates.

## **7. Synthesis of direct IgG-MTX conjugates**

Conjugates with MTX linked directly to mAb K20 were also prepared for comparison with site-specific and non-site-specific ternary conjugates with respect to retention of antibody binding activity and cytotoxicity. mAb IgG<sub>1</sub>-MTX direct conjugates were also prepared as controls for cytotoxicity testing.

Direct IgG-MTX conjugates were synthesized by reaction of mAb IgG<sub>1</sub> or mAb K20 with MTX-AE prepared using a 1:1:1 molar ratio of MTX, DCC and NHS. The molar incorporation of MTX into IgG under these conditions was between 25% and 50% of the amount of MTX-AE added. A large amount of precipitation of mAb K20 occurred during coupling where none was seen with mAb IgG<sub>1</sub>. This loss due to precipitation is reflected in the low recovery of mAb K20 conjugates (Table 7). Yields of mAb K20 in mAb K20-MTX were 29% at an incorporation of 8.4 MTX/mAb K20 and 77% at an incorporation of 4.2 MTX/mAb K20, whereas mAb IgG<sub>1</sub> yields were 100% for similar incorporation levels. Analysis of mAb K20 and mAb IgG<sub>1</sub> conjugates by SDS PAGE following removal of unreacted MTX and precipitate showed that a substantial amount of polymerization of mAb K20 had occurred during coupling whereas there was none with mAb IgG<sub>1</sub> (Figure 15, lanes 1 and 2, and 7 to 10).

## **8. Characterization of mAb K20 conjugates**

### **8.1 Determination of the ratio of HSA-MTX to IgG**

The ratio of HSA to IgG in the isolated product was determined using a dual labelling experiment in which <sup>125</sup>I-HSA-MTX was conjugated to <sup>131</sup>I-NRG-GMBS. In this case, HSA was activated for coupling by direct reduction of HSA-MTX disulfides with DTT and allowed to react with maleimide-containing NRG. The reaction mixture was separated by SDS PAGE and stained with Coomassie Blue. The band migrating directly

above NRG was cut out and counted for both  $^{125}\text{I}$  and  $^{131}\text{I}$  from eleven different lanes. From the known specific activity of both isotopes, the ratio of HSA to NRG in these bands was calculated to be  $0.88 \pm 0.10$ . This showed that the first band from the conjugation mixture which migrated directly above IgG on SDS PAGE was the MTX-containing 1:1 HSA:IgG conjugate.

## **8.2 Evidence for carbohydrate linkage in site-specific conjugates**

In order to localize the site of the hydrazide reactivity with oxidized IgG, mAb K20 was either derivatized site-specifically by oxidation and reaction with biotin-hydrazide or non-site-specifically with a succinimidyl ester derivative of biotin. Each of these was digested with pepsin or papain and analyzed by SDS PAGE and Western blotting. It can be seen that mAb K20 modified with either form of biotin was completely digested to  $\text{F}(\text{ab}')_2$  by pepsin (lanes 1 to 4, Figure 18A). When stained for biotin, both site-specific and non-site-specifically derivatized whole antibodies stained positive (lanes 7 and 8, Figure 18A), but only the  $\text{F}(\text{ab}')_2$  from the non-site-specifically derivatized mAb stained positive (lanes 5 and 6, Figure 18A). The cleavage site for pepsin is below the interchain disulfide bonds joining the two heavy chains as shown in Figure 19. This cleavage gives rise to  $\text{F}(\text{ab}')_2$  and a number of small fragments since the  $\text{Fc}$  portion is degraded by pepsin. The lack of staining of the site-specifically derivatized mAb  $\text{F}(\text{ab}')_2$  is consistent with labelling of the oxidized carbohydrate moiety, the location of which is known to be below the interchain disulfide bonds and therefore also below the pepsin cleavage site. Under reducing conditions, both biotin-labelled whole antibodies are broken down to heavy and light chains as shown in lanes 1 and 2 of Figure 18B. When probed for biotin, both heavy and light chains were seen to be labelled approximately to the same extent with the non-site-specific biotin derivative, this being consistent with a random modification of IgG by succinimidyl ester compounds (lane 7, Figure 18B). The site-specific biotin-mAb K20

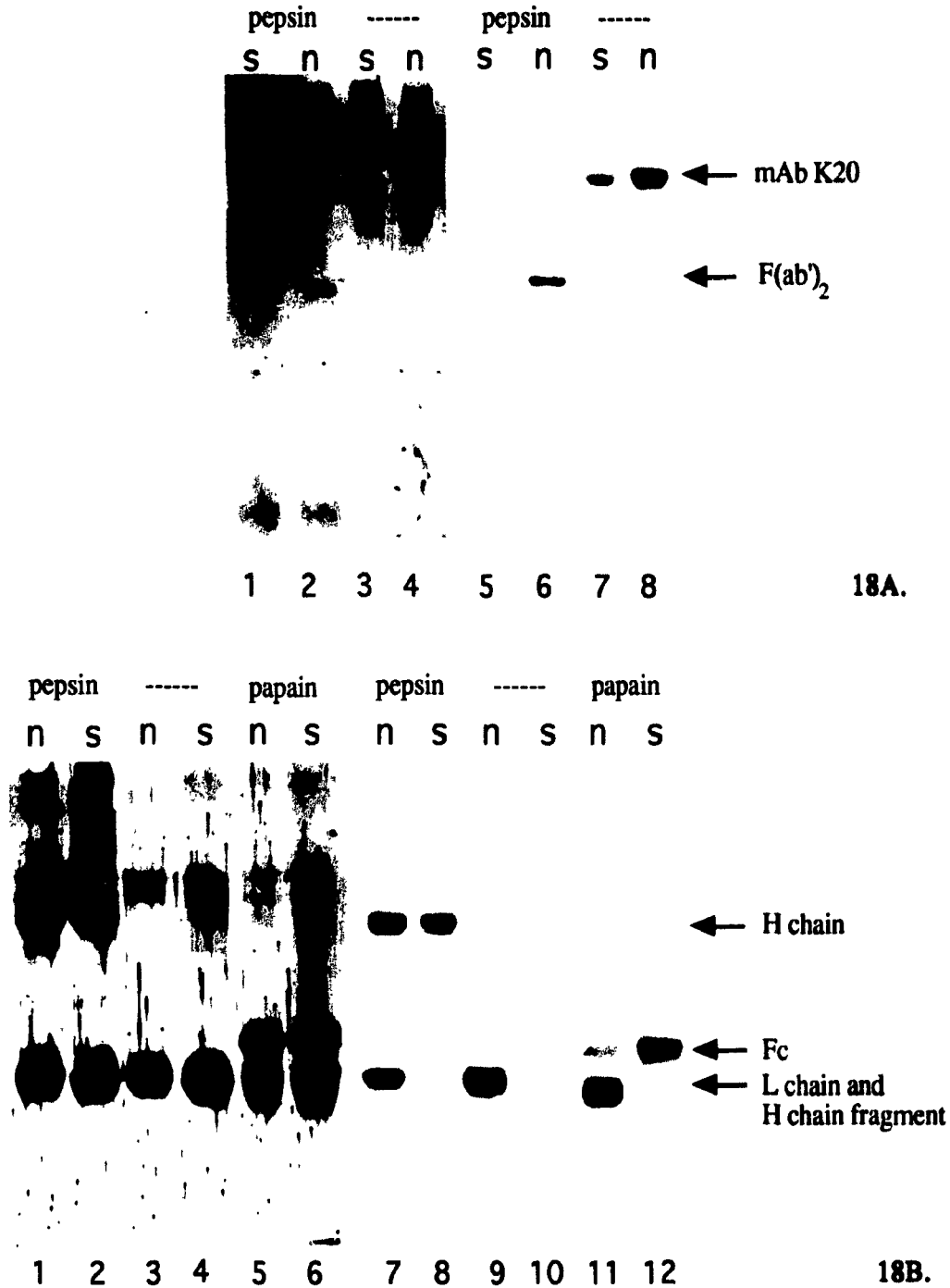


**Figure 18. Localization of sites on mAb K20 reactive toward site-specific and non-site-specific derivatives of biotin.** mAb K20 was labelled site-specifically with biotin hydrazide (s) or non-site-specifically with sulfosuccinimidyl 6-(biotinamido)hexanoate (n), digested with papain or pepsin, separated by SDS PAGE either under non-reducing (7% gels, 18A) or reducing (12% gels, 18B) conditions. Gels were run in duplicate, transferred to nitrocellulose and either stained for total protein with India ink (left panels) or for biotin with extravidin-peroxidase (right panels). H chain, heavy chain of IgG; L chain, light chain of IgG.

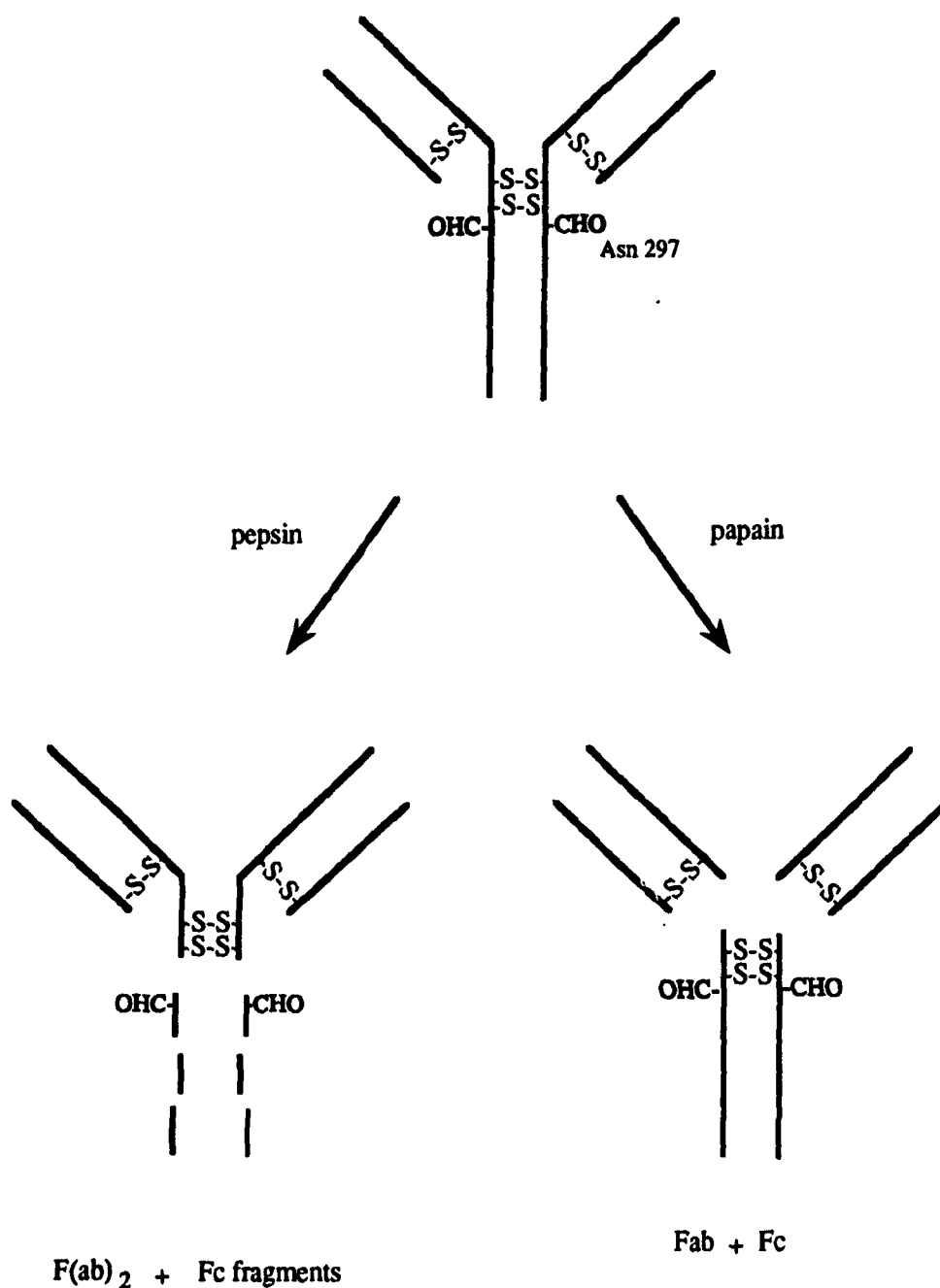


**Figure 19. Digestion of mouse IgG1 by pepsin and papain.** Pepsin cleaves mouse IgG1 below the interchain disulfide bonds linking the two heavy chains resulting in the production of F(ab')<sub>2</sub>, with a molecular weight of approximately 100 kDa. The Fc portion contains additional pepsin cleavage sites and is degraded to low molecular weight fragments. Papain cleaves at a site above the interchain disulfide bonds resulting in the formation of two identical Fab fragments and an Fc fragment, each of approximately 50 kDa.

showed labelling of the heavy chain only, again supporting the presumption of specific carbohydrate labelling by hydrazides (lane 8, Figure 18B). Pepsin-digested samples analyzed under reducing conditions (lanes 3 and 4, Figure 18B) showed that both the light chain and the heavy chain fragments appear to migrate the same distance on these gels. As expected, only the non-site-specifically labelled sample stained positive for biotin since it was shown that the biotin label is in the degraded Fc fragment in the site-specific sample (lanes 9 and 10, Figure 18B). Analysis of papain-digested samples under reducing conditions (lanes 5 and 6) shows two bands staining for total protein, one with a migration position expected for the light chain and a second slower migrating species. This second band stained positive for biotin in the site-specific sample (lane 12), and therefore represents the Fc portion of mAb K20 since it was established with the pepsin digests (Figure 18A) that the biotin label must be in this portion of the molecule for the site-specific sample. In the non-site-specific case, the intensity of the lower band is much greater than that of the Fc band. The lower band contains both the light chain and that portion of the heavy chain above the papain cleavage site since it was shown in lanes 3 and 4 of Figure 18B that a similar sized fragment, namely the portion of the heavy chain above the pepsin cleavage site, migrates with the light chain. The difference in staining intensities between Fc and Fab fragments with the non-site-specific biotin derivative indicates a preference for reaction with the Fab portion of mAb K20.

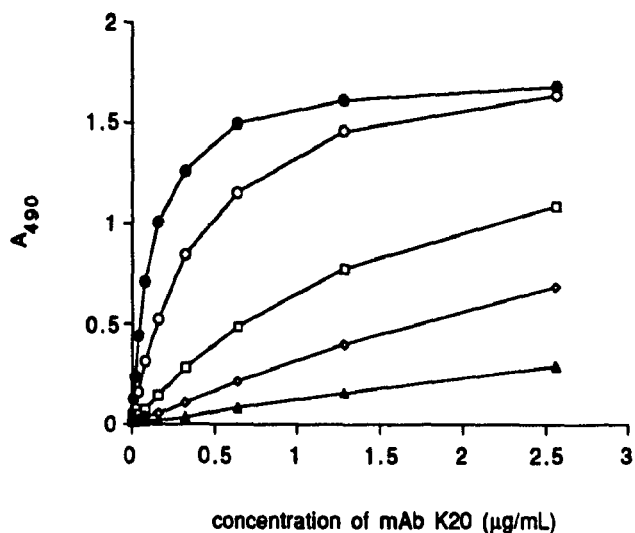
### **8.3 Effect of modifications and conjugation on mAb K20 binding activity**

The retention of mAb K20 binding activity was determined after each step in conjugate synthesis. Antibody binding activity was assessed initially using a direct cell-binding assay in which fixed Caki-1 cells in 96-well ELISA plates were used as the source of antigen and incubated with either dilutions of native mAb K20 or modified mAb K20. The amount of mAb K20 bound to cells was then determined using a second anti-mouse IgG antibody containing a peroxidase label. The assumption made in this assay is that all

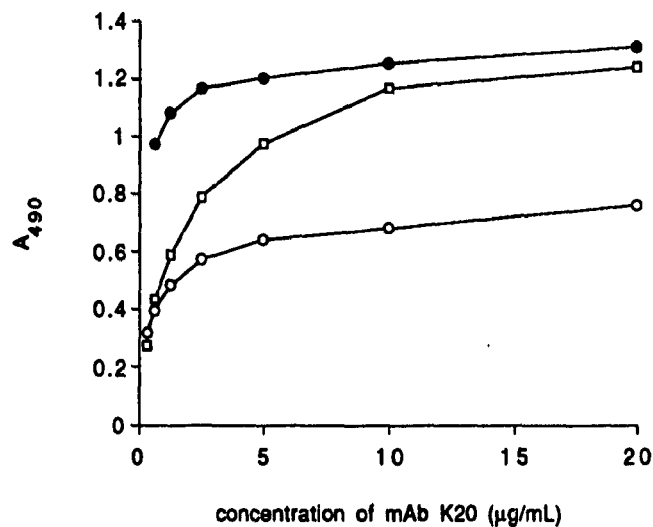
cell-bound mAb K20, either native or modified, is recognized by the second antibody with the same efficiency, and therefore that peroxidase activity and colour production are proportional to the amount of mAb K20 present. An example of this analysis is shown in Figure 20A, where direct mAb K20-MTX conjugate binding was examined. It is apparent from the binding curves that increased loading of MTX resulted in decreased binding of the conjugate. Antibody binding activity results for all conjugates are summarized in Table 8. Binding activity was 35% and 8% of that of native mAb K20 at incorporation levels of 4 and 8 mol MTX/mol mAb K20, respectively. Radioiodination of mAb K20 to a level similar to that used for IRF determination was found to have no effect on antibody activity.

mAb K20-HSA binary conjugates prepared site-specifically or non-site-specifically were also compared with native antibody using this direct cell-binding assay (Figure 20B). The binding curve for the non-site-specific conjugate exhibited a plateau at a level similar to that for native mAb, whereas the curve for the site-specific conjugate gave a plateau at a value approximately half that of native antibody. These differences in saturation indicated that the two conjugates were not recognized by the second antibody to the same extent, and therefore that this type of assay was not appropriate to assess antibody activity in site-specific conjugates.

In order to define the retention of binding activity in mAb K20-HSA conjugates, an assay based on competitive binding was developed. Initially, the assay used was one in which a fixed amount of  $^{125}\text{I}$ -labelled mAb K20 was allowed to compete for binding to Caki-1 cells with increasing amounts of either native mAb or mAb K20-HSA conjugates as shown in Figure 21. Comparison of the  $\text{IC}_{50}$  values of these three samples showed that the non-site-specific mAb K20-HSA retained 9% activity and the site-specific conjugate retained 32% activity relative to native mAb K20 (Table 8). These findings confirmed that the ELISA based assay was not appropriate to assess binding activity in site-specific conjugates, although it appears to be valid for non-site-specific conjugates and direct conjugates.



20A.



20B.

**Figure 20. Analysis of binding of conjugates by ELISA.**

Direct mAb K20-MTX conjugates (20A) and mAb K20-HSA binary conjugates (20B) at the concentrations shown were incubated with Caki-1 cells in 96-well ELISA plates. Binding was quantitated using goat anti-mouse IgG-peroxidase conjugate and o-phenylenediamine to detect peroxidase activity as described in Section 14.1 under Materials and Methods. Peroxidase activity was quenched with 2.5 M H<sub>2</sub>SO<sub>4</sub> and the absorbance at 490 nm measured in an ELISA plate reader.

**Figure 20A:** native mAb K20 (filled circles) was compared with direct conjugates containing: 3.7 (open circles), 8 (open squares), 13 (open diamonds), and 17 (filled triangles) moles MTX per mole mAb K20.

**Figure 20B:** native mAb K20 (filled circles) was compared with the non-site-specific mAb K20-HSA binary conjugate (open squares), and the site-specific mAb K20-HSA binary conjugate (open circles).

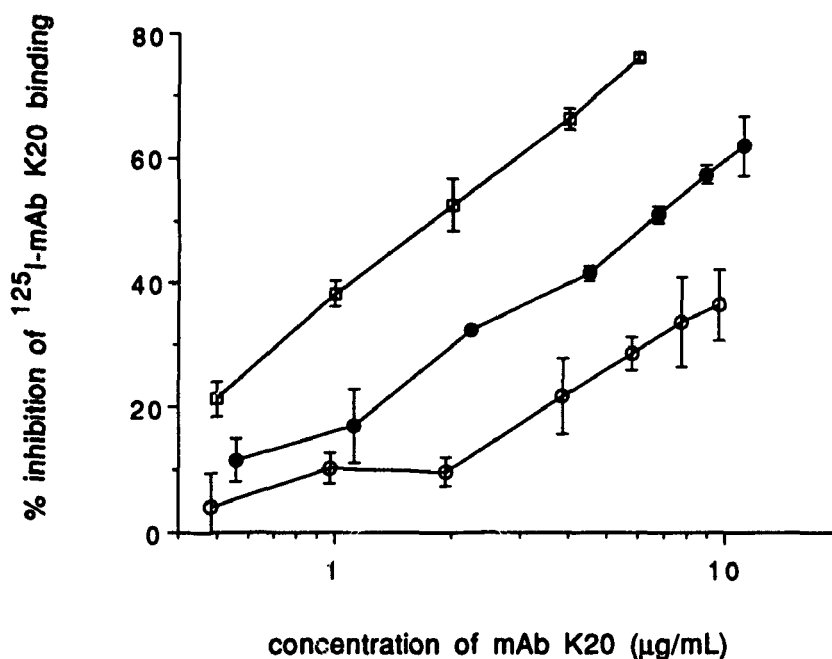


**Figure 21. Competitive binding of binary conjugates measured with  $^{125}\text{I}$ -mAb K20.**

Conjugates or native mAb K20 were mixed with  $^{125}\text{I}$ -mAb K20 ( $3.38 \mu\text{Ci}/\mu\text{g}$ ) to give a final concentration of  $1.25 \mu\text{g}/\text{mL}$  radiolabelled mAb K20 and the concentrations indicated for native and conjugated mAb K20. Duplicate samples were incubated with Caki-1 cells in test tubes at  $4^\circ\text{C}$  for 2h, cells washed, and cell-associated radioactivity measured in a gamma counter. The percent inhibition of  $^{125}\text{I}$ -mAb K20 binding was determined as described in Section 14.1 under Materials and Methods. Error bars represent the standard deviation from duplicate determinations. Native mAb K20 (open squares), non-site-specific mAb K20-HSA binary conjugate (open circles), site-specific mAb K20-HSA binary conjugate (filled circles).

A second competition assay was developed for the routine measurement of antibody activity. mAb K20 was derivatized with a succinimidyl ester derivative of biotin and allowed to compete for cell binding with either native mAb K20 or conjugates, and the amount of biotinylated mAb K20 bound detected with avidin-peroxidase. This assay proved to be more convenient than the  $^{125}\text{I}$ -mAb K20-based competition method since the assay could be performed in ELISA plates. Using this assay system, mAb K20-HSA-MTX ternary conjugates were evaluated as shown in Figure 22. It is apparent that the site-specific conjugate retained more activity than the non-site-specific conjugate, since a lower concentration of the former was required to inhibit binding of mAb K20-biotin. Analysis of these results showed that the site-specific conjugate retained 56% activity and the non-site-specific conjugate retained 11% activity. Results from this and other competition experiments are summarized in Table 8. Site-specific conjugates had binding activities ranging from 32% to 56% relative to native mAb K20, whereas all non-site-specific conjugates, whether binary or ternary, had binding activities in the range of 9% to 16%. The large loss of activity seen with non-site-specific conjugates is not surprising considering that simply reacting mAb K20 with SPDP resulted in a 60% loss of activity. Both oxidation with 150 mM periodate and reduction with 15 mM cyanoborohydride had no effect on mAb K20 binding activity but the incorporation of AUPDP resulted in a 34% loss of activity. It would be expected that AUPDP incorporation should not affect binding if it is in the carbohydrate moiety. A possible explanation for the observed loss of activity is that the hydrophobic nature of the spacer resulted in aggregation or precipitation of the modified mAb during the assay, rather than the spacer exerting a direct effect on binding activity.

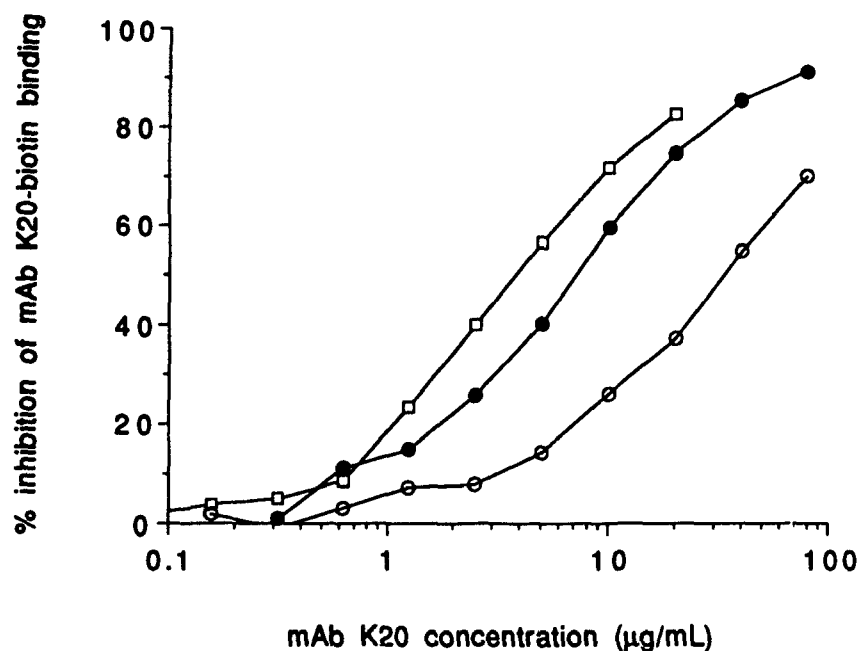


**Figure 22. Competitive binding of ternary conjugates measured with mAb K20-biotin.**

Conjugates or native mAb K20 were mixed with mAb K20-biotin to give a final concentration of 2.5 µg/mL mAb K20-biotin and the concentrations indicated for native mAb K20 and conjugates. Triplicate samples were incubated with Caki-1 cells in 96-well ELISA plates. Plates were washed after 1 h and the extent of mAb K20-biotin binding was measured by incubation with avidin-peroxidase, and peroxidase activity detected with o-phenylenediamine. Colour development was quenched after 10 min with 2.5 M H<sub>2</sub>SO<sub>4</sub> and the absorbance at 490 nm measured in a ELISA plate reader. Percent inhibition of mAb K20-biotin binding was calculated as described in Section 14.1 under Materials and Methods. Native mAb K20 (open squares), non-site-specific mAb K20-HSA-MTX ternary conjugate (open circles), site-specific mAb K20-HSA-MTX site-specific conjugate (filled circles).

Type of mAb K20 conjugate or chemical modification	% activity <sup>a</sup> (ELISA <sup>b</sup> )	% activity <sup>a</sup> (competition <sup>c</sup> )
<b>Direct MTX conjugates</b>		
4 MTX/mAb	34.5 ± 0.8	
8 MTX/mAb	8.3 ± 0.1	
13 MTX/mAb	2.9 ± 0.1 <sup>d</sup>	
4 MTX/mAb		28.2 ± 0.3
8 MTX/mAb		7.1 ± 0.4
<b>Ternary conjugates</b>		
non-site-specific, 28 MTX/mAb		10.6 ± 0.5
non-site-specific, 35 MTX/mAb		15.8 ± 1.4
site-specific, 28 MTX/mAb		56.1 ± 3.8
site-specific, 35 MTX/mAb		35.1 ± 2.9
<b>Binary conjugates</b>		
non-site-specific	11.1 ± 0.3	9.36 ± 0.01 <sup>d,e</sup>
site-specific	6.5 ± 0.3	32.2 ± 1.4 <sup>e</sup>
<b>Chemical modifications</b>		
<sup>125</sup> I labelling at 0.54 μCi/μg	106.4 ± 7.6	
periodate oxidation		97.3 ± 4.5
oxidation and BH <sub>3</sub> reduction		92.6 ± 7.6
oxidation and AUPDP incorporation		65.7 ± 4.5
SPDP incorporation		40.4 ± 0.3

**Table 8. Retention of mAb K20 binding activity following chemical modification and conjugation.**

<sup>a</sup> activity ± SD expressed as percentage of activity relative to native mAb K20.

<sup>b</sup> ELISA was by direct cell binding assay with detection by goat anti-mouse-peroxidase.

<sup>c</sup> competition with mAb K20-biotin.

<sup>d</sup> activity determined from the amount of mAb K20 required to give one third saturation.

<sup>e</sup> competition with <sup>125</sup>I mAb K20.

#### 8.4 DHFR inhibition by MTX-containing conjugates

The effect of incorporation of MTX into both HSA and IgG on the ability of MTX to inhibit DHFR was studied using the method of Peterson (189) with the exception that the assay was performed at pH 7.5 instead of pH 5.0. This change in pH was necessary because HSA-MTX or ternary conjugates containing HSA-MTX precipitate at pH values below 6. Increasing concentrations of either free or conjugated MTX were incubated with DHFR prior to addition of dihydrofolate, and the concentration of MTX required to inhibit DHFR activity by 50% (IC<sub>50</sub>) was determined.

Conjugate	Incorporation of MTX <sup>a</sup>	DHFR IC <sub>50</sub> <sup>b</sup> (nM MTX)
<b>MTX</b>	-	0.5
<b>Direct conjugates</b>		
mAb K20	8.4	235
mAb K20	4.2	169
mAb IgG <sub>1</sub>	4.6	184
mAb IgG <sub>1</sub>	2.6	202
HSA-MTX	28	443
<b>Ternary conjugates</b>		
non-site-specific mAb K20	28	405
non-site-specific mAb IgG <sub>1</sub>	28	477
site-specific mAb K20	28	393

**Table 9. DHFR inhibition by MTX-containing conjugates.**

<sup>a</sup> mol MTX/mol IgG or mol MTX/mol HSA

<sup>b</sup> concentration of MTX to give 50% inhibition of DHFR activity

As shown in Table 9, the general trend was that the IC<sub>50</sub> increased as the molar incorporation of MTX into IgG or HSA increased. All direct IgG-MTX conjugates with incorporations between 3 and 8 MTX/IgG had an IC<sub>50</sub> of approximately 200 nM and all ternary conjugates as well as HSA-MTX had an IC<sub>50</sub> of approximately 400 nM. These high values for conjugated MTX relative to free MTX (IC<sub>50</sub> of 0.5 nM) indicate that MTX bound to protein is a much weaker inhibitor of DHFR compared to free MTX.

### 8.5 Cytotoxicity of MTX-containing conjugates

mAb K20 and mAb IgG<sub>1</sub> conjugates were compared with respect to cytotoxicity toward a target cell line for mAb K20 (Caki-1) and a cell line toward which neither mAb displayed any specificity (D10-1). Cells from both lines were incubated with increasing amounts of either free or conjugated MTX for 6 h, after which the test agent was removed and replaced with growth medium. The number of Caki-1 cells per treatment group was determined after 3 days by using the crystal violet assay, and the numbers of D10-1 cells determined by direct counting of cells. Crystal violet staining was found to be directly proportional to the number of cells present in the range used in the cytotoxicity assays. As shown in Table 10, the concentration required to inhibit growth by 50% (the IC<sub>50</sub>) of free MTX was 0.5  $\mu$ M for both cell lines whereas the IC<sub>50</sub> for all conjugates was substantially greater, indicating that all were less cytotoxic than free MTX toward either cell line. Of all the conjugates tested, the site-specific mAb K20-HSA-MTX ternary conjugate was found to be the most effective in inhibiting the growth of Caki-1 cells with an IC<sub>50</sub> of 11  $\mu$ M, or 24 times that of free MTX. The site-specific conjugate was twice as effective as the non-site-specific mAb K20 conjugate (IC<sub>50</sub> of 25  $\mu$ M), indicating that the greater antibody binding activity in the site-specific conjugate (56% versus 11%) resulted in greater cytotoxicity since both conjugates contained an equivalent amount of MTX. Both these conjugates were more potent than either HSA-MTX or the mAb IgG<sub>1</sub>-HSA-MTX control conjugate, showing that conjugation to mAb K20 resulted in specificity toward Caki-1 cells. In the case of direct mAb K20-MTX conjugates, there was no correlation between antibody activity and cytotoxicity since the conjugate containing 8 MTX/mAb K20 was more cytotoxic than the conjugate containing 4 MTX/mAb K20, although the latter retained four times the antibody binding activity. The control mAb IgG<sub>1</sub>-MTX direct conjugates also showed considerable cytotoxicity against Caki-1 cells and were found to be as potent as the mAb K20 direct conjugates. However, unlike the mAb IgG<sub>1</sub> direct conjugates, the

Conjugate	MTX incorporation <sup>a</sup>	Retention of antibody activity (%)	IC <sub>50</sub> <sup>b</sup> for Caki-1 cells (μM MTX)	Sensitivity ratio <sup>c</sup> for Caki-1 cells	IC <sub>50</sub> <sup>b</sup> for D10-1 cells (μM MTX)	Sensitivity ratio <sup>c</sup> for D10-1 cells	Selectivity ratio <sup>d</sup>
<b>direct</b>							
mAb K20	4.2	28.2 ± 0.3	55.5 ± 0.6	116	39.2 ± 2.6	80	1.5
mAb K20	8.4	7.1 ± 0.4	33.9 ± 1.6	71	55.2 ± 11.6	113	0.6
mAb IgG1	2.6	--	31.0 ± 0.9	65	9.3 ± 0.8	19	3.4
mAb IgG1	4.6	--	40.5 ± 1.1	84	21.6 ± 1.6	44	1.9
<b>ternary</b>							
site-specific mAb K20	28	56.1 ± 3.8	11.4 ± 0.9	24	23.9 ± 2.9	49	0.5
non-site-specific mAb K20	28	10.6 ± 0.5	25.4 ± 0.6	53	21.22 ± 2.8	43	1.2
non-site-specific mAb IgG1	28	--	104.2 ± 7.3	217	26.12 ± 18.4	53	4.1
<b>HSA-MTX</b>	28	--	59.2 ± 1.9	123	55.2 ± 8.9	113	1.1
<b>MTX</b>	--	--	0.48 ± 0.04	--	0.58 ± 0.13	--	--

**Table 10. Cytotoxicity of conjugates toward Caki-1 and D10-1 cells.**

<sup>a</sup> mol MTX/mol protein.

<sup>b</sup> concentration of MTX ± SD required to inhibit growth by 50% following 6 h pulse exposure as described in Section 14.2 of Materials and Methods.

<sup>c</sup> IC<sub>50</sub> for conjugate/IC<sub>50</sub> for free MTX.

<sup>d</sup> sensitivity ratio for Caki-1 cells/sensitivity ratio for D10-1 cells.

control mAb IgG<sub>1</sub>-HSA-MTX ternary conjugate showed very little cytotoxicity in this assay.

In testing for cytotoxicity toward the non-target D10-1 cell line, all three ternary conjugates were found to be equally potent with an IC<sub>50</sub> value approximately 50 times that of free MTX. mAb K20 direct conjugates were from 80 to 110 times less potent than free MTX whereas mAb IgG<sub>1</sub> direct conjugates were from 20 to 40 times less potent than free MTX. Taken together, these results indicate that the site-specific ternary conjugate was the most potent conjugate to target cells and showed some specificity since it was less cytotoxic to non-target cells.

### **8.6 Long term stability of mAb K20-HSA binary conjugates**

Binary site-specific and non-site-specific mAb K20-HSA conjugates as shown in Figure 12A, lanes 3 and 4, respectively, were analyzed by SDS PAGE after storage for 16 months at 4 °C. Comparison of lanes 2 and 3 in Figure 23 for site-specific and non-site-specific conjugates, respectively, shows that both conjugates exhibited some breakdown after long term storage. Both contained small amounts of material migrating at positions expected for mAb K20 and HSA along with a band migrating between these two. The conjugates appear to show both a similar degree and pattern of breakdown.

## **9. Characterization of native mAb K20**

### **9.1 Isolation of mAb K20**

mAb K20 was isolated from ascites fluid either by caprylic acid precipitation or Protein A chromatography. Average yields of mAb K20 were 1.2 mg/mL ascites by caprylic acid and 2.7 mg/mL ascites by Protein A affinity chromatography. Purity of mAb K20 isolated by both techniques was comparable as seen by SDS PAGE. Typical patterns for purified mAb K20 are shown in Figure 15, lane 2 and Figure 12A, lane 1.

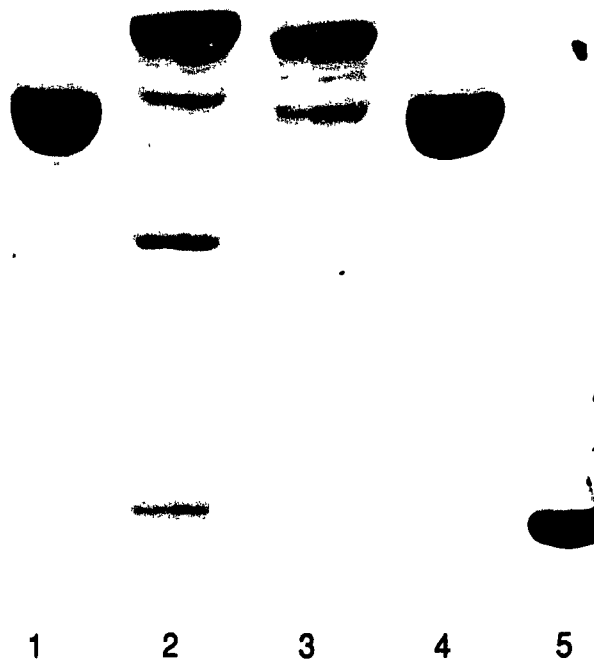


**Figure 23. Long term stability of site-specific and non-site-specific mAb K20-HSA binary conjugates.**

The purified site-specific and non-site-specific binary mAb K20-HSA conjugates shown in Figure 12 were stored at 4 °C in PBS containing 0.02% (w/v) sodium azide for 16 months and analyzed by SDS PAGE under non-reducing conditions.

Lanes 1 and 4, mAb K20; lane 2, site-specific mAb K20-HSA binary conjugate; lane 3, non-site-specific mAb K20-HSA binary conjugate; lane 5, HSA.

## 9.2 Immunoreactive Fraction

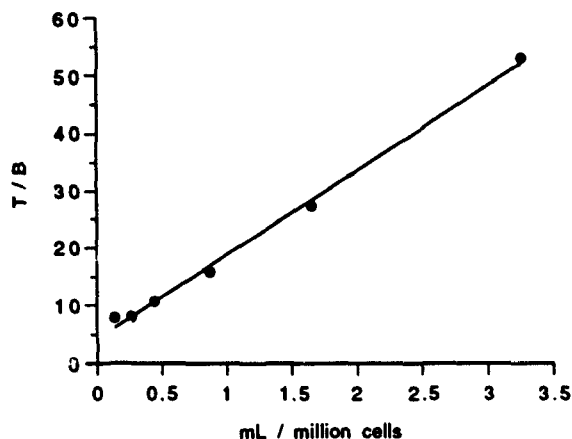
The immunoreactive fraction (IRF) of mAb K20 was measured using the method of Lindmo and Bunn(45) in which increasing concentrations of Caki-1 cells were incubated with either  $^{125}\text{I}$ -labelled mAb K20 or mAb IgG<sub>1</sub> at 4 °C. Non-specific binding as measured by mAb IgG<sub>1</sub> binding, was subtracted from mAb K20 counts to determine the amount of specific binding. For determination of IRF, the inverse of the cell concentration was plotted against the inverse of the fraction bound (T/B where T is total counts added and B is the counts bound) as shown in Figure 24A. Extrapolation to the intercept with the ordinate gives the theoretical amount of mAb K20 which is capable of binding to cells at infinite antigen excess. As shown in Figure 24A, extrapolation to infinite antigen excess gives an IRF of 0.24, indicating that 24% of the antibody molecules in the preparation are capable of binding to Caki-1 cells. These data were also plotted as T/B versus the inverse of the number of free binding sites per sample to correct for the lack of antigen excess (not shown). The value of  $3.5 \times 10^5$  binding sites per cell (see below) was used to calculate the total number of free sites. Results taking this correction factor into account were comparable to the IRF obtained without correction.

## 9.3 Number of bindings sites and apparent affinity constant for Caki-1 cells.

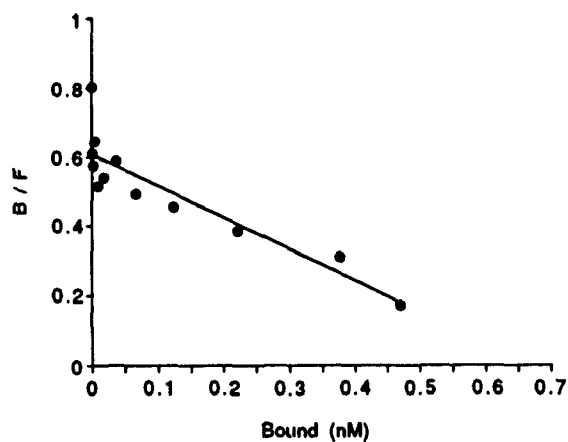
$^{125}\text{I}$ -mAb K20 binding to target Caki-1 cells was also examined by Scatchard analysis. In this case, Caki-1 cells were incubated with increasing amounts of  $^{125}\text{I}$ -labelled mAb K20 at 4 °C to decrease endocytosis of bound antibody. The binding data were corrected for the IRF of mAb K20 (0.24) and the Scatchard plot of this data is shown in Figure 24B. From these data, it was determined that mAb K20 has an apparent  $K_a$  of  $9.1 \times 10^8 \text{ M}^{-1}$  for Caki-1 cells and  $3.5 \times 10^5$  binding sites are present per cell.

#### **9.4 IEF of mAb K20**

mAb K20 was subjected to isoelectric focusing under either denaturing conditions in the presence of urea or under native conditions. In the former case a pH gradient of 3 to 10 was used to resolve different molecular species in the preparation. As seen in lane 1 of Figure 25, Protein A-purified mAb K20 shows the presence of three major bands in the pI range from 7.0 to 8.1. Under native conditions using a pH gradient of 5 to 8, mAb K20 showed at least four bands, with two major bands in the center and a minor band on either side of the major bands (not shown).



24A.



24B.

**Figure 24. Analysis of mAb K20 binding to Caki-1 cells.**

**Figure 24A:** The immunoreactive fraction of mAb K20 was determined by incubating the dilutions of cells shown with  $^{125}\text{I}$ -mAb K20 ( $0.18 \mu\text{g}$ ,  $0.27 \mu\text{Ci}/\mu\text{g}$ ) in a total volume of  $0.3 \text{ mL}$  at  $4^\circ\text{C}$ . Cells were washed after  $1 \text{ h}$  and cell-associated radioactivity determined. Counts were corrected for non-specific binding as determined by incubation of cells with with an equivalent amount of  $^{125}\text{I}$ -mAb IgG1. The inverse of the fraction of counts bound (B) relative to total counts added (T) at each cell concentration is plotted against the inverse of the cell concentration. Extrapolation to the ordinate represents the inverse of the theoretical amount of mAb K20 bound at infinite antigen excess. The IRF was found to be  $0.24$ .

**Figure 24B:** The apparent affinity constant and number of binding sites for mAb K20 on Caki-1 cells was determined by Scatchard analysis. Serial dilutions of  $^{125}\text{I}$ -labelled mAb K20 ( $3.38 \mu\text{Ci}/\mu\text{g}$ ) were added to  $4.56 \times 10^5$  Caki-1 cells at  $4^\circ\text{C}$  in a total volume of  $0.4 \text{ mL}$  to give a range of  $0.4$  to  $770 \text{ ng}$  of mAb K20 added. After  $90 \text{ min}$ , cells were washed and cell-associated radioactivity determined. The ratio of bound mAb K20 (B) to free mAb K20 (F) was plotted against the amount bound. The apparent  $K_a$  was determined from the negative slope of the line, and the maximum amount of binding determined by extrapolation to the abscissa. The free mAb K20 concentration was corrected according to the IRF determined in Figure 24A. No correction for non-specific binding was made as this was found to be negligible. mAb K20 was found to have an apparent  $K_a$  of  $9.1 \times 10^8 \text{ M}^{-1}$  and  $3.5 \times 10^5$  binding sites were present per cell.

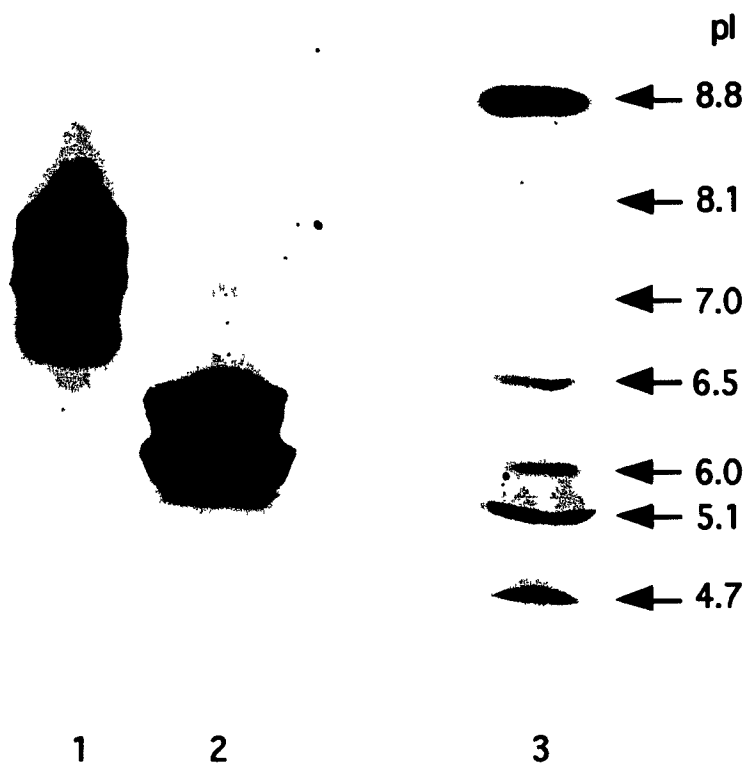


**Figure 25. Isoelectric focusing (IEF) analysis of mAb K20.**  
mAb K20 isolated from ascites fluid was analyzed by IEF under denaturing conditions using a pH gradient from 3 to 10 in the presence of 8 M urea.

Lane 1, purified mAb K20; lane 2, mAb K20 hybridoma culture supernatant; lane 3, IEF standards.

#### **IV. Discussion**

It is generally recognized that to be therapeutically effective, drug-antibody conjugates should incorporate relatively large amounts of drug and yet retain antigen binding activity. The majority of drug-antibody conjugates synthesized to date have focused on the direct incorporation of drug into the antibody molecule. Overall, this approach appears to be limited since antibody activity typically decreases with increased drug loadings (1,73). In an attempt to prepare more potent drug-antibody conjugates for targeted therapy, two approaches were taken in the present study. The first was the use of a carrier which was loaded with drug and linked to an anti-tumor IgG antibody. Such a method of drug linkage was predicted to minimize the loss of antibody activity while at the same time increasing the amount of drug load per antibody molecule. Second, the drug-loaded carrier was linked to the carbohydrate moiety of the antibody molecule since it was expected that linkage to this site would further preserve antigen binding activity.

The antibody used in this study was mAb K20, an IgG<sub>1</sub> mouse monoclonal antibody directed against a cell-surface component of the human kidney cancer cell line Caki-1. mAb K20 (185) was chosen on the basis of its availability as well as on the knowledge of its internalization following binding to Caki-1 cells. The control antibody was a non-specific mAb IgG<sub>1</sub>, a mouse myeloma IgG<sub>1</sub> monoclonal antibody shown not to react with Caki-1 cells. MTX was used as the model drug for this study because of its use in a number of ternary conjugates which had been reported prior to this work (107,110,119,120), and also on the grounds that the linkage chemistry of MTX to proteins as well as its primary mode of action have been established. One of the objectives of this study was to isolate well-defined homogeneous conjugates for evaluation of antibody and cytotoxicity activity. Although the isolation of well-defined conjugates is an obvious prerequisite for proper conjugate characterization, reports of previous ternary conjugates

which have been synthesized failed to demonstrate the use of well-defined conjugates. HSA was chosen as the drug carrier for the following reasons: i) it has a large number of amino groups for the incorporation of a relatively large amount of MTX; ii) it is highly water soluble and should be capable of carrying large amounts of hydrophobic MTX; and iii) unlike other synthetic polymers such as dextran and polyglutamic acid which exhibit a distribution of molecular weights, HSA is homogeneous in this respect. This last feature of HSA was expected to facilitate the subsequent isolation of homogeneous conjugates.

This discussion will be divided into three sections: i) synthesis of the drug-carrier intermediate, HSA-MTX; ii) synthesis and physical characterization of ternary conjugates; and iii) functional characterization of ternary conjugates.

## **1. Synthesis of HSA-MTX**

In the synthesis of HSA-MTX for use as a drug carrier for subsequent conjugation to anti-tumor mAb, the goal was to produce a homogeneous drug-loaded intermediary containing a large amount of MTX. The activation of MTX was studied first to establish conditions which would give high drug loadings into HSA and use MTX efficiently. The general trend seen in studies on the preparation of MTX-AE using different ratios of reactants was that an excess of both NHS and DCC over MTX resulted in activation of a larger amount of the MTX activation as measured functionally by the acylating ability of the product. Analysis of the reaction mixtures by TLC showed that a number of products were formed, the proportions of these being dependent on the molar ratios of reactants. The first product to be formed would be expected to be the MTX-O-acylisourea intermediate resulting from reaction of MTX carboxyl(s) with DCC, and conversion of this intermediate to an acylating species. The formation of such an intermediate is consistent with TLC data obtained, which showed that a product with a higher mobility than MTX was formed initially, but was no longer present after 24 h. An increased mobility on TLC would be

predicted for any product which blocks one or both carboxyl groups of MTX. The disappearance of this intermediate and formation of higher mobility products suggests that the intermediate was the mono-substituted O-acylisourea which was either converted to the di-substituted O-acylisourea or other products.

MTX contains two carboxyl groups in the glutamic acid portion of the molecule. Theoretically, one or both of these carboxyls can be converted to the succinimidyl ester, the proportion of each probably determined by the molar ratio of reactants. Alternatively, a cyclic anhydride may be formed once one carboxyl group is activated, forming a stable six-membered ring. This latter possibility was proposed by Burnstein and Knapp (105) in their experiments on MTX activation with acetic anhydride. However, they determined that the major activated species was the double mixed anhydride and not an intramolecular anhydride, this most likely being due to the large excess of anhydride over MTX during activation. All three of these compounds, the monoester, diester, and intramolecular anhydride of MTX, are potential acylating species which may be formed during the activation of MTX under conditions studied in the present experiments.

Endo et al. (119) monitored the distribution between monoester and diester forms of MTX by HPLC following the activation of MTX with equimolar amounts of DCC and NHS. The succinimidyl esters were not separated directly, but instead converted to the amide derivatives by reaction with isopropylamine prior to separation. They determined that the proportions of monoester and diester were 38% and 20%, respectively, following activation of MTX under these conditions. They found that the distribution between the two products could be altered by first reacting MTX with DCC for 15 h, followed by the reaction with NHS. Under these conditions, the amounts of monoester and diester were 58% and 12%. It was proposed that reaction between MTX and DCC resulted in the formation of an intramolecular anhydride, which gave the active ester upon reaction with NHS.

Rosowsky and Yu (193) studied the esterification of MTX with diethyl L-glutamate using DCC. They found that, under conditions of equimolar reactants, mono- and disubstituted MTX derivatives were formed in the ratios 31%, 17%, and 11% for the  $\alpha$ -monoglutamate,  $\gamma$ -monoglutamate, and  $\alpha,\gamma$ -diglutamate, respectively. Reaction using a 1:2:2 (MTX:DCC:diethyl L-glutamate) molar ratio was found to increase the amount of disubstituted product, but also result in the formation of two new products which were identified as the  $\alpha$ - and  $\gamma$ -monoglutamate containing the acylurea product on the  $\gamma$ - and  $\alpha$ -carbonyl groups, respectively. They also pointed out that the use of DCC as well as other peptide-forming agents led to the racemization of the glutamate moiety of MTX. The mechanism proposed to account for the racemization was formation of an oxazolone intermediate involving the benzoic acid carbonyl group and the DCC-activated  $\alpha$ -carbonyl group of the glutamic acid portion of MTX which could form a resonance stabilized five-membered ring. It is the existence of a number of resonance structures which leads to the racemization of MTX. This racemization may affect the cytotoxicity of MTX derivatives as discussed in a later section. This oxazolone intermediate can also be considered an acylating species and may be one of the products formed during the activation of MTX in the present study.

The preferential activation of the  $\alpha$ -carboxyl of MTX may be undesirable since it is known that this carboxyl group is important in binding to DHFR (194) (see below). Studies have also shown that  $\gamma$ -substituted MTX derivatives are much more effective than the corresponding  $\alpha$ -substituted MTX derivative in inhibition of human lymphoblastic leukemia cells *in vitro* as well as L1210 murine leukemia tumors *in vivo* (193). It is not known which carboxyl group of MTX was preferentially activated in the present study. However, as shown by Rosowsky (193), the proportion of disubstituted ester increases with an increase in the ratio of DCC over MTX. Thus, the final product in this study likely contained a number of different species which were not resolved by TLC, i.e. not a single "active ester", but instead, a mixture of compounds which have acylating ability.

The reaction mixture obtained by activation of MTX with an excess of DCC and NHS could not be used directly for reaction with HSA since there was precipitation on addition to aqueous solutions, resulting in low incorporations of MTX into HSA. This was most likely due to the poor water solubility of the excess reagents which caused the co-precipitation of MTX at the concentrations used for large scale HSA-MTX preparations. MTX and not HSA-MTX was the species which precipitated since the precipitate was yellow (MTX is yellow), but there was little loss of HSA during the reaction. Precipitation of MTX was eliminated by the purification step using ether to precipitate MTX, while removing excess DCC and NHS.

It was found that both the molar excess of MTX over HSA as well pH had an effect on incorporation, with the greatest incorporations achieved at high molar excess and high pH. HSA contains 58 lysine residues (136), although there are many known genetic variants which have an increased lysine content (195). HSA obtained from commercial sources may therefore be expected to display some heterogeneity since blood products are usually pools derived from the general population. The "active ester" of MTX is believed to react primarily with protein amino groups to form an amide linkage between the protein and MTX (73), and hence an upper limit for the molar incorporation of MTX into HSA of approximately 58 would be predicted. As the unprotonated amino group is likely to be the most significant nucleophile present, the increase seen with increasing pH was expected. It is likely that both molar excess and pH affect the distribution between the two competing reactions, namely hydrolysis of the acylating species and reaction with HSA. HSA-MTX which was prepared for subsequent conjugation with IgG typically had molar incorporations between 30 and 35 mol MTX/mol HSA. These incorporations were lower than those found during studies of the effect of pH on incorporation into HSA, and is probably due to the efficiency of removal of unbound or weakly bound MTX by desalting as compared to dialysis. The incorporations of MTX into HSA which were achieved in the

present study were comparable to those reported by others which ranged from 24 to 38 mol MTX/mol HSA (107,110,162).

It is possible that other nucleophiles present in HSA may also react with activated MTX, particularly at higher pH values. Halbert et al. (108) found that MTX linked to BSA showed some degree of instability. Following extensive dialysis approximately 15% of bound MTX was released from BSA. Furthermore, release of MTX was found to be biphasic, suggesting the presence of two distinct types of linkages.

Endo et al. (118) examined the conjugates formed between MTX-AE and a number of carriers in an attempt to determine the types of linkages formed. Reaction of the active ester with dextran produced conjugates which contained MTX, presumably bound through an ester linkage. These conjugates were unstable as 100% of the MTX could be removed by treatment with hydroxylamine. MTX-AE which had been reacted with polylysine on the other hand, produced conjugates which retained 80% of the MTX following hydroxylamine treatment. They further showed that IgG which had been previously succinylated to block amino groups (93% blocked) also incorporated MTX, the majority of which could be removed with hydroxylamine, indicating that the MTX which was bound was probably linked through ester linkages. Cytotoxicity of mAb-MTX conjugates with and without hydroxylamine treatment also differed significantly. The conjugate that was not treated with hydroxylamine was more cytotoxic. However, when conjugates were assayed in the presence of thiamine pyrophosphate, an inhibitor of the MTX active transport system, both conjugates showed similar low cytotoxicity. These results indicated that free MTX was likely released from the untreated samples and resulted in the increased cytotoxicity as compared to conjugates which had weakly bound MTX removed by hydroxylamine treatment. It is possible that HSA-MTX conjugates produced in the present study also contained MTX linked by more than one type of linkage. If present, weakly bound MTX could result in the release of free MTX during cytotoxicity assays resulting in erroneously higher cytotoxicity to cells. However, there was no evidence of such release,

since the non-specific control ternary mAb IgG<sub>1</sub>-HSA-MTX conjugate as well as HSA-MTX itself exhibited very low cytotoxicity toward cells, as will be discussed later. Weakly bound MTX, if present, could have been removed during the extensive purification of the conjugates.

It was found that dimers and trimers of HSA-MTX were formed during the incorporation procedure. These were readily removed by gel filtration and only the monomer was used for the subsequent conjugation with IgG, since contamination with ternary conjugates containing HSA-MTX polymers would be expected to make the separation of the 1:1 IgG:HSA-MTX conjugate more difficult and reduce the yield of the desired conjugate. The mechanism of HSA-MTX cross-linking is not readily apparent since the polymers were formed in spite of the fact that excess NHS and DCC were removed in purifying MTX-AE. The linkage was not reducible by low MW thiol compounds and so was probably not due to disulfide formation. The product resulting from the direct coupling of MTX to mAb K20 also formed polymers. However, under the same conditions and using the same MTX-AE preparation, the mAb IgG<sub>1</sub> product did not show this type of polymerization.

## **2. Synthesis of Ternary Conjugates**

Since no heterobifunctional site-specific cross-linkers were commercially available at the time of the present study, two such spacers were synthesized for use in the site-specific attachment of HSA-MTX to mAb K20. The design of HPDP and AUPDP was based on the structure of SPDP for the following reasons: i) the acylating potential of SPDP offered a convenient synthetic route to the cross-linkers; and ii) the thiol reactions of the site-specific derivatives would be expected to be similar to those of SPDP. Both spacers contained a hydrazide group for reaction with aldehyde groups, and a pyridyl disulfide group for reaction with thiol groups. Zara et al (169) have recently and

independently reported the synthesis of HPDP for use in site-specific conjugation of antibodies with toxins. Their synthesis differed from that used in the present study in that they reacted 3-(2-pyridyldithio)propionic acid with *tert*-butyl carbazate in the presence of DCC to give the protected hydrazide, followed by removal of the *tert*-butyloxycarbonyl protecting group with HCl. Their yield of HPDP (from 3-(2-pyridyldithio)propionic acid) was 40% compared to 27% (from SPDP) achieved by reaction of SPDP with hydrazine as reported here. This low yield was mostly due to the poor crystallization which was achieved. Conversion of HPDP to the hydrochloride might have facilitated its isolation and resulted in a higher yield of HPDP. The synthetic route devised in the present study for AUPDP gave a yield of 56% from SPDP. The fact that AUPDP was already crystalline following removal of solvent contributed to the better yield compared to HPDP.

Site-specific spacers were incorporated into IgG by reaction of IgG aldehyde groups with cross-linker hydrazide groups resulting in the formation of hydrazone bonds between IgG and the spacers. Aldehyde groups are usually generated from IgG oligosaccharides by periodate oxidation. In studying the oxidation level required for the subsequent incorporation of approximately four mol of HPDP or AUPDP per mol IgG, it was determined that the concentration of periodate required to generate sufficient aldehyde groups was approximately 10-fold higher than that typically used by others. It had been reported that, with periodate concentrations between 1 and 10 mM at pH 5.5 and 0 °C, the terminal sialic acid residues are selectively oxidized (172,176,177). Under these mild conditions, both reactivity toward AUPDP and HPDP as well as subsequent reactivity of the incorporated pyridyldithio groups with HSA were found to be low. The need for more spacer groups to achieve efficient conjugation with HSA observed in this study suggests that those incorporated as a result of mild oxidation conditions differ from those incorporated after oxidation under harsher conditions with respect to their reactivity towards HSA. This difference may be due to the location of the spacer incorporation

within the carbohydrate chain, and reflect the steric accessibility of the spacer for reaction with HSA.

It has been shown that periodate can oxidize certain free amino acids (196), although relatively harsh conditions (120 mM periodate at RT for 6-12 h) are required for the destruction of tyrosine and sulfur containing amino acids contained in polypeptides (197). Chua et al. (179), reported that periodate oxidation of IgM at 0 °C with 10 mM periodate resulted in the loss of 4% of tyrosine residues after 30 min, and 19% loss after 1 h, although antibody binding affinity was not altered. The oxidation conditions used in the present study could be considered harsh compared to those typically used by others. It is not known whether oxidation of susceptible amino acids occurred, but the oxidation conditions used for the incorporation of HPDP and AUPDP into mAb K20 did not result in any loss of antigen binding activity.

The major functional difference between AUPDP and HPDP is the distance between the two reactive groups. This difference in length had a significant effect on the ability to form conjugates between mAb K20 and HSA. As mentioned above, the synthesis and use of HPDP has recently been reported by Zara et al. who used it to conjugate an IgM mAb with ricin A-chain or barley toxin (169). They found that the use of an internal thiol present in ricin A-chain for conjugation with HPDP-derivatized IgM resulted in low conversion to conjugates, and showed that the incorporation of an SPDP-derived thiol into barley toxin was required to achieve conjugation between IgM and the toxin. These results indicated that the internal thiol of ricin A-chain was probably not sterically accessible for reaction with the carbohydrate-linked spacer. Similarly, in the present study, mAb K20 which was modified with AUPDP was found to be superior to the shorter HPDP with respect to the amount of conjugate formed after reaction with HSA. A direct correlation was found between the total length of spacer(s) between mAb K20 and HSA, and the yield of conjugates. The presence of MTX on HSA lowered the yields, and only AUPDP-derivatized mAb K20 showed any appreciable conjugate formation with

HSA-MTX, indicating that MTX itself imposes a further steric barrier to conjugation. These findings are not surprising considering the location of the carbohydrate moiety within the IgG molecule. The majority of carbohydrate is present at the conserved N-glycosylation site at Asn 297 of both heavy chains on all IgG (21). Structural studies on a number of IgGs have shown that the carbohydrate lies between the two  $C_{H2}$  domains of the molecule (25,26), which would explain the apparent steric constraints seen with the conjugation of HSA to this location. These results suggest that, although HPDP may have some applications in the conjugation of non-sterically hindered proteins, it is too short to allow for good conjugate yields when using IgG-associated carbohydrate and a second protein. The finding that the presence of MTX on HSA resulted in a decrease in conjugate yield when reacted with AUPDP-derivatized mAb K20 indicates that a longer spacer or combination of spacers may be required for optimal conjugate yield under sterically demanding conditions.

Unlike mAb K20, NRG could be efficiently conjugated with HSA using both site-specific cross-linkers and did not display the same steric constraints which were found with mAb K20. This may be due to the fact that NRG is polyclonal, and therefore contains a number of different immunoglobulin species. It has been shown that a number of immunoglobulins in serum also possess carbohydrate structures in their light chains (15,17,194). These carbohydrate chains are probably not buried as in the case of  $C_{H2}$ -linked carbohydrate. The presence of sterically accessible carbohydrate residues may therefore explain the differences in conjugation yields seen between mAb K20 and NRG.

Steric hindrance did not present a problem in synthesis of non-site-specific mAb K20 conjugates using SPDP-derivatized mAb K20 since good yields of conjugates were obtained. Furthermore, the presence of SPDP on HSA or HSA-MTX to increase the distance between HSA and the thiol, was found not to significantly increase the yield of conjugates. These findings are consistent with the incorporation of spacers by reaction with amino groups which would be expected to be present on the exposed surface of the

IgG rather than buried. Incorporation of SPDP on the surface of IgG would be predicted to allow efficient reaction between IgG spacers and HSA thiols.

The site-specific mAb K20-HSA conjugates which were formed by reaction of AUPDP-derivatized mAb K20 and thiol-containing HSA could not be isolated by either gel filtration or preparative electrophoresis. Following purification by either method, both free mAb K20 and HSA as well as conjugates were found to be present. In contrast, non-site-specific mAb K20-HSA conjugates containing a disulfide linkage between the two proteins, were isolated by both techniques free of contaminating HSA and mAb K20, indicating that the site of breakdown was likely the hydrazone linkage. This conclusion was supported by the observed release of DNP-groups from DNP-AU-hydrazide-derivatized IgG. A number of recent reports are in agreement with these findings, showing that hydrazone-linked antibody-<sup>99m</sup>Tc (162), antibody-adriamycin (75,165) or antibody-MTX (128) conjugates are unstable, particularly at pH values below 6. In fact, the instability of the hydrazone bond has been taken advantage of to release free adriamycin from antibody-adriamycin conjugates in the acidic lysosomal compartment once the conjugate has been internalized (75,83,165).

Several workers have reported the isolation of stable protein-protein conjugates formed through hydrazone bonds (169,177,178). King et al. (178) synthesized hydrazone-linked ovalbumin-ovalbumin conjugates by reaction of aldehyde- and hydrazide-derivatized ovalbumins. Aldehydes were introduced by acylation of ovalbumin amino groups with the N-hydroxysuccinimide ester of p-carboxybenzaldehyde and hydrazides were introduced by a two-step procedure in which ovalbumin was reacted first with N-(bromoacetyl)- $\beta$ -alanyl N-hydroxysuccinimide ester, then with N-acetylhomocysteinyl hydrazide. They reported that ovalbumin-ovalbumin conjugates isolated by gel filtration chromatography were stable for at least 30 days at pH 7.0, with little or no breakdown to ovalbumin monomers. However, the addition of an excess of acetyl hydrazide did result in breakdown of the conjugates indicating that the hydrazones were susceptible to hydrolysis

under these conditions. Furthermore, this breakdown could be prevented if hydrazone bonds were reduced with sodium cyanoborohydride prior to treatment with acetyl hydrazide. The stability of the ovalbumin conjugates was found to be significantly greater than that seen with model hydrazones which were also examined by King et al. (179), and the difference was attributed to the presence of multiple hydrazone linkages between the proteins. The presence of multiple hydrazone bonds was probable in these conjugates as the ovalbumins contained approximately five aldehyde groups and six hydrazide groups. These aldehyde and hydrazide groups would be expected to be randomly distributed on the surface of the ovalbumins because they were introduced by acylation of amino groups by succinimidyl esters. The apparent difference in stability between my site-specific mAb K20-HSA conjugates and the ovalbumin conjugates could also be explained on this basis. It was found that the carbohydrate-linked site-specific cross-linkers were not readily accessible for reaction with thiol-containing HSA, presumably due to steric factors. This implies that few hydrazone bonds between mAb K20 and HSA would be present in the conjugates which were formed, resulting in a less stable product than if multiple hydrazone bonds were present. The nature of the immediate environment of the hydrazone linkages in the present conjugates and those of King also differed significantly. In the case of the ovalbumin conjugates, the aldehyde-donating substituent was p-carboxybenzaldehyde, whereas with mAb K20 conjugates, aldehyde groups were derived from the carbohydrate of mAb K20. As was shown by King et al. (179) with model compounds, the equilibrium constants for hydrazone bond formation between i) acetyl hydrazide and p-carboxybenzaldehyde and ii) acetyl hydrazide and acetaldehyde were  $4.2 \times 10^4 \text{ M}^{-1}$  and  $5 \times 10^3 \text{ M}^{-1}$ , respectively, showing that the immediate environment of the hydrazone bond had an effect on stability of the bond. They further showed that hydrazones formed from benzaldehyde that contained electron-withdrawing groups were more stable than those formed with benzaldehyde that contained electron-donating groups. Zara et al. (169) used HPDP to conjugate IgM containing 7 HPDP/IgM with barley toxin containing 4.3

SPDP/toxin molecule and reported that conjugates could be isolated without reductive stabilization. Unlike IgG where the majority of carbohydrate is located in one area of the molecule, each heavy chain of the pentameric IgM has N-linked carbohydrate. With the presence of multiple spacers at different locations on both IgM and on barley toxin, it is again probable that the conjugates which were isolated contained multiple hydrazone bonds. In summary, it is likely that differences in the number of hydrazone bonds contributes to the differences in stability seen among ovalbumin, IgM and mAb K20-HSA conjugates.

During their studies on the site-specific immobilization of oxidized horseradish peroxidase to a hydrazide-containing Sepharose matrix, O'Shannessy and Hoffman (160) found that hydrazone-linked peroxidase continuously leaked from the matrix. However, they attributed this leakage to instability of the matrix because peroxidase coupled through amino groups using cyanogen bromide showed a similar pattern of leakage. They concluded that the hydrazone bonds were stable. This might have been an erroneous conclusion because the cyanogen bromide coupled product is an N-substituted imidocarbonate which itself has limited stability (132).

Having established that the hydrazone bonds between HSA and mAb K20 possessed limited stability, it was necessary to stabilize the bonds to allow isolation of site-specific mAb K20-HSA-MTX conjugates. Using model hydrazones, King et al. (178) showed that stabilization could be achieved by reduction of the bond with cyanoborohydride in a manner similar to that used for stabilization of Schiff bases. Reduction was found to be faster at lower pH and with high concentrations of reducing agent (31). In the present study, a preliminary assessment of the conditions for hydrazone bond stabilization by cyanoborohydride was made using a DNP-containing hydrazide probe. The use of such a probe was necessary because pyridyldithio groups of HPDP and AUPDP were found to be reduced by cyanoborohydride, resulting in the loss of reporter function of the pyridyldithio group. It was seen that the hydrazone-linked probe was

unstable during extended periods of dialysis and was susceptible to an exchange reaction with propanal. It was found that 60% of hydrazone-linked DNP groups could be stabilized by treatment with 15 mM sodium cyanoborohydride at pH 4.0 for 90 min. The reduction process itself appeared to result in the release of a fraction of the DNP-probe from IgG, and this may be a reflection of the mechanism of reduction by cyanoborohydride, in which an intermediate of the reduction process can either form the reduced disubstituted hydrazide or result in hydrolysis of the bond. Approximately 20% of the hydrazone-linked probe appeared to be stable without reduction, as neither dialysis nor propanal competition could remove 100% of the DNP groups. This may be an indication that some of the hydrazone bonds which were formed are stable as a result of the immediate environment around them. Alternatively, the fraction of probe groups which could not be removed may represent reaction of the probe elsewhere in IgG with group(s) other than the oxidized carbohydrate, resulting in the formation of stable linkages. Control reactions in which oxidized IgG was incubated with the DNP-AU-OMe, or where non-oxidized IgG was incubated with DNP-AU-hydrazide failed to show incorporation of the DNP label, indicating the specificity of the hydrazide group for oxidized IgG. As discussed previously, certain amino acid side chains are known to be oxidized by periodate under harsh conditions, and may become sites of label incorporation. If reaction with certain oxidized amino acids did occur, this should have resulted in at least some biotin hydrazide incorporation into the F(ab')<sub>2</sub> portion of oxidized IgG. This possibility therefore seems unlikely since it was shown that biotin hydrazide was selectively incorporated into the Fc portion of IgG under the same oxidation conditions used for DNP-probe incorporation.

When the reduction conditions used to stabilize the DNP-probe were applied to mAb K20-HSA conjugates, a proportion of the hydrazone bonds between IgG and HSA were apparently reduced, since conjugates could be isolated following reduction. The reduced hydrazone appeared to be similar in stability to an amide bond as both site-specific and non-site-specific conjugates showed a similar pattern and a similar degree of

breakdown on extended storage at pH 7.2, 4 °C. Both conjugates contained disulfide linkages which are known to be less stable than thioether linkages because of the possibility of disulfide exchange. A new site-specific cross-linker recently reported by Chammow et al. (177) containing hydrazide and maleimide functional groups may be an alternative method of linkage to produce more stable conjugates.

Evidence for the selective modification of oxidized IgG carbohydrate by hydrazides in the present study is based on the findings that i) oxidation of IgG is a prerequisite for the incorporation of hydrazide-containing compounds, and ii) that a biotin-hydrazide label was selectively incorporated into the Fc portion of IgG, this being consistent with the known location of the conserved glycosylation site. Others have described similar findings (198), and have further demonstrated that endoglycosidase F which releases N-linked oligosaccharides could remove a biotin-hydrazide label from oxidized IgG.

It is important to note that a number of authors have claimed that site-specific conjugates have been isolated (169,177,178), but, as is often the case in the conjugation literature, little evidence of purity in the form of electrophoretic or chromatographic analysis was given. If the site-specific conjugates prepared by these authors were impure, and the preparations contained unbound components, the lack of stability of the hydrazone bond would not be readily apparent. The failure to purify conjugates would also affect subsequent antibody activity assays, giving erroneously high activity levels if unreacted antibody was present. In the present study, purification of stable conjugates was achieved. Purification of binary conjugates was more difficult than that of the ternary conjugates because, in the latter case, the presence of MTX allowed the removal of unreacted IgG by ion exchange chromatography which simplified the subsequent separation by gel filtration. In the case of binary conjugates, species with predicted MWs of 150 kDa (IgG), 217 kDa (IgG + 1 HSA), 284 kDa (IgG + 2 HSA) were separated by gel filtration alone. It was established that the non-site-specific ternary conjugates which migrated to a position directly above IgG on SDS PAGE were 1:1 HSA:IgG conjugates by using a dual-labelling

experiment. The conclusion that the site-specific conjugates isolated were also 1:1 IgG:HSA-MTX conjugates is based on their mobility which was closely similar to that of the non-site-specific conjugates. The binary and ternary conjugates which were isolated by gel filtration were also 1:1 conjugates since these were shown to migrate directly above IgG on SDS PAGE. One of the difficulties encountered in the purification of conjugates by gel filtration was the low resolution achieved in the region of 200 kDa. Bio Gel P-300 was found to give the best resolution in this region. A number of matrices including Sephadex G-200, Sephacryl HR-200, and Ultrogel AcA 34 were found to be unsatisfactory for this separation.

One of the problems encountered with the use of AUPDP in site-specific conjugation was its poor water solubility. Although the presence of 25% DMF in the reaction mixture prevented precipitation, solutions of mAb K20 derivatized with 4 to 5 AUPDP were cloudy once DMF was removed. Following reaction with HSA and stabilization, solutions were once again clear. This was most likely due to a solubilizing effect by HSA. Recovery of mAb K20 in the form of the site-specific binary mAb K20-HSA conjugate was comparable to that in the corresponding non-site-specific conjugate, with yields of 15% and 20%, respectively. Yields of site-specific conjugates synthesized with HSA containing MTX were much lower, with the best yield being 2.5%, compared to 11% for the corresponding non-site-specific conjugate. Similar mAb-HSA-MTX non-site-specific ternary conjugates have been prepared by others (107,110,111,119), but recoveries of mAb in the isolated conjugates were not reported. The low recovery of the site-specific conjugates in the present study probably reflects the lower water solubility of HSA-MTX compared to HSA, and therefore the lower degree of solubilization by HSA-MTX. Similarly, Hurwitz et al. (144) found that the site-specific incorporation of polyglutamyl hydrazide did not affect the solubility of the IgG, but the subsequent incorporation of daunorubicin into the carrier resulted in irreversible precipitation of IgG. It is well known that the incorporation of hydrophobic drugs directly into IgG can result in

IgG precipitation, with recovery decreasing as drug incorporation increases (73). Because IgG-associated carbohydrate is believed to play a role in IgG solubility (17), it is possible that the incorporation of a large hydrophobic entity into this area diminishes the solubilizing effect of the carbohydrate residues, and results in a product which is less soluble than the corresponding non-site-specific conjugate.

### **3. Characterization of Conjugates**

Conjugates as well as conjugation intermediates were evaluated for retention of antigen binding activity. It was found that neither oxidation with periodate nor reduction by cyanoborohydride resulted in loss of antibody activity, whereas derivatization with 4 AUPDP/mAb K20 resulted in a 35% loss of antibody activity. According to a number of reports, antibody derivatized site-specifically with low MW hydrazides such as biotin hydrazide (165,166), HPDP (IgM) (169), MTX-hydrazide (128), and adriamycin-hydrazide (75) retained full antibody activity following derivatization. The reason for the apparent loss of mAb K20 antigen binding activity following derivatization with AUPDP may be related to a decrease in solubility of AUPDP-derivatized mAb K20. It is possible that aggregation of mAb K20 occurred during the assay of antibody activity, thereby reducing the effective mAb K20 concentration in the assay.

mAb K20 which had been modified with SPDP, showed a much greater loss of antibody activity, with a loss of 60% following derivatization with 3 SPDP/mAb K20. Such losses of antibody activity have been reported by others following derivatization of antibody amino groups with biotin (166), MTX-AE (73), or vinblastine (199), and the degree of activity loss was directly proportional to the level of derivatization. In the present study, mAb K20 which was derivatized directly with MTX using the MTX-AE method also showed high levels of loss of antibody activity, with losses of 70%, 92%, and 97% for incorporations of 4, 8, and 13 MTX/mAb K20, respectively. It would appear that

modification of amino groups of mAb K20 results in direct modification of residues at or near the antibody binding site. Experiments with non-site-specifically labelled mAb K20 confirmed that this area was preferentially labelled by the succinimidyl ester of biotin.

Based on size alone and the assumption that amino groups are randomly distributed throughout the antibody, it would be predicted that the ratio of Fab to Fc labelling would be 2:1 since Fab and Fc have MWs of approximately 50 kDa each, and, for each IgG, two Fab and one Fc fragment are generated by papain digestion. However, Fab fragments were found to be labelled to a much greater extent than the predicted 2:1 (Fab:Fc) ratio. These results indicate that amino groups in the Fab and/or antigen binding region were much more susceptible to acylation. It is likely that the  $\alpha$ -amino groups of the terminal residues of the heavy and light chains are preferentially acylated. The  $\alpha$ -amino groups are present in the area of the antigen binding site and have a lower pKa than lysine  $\epsilon$ -amino groups, so they would be predicted to be more nucleophilic than  $\epsilon$ -amino groups at neutral pH. Preferential labelling of these terminal residues would explain the high reactivity towards acylating compounds as well as the decrease in antibody binding activity following acylation.

It is known that not all mAbs are susceptible to loss of antibody activity following amino group modification. As a preliminary screening tool, mAbs have been reacted with fluoro-2,4-dinitrobenzene to determine whether the mAb in question is susceptible to loss of binding activity due to amino group modification (200). Methods to minimize the damage caused by chemical modification of mAbs have also been employed. Endo et al. (72) used the reversible reaction of 2,3-dimethylmaleic anhydride with protein amino groups for protection of the antigen binding site. The rationale of this modification was based on the finding that, in some cases, the acylation of only a small number of amino groups was sufficient to result in a large decrease in antigen binding activity. This suggested that the most reactive amino groups were also important in antigen binding. Blockage of these groups with the anhydride would be expected to prevent their subsequent

reaction with MTX-AE. Following the loading of MTX, dimethylmaleyl groups were removed by treatment with hydroxylamine to regenerate the free amino groups. Using this method, they found antibody activity could be preserved with two mAbs which were tested. Further attempts to preserve mAb binding activity include those in which the mAb (201) or polyclonal antibody (202) was bound to solid-phase antigen prior to chemical modification. One of the problems with this technique in the past has been the poor recovery of IgG from the solid phase. These methods can now be optimized for a particular mAb and quantitative yields have been reported by Ramjeesingh et al. (201). They found that antigen binding activity of mAbs undergoing a variety of chemical modifications could be preserved using such an active site protection method. Such protection may also be useful for the preservation of antibody activity in conjugates utilizing those mAbs which are susceptible to damage following amino group acylation.

The assay initially used to measure antibody activity of the conjugates in the present study was a direct cell-binding assay in which Caki-1 cells were used as antigen, and cell-bound mAb K20 was detected with a second antibody-peroxidase conjugate. It was found, however, that mAb K20-HSA site-specific conjugates were not recognized as efficiently as native mAb K20 by the second antibody. Non-site-specific and direct conjugates did not show this effect, and results from assays based on competition with either radiolabelled or biotinylated mAb K20 were comparable with those from direct binding assays. Based on the findings that mAb K20 is modified preferentially in or near the region of the antigen binding site with amino group-reactive reagents, it is likely that HSA is also linked near the amino termini of mAb K20 in the non-site-specific conjugates. In contrast, HSA is bound to the hinge region in the site-specific conjugates. Considering that HSA has a MW greater than that of one heavy chain, it is likely that HSA blocks a large portion of one face of IgG when it is linked to the C<sub>H</sub>2 domain. The second antibody used was polyclonal and so a number of different epitopes on mAb K20 should be recognized. The finding that site-specific conjugates showed saturation at a value

approximately half that of native mAb K20 would seem to indicate that half the molecule is blocked by HSA in site-specific conjugates, and only the other half is available to bind with the second antibody. Non-site-specific conjugates did not show this effect, presumably because the HSA was likely linked near the amino termini and did not block a large portion of the IgG.

Because the direct binding assay underestimated the activity retained in site-specific conjugates, their activity was measured using an assay based on competition. The advantage of a competition assay is that no second antibody was involved and only the ability to bind to cells was detected. The activities found for three different non-site-specific conjugate preparations ranged from 10% to 16%, and for three different site-specific conjugates between 32% and 56%, clearly showing that the site-specific conjugates consistently retained from two to three times more activity than the non-site-specific conjugates. The reason for the large loss of antibody activity in the non-site-specific conjugates can be explained by the direct blockage of the antigen binding site by HSA as was shown for both SPDP and MTX-AE. The values of 10% to 16% retention of binding activity found in the non-site-specific conjugates appears to correlate very well with the relative staining intensities of Fab and Fc fragments following non-site-specific linkage of biotin to mAb K20, where it was seen that approximately 90% of the label was in the Fab portion and the remainder in the Fc. It is therefore possible that 90% of the HSA molecules were linked to the Fab portion of mAb K20 and 10% to the Fc portion, and only the latter retained antigen binding activity. Endo et al. (119) and Baldwin's group (107,110,111) have previously synthesized similar mAb-HSA-MTX non-site-specific ternary conjugates. They reported antibody activities ranging from 28% to 35% for the conjugates. These results should be interpreted cautiously, however, since their relatively impure preparations likely contained unreacted mAb that would increase the apparent activity of the conjugates.

The site-specific conjugates obtained in the present study, although having greater antigen binding activity compared to the non-site-specific conjugates, still showed a

decrease in antibody activity. This may be related to the steric factors imposed by HSA itself, where HSA may physically interfere with the antibody-antigen interaction. The use of a smaller  $\gamma$  protein for site-specific conjugation to IgG may be more appropriate for this reason. Rose et al. (203) recently described a method to specifically introduce hydrazide groups at the carboxyl terminus of insulin by using reverse proteolysis. They showed that a number of enzymes could effect incorporation of carbohydrazide under suitable pH and substrate conditions. Such a method may prove useful for IgG modification if carbohydrazide incorporation can be restricted to the heavy chains carboxyl groups, as this would be predicted to eliminate any antibody activity loss due to steric factors imposed by drug carriers linked to this location.

Shih et al. (117) synthesized a site-specific mAb-dextran-MTX ternary conjugate using Schiff base formation between amino-dextran (average MW 40 kDa) and oxidized IgG-associated carbohydrate. The conjugate was reported to retain 100% of antibody binding activity. It is interesting to note that activity was assayed using a second antibody and that the conjugate did not show the same blockage of IgG epitopes by carbohydrate-linked dextran as was seen in the present study. Similarly, Zara et al (169) prepared site-specific IgM-barley toxin conjugates using HPDP and reported full retention of antibody activity. Purification of both the above conjugates was by gel filtration chromatography, although the degree of purification was not shown. It is possible that IgM is less susceptible to activity loss due to its pentameric structure, and blockage of a limited number of antigen binding sites by the toxin may not be reflected in decreased activity, since other binding sites present on IgM are still functional.

Native mAb K20 was found to be only 24% immunoreactive (IRF of 0.24). Possible reasons for this include clonal heterogeneity of the mAb K20 hybridoma (199), contamination by normal mouse IgG since the antibody was obtained from ascites, or damage arising from purification methods. Radiolabelling of mAb K20 to a similar specific activity as that used for IRF determination was shown not to affect antibody activity so the

low IRF is not due to the iodination procedure. The apparent binding affinity of mAb K20 for target Caki-1 cells was found to be approximately  $9 \times 10^8 \text{ M}^{-1}$ , which is considered acceptable for targeting purposes (44).

The percent retention of antibody activity has been expressed in terms of the relative ability of the conjugate and unmodified mAb K20 to compete for cell surface binding sites. All ternary conjugates were less active than the starting mAb, for example the site-specific and non-site-specific conjugates had 56% and 11% of the ability of native mAb K20 to compete for sites, respectively. According to the simplest interpretation, all activity loss following conjugation would be due to a loss of immunoreactivity, and all active mAbs in the final conjugate preparations homogeneous with respect to binding properties. This simplest interpretation is unlikely and the activity which was measured in the isolated conjugates is probably a composite of both immunoreactivity (can the mAb bind) as well as affinity (how well does the mAb bind). Unfortunately, the starting mAb contained only 24% of molecules capable of binding (based on its IRF of 0.24). These inactive IgG molecules were also conjugated and contributed to non-specific background in the cytotoxicity assays (see below).

The heterogeneity of native mAb K20 as seen by IEF analysis has been reported by others (199,204) who showed that different mAb preparations contained from four to six bands within a narrow isoelectric point range. It is conceivable that this microheterogeneity represents species containing variable amounts of sialic acid in the carbohydrate portion of the mAb. One study, however, showed that this was not the case, since digestion with neuraminidase to remove sialic acid failed to result in convergence of the bands (204). Another possible origin for the heterogeneity of mAb preparations is as a result of variable post-synthetic deamidation of glutamine and/or asparagine residues. This has been demonstrated in both heavy and light chains in myeloma proteins (205). Others have found that hybridomas can also express irrelevant IgG (199) which would increase the apparent heterogeneity seen by IEF analysis.

The DHFR inhibition of MTX in all conjugates was found to be from 20- to 40-times less than that of free MTX. Such losses of inhibition activity following conjugation have been reported previously (73,190) and are not necessarily an indication that MTX itself was damaged by coupling to either HSA or IgG. Two likely explanations for this effect are based on steric factors. First, the linkage of MTX to protein is likely to interfere with its ability to interact optimally with DHFR. Second, the distribution of MTX on the protein surface is likely to be such that there are "local high concentrations" of MTX (protein-bound MTX) which would preclude all MTX binding to DHFR at the same time. The finding that DHFR inhibition activity decreased with increasing MTX incorporation supports the latter point. Alternatively, a proportion of MTX which was bound to protein may have undergone racemization. As discussed previously, Rosowsky and Yu (195) found that activation of MTX by DCC led to partial racemization of the glutamate moiety of MTX and showed that the D-enantiomer was less cytotoxic to human lymphoblastic leukemia cells in culture compared to the L-enantiomer. This effect could have been due to differences in either transport or DHFR inhibition capacity of the two enantiomers.

The ultimate goal in the synthesis of drug-antibody conjugates is the production of conjugates which show cytotoxicity to target cells. Furthermore, to be therapeutically effective, conjugates should also show antibody-based selectivity between target and non-target cells, i.e. they should be more toxic to target cells than to antigen-negative non-target cells. It was predicted that conjugates which retained greater antigen binding capacity should be more cytotoxic to target cells. This was found to be the case with the ternary conjugates synthesized in the present study, for which cytotoxicity correlated with the retention of antibody binding activity. The site-specific ternary conjugate which had the greatest antibody binding activity also showed the greatest inhibition of proliferation of target Caki-1 cells, with a sensitivity ratio of 24 (i.e. 24 times weaker than free MTX). The non-site-specific mAb K20 and the control IgG<sub>1</sub> ternary conjugates had much lower sensitivities i.e. sensitivity ratios of 53 and 217, respectively. HSA-MTX itself also

exhibited a low sensitivity (sensitivity ratio of 123). These results showed that the presence of mAb K20 in the conjugates was responsible for the greater cytotoxicity of the ternary conjugates. The cytotoxicity was not directly proportional to antibody activity since the site-specific ternary conjugate showed approximately five times the antibody activity, but only twice the cytotoxicity compared to the non-site-specific mAb K20 ternary conjugate. It would be expected that more potent conjugates would have been obtained if the initial IRF of mAb K20 was higher.

Direct mAb K20-MTX conjugates showed little correlation between antibody activity and cytotoxicity. Direct conjugates synthesized using irrelevant IgG showed growth inhibition comparable to the mAb K20 conjugates. A possible explanation for this apparent lack of specificity is high levels of non-specific binding during the assay. Conjugates were compared on the basis of MTX concentration, and therefore those with lower incorporations of MTX had higher IgG concentrations during the assay which would make non-specific binding more likely. The most cytotoxic mAb K20 direct MTX conjugate had an incorporation of 8 MTX/mAb K20 and showed a sensitivity ratio of 71, whereas the mAb K20 site-specific ternary conjugate had an incorporation of 28 MTX/mAb K20 with a sensitivity ratio of 24, indicating that the ternary conjugate was a more effective inhibitor of cell proliferation. These sensitivity ratios are based on MTX concentrations. Had they been based on mAb K20 concentration, the difference between the two conjugates would be much greater, indicating that ternary conjugates with their increased loading are more potent than direct conjugates on a per IgG basis, as was predicted.

The ternary conjugates were also shown to be target-selective since the mAb K20 and the non-specific IgG ternary conjugates all showed similar cytotoxicity toward the antigen-negative D10-1 cell line. Of these, the mAb K20 site-specific ternary conjugate was the most selective with a selectivity ratio of 0.5 (sensitivity to target cells + sensitivity to non-target cells) indicating that it was twice as cytotoxic to target cells than to non-target cells. The D10-1 cell line is a B-cell lymphoma line and therefore as all B-cells, have Fc $\gamma$

receptors on their surface. The presence of these receptors may have contributed to non-specific binding and subsequent toxicity of conjugates. It is likely, however, that all conjugates would be equally non-specifically cytotoxic to these cells, and the presence of non-specific cytotoxicity would therefore be expected to decrease the selectivity ratio proportionally for all conjugates.

The mAb-HSA-MTX ternary conjugates synthesized by other groups (107,110,119) were found to retain from 28% to 35% antibody activity. One difficulty in comparing different conjugates is that different assays were used to measure cytotoxicity, the variables being the conditions of exposure and method of cytotoxicity determination. In two reports (107,119), the cytotoxicity of conjugates was found to be less than that of free MTX and conjugates showed specificity in that they were more cytotoxic to target cells than non-target cells as was found for the site-specific ternary conjugate in the present study. These conjugates were assayed using a continuous exposure to cytotoxic agent, unlike the 6 h pulse exposure employed here. Garnett et al. (107) also assayed conjugates using a 15 min pulse exposure which was designed to mimic the *in vivo* situation more closely, where circulating conjugates only briefly encounter either tumor or normal non-target cells. In this assay, the same conjugate which was weaker than free MTX in a continuous assay, showed much greater cytotoxicity to target cells than did the free drug. A second ternary conjugate prepared using the same mAb was also studied by this group (110). The synthesis of this conjugate differed from that previously reported, in that the incorporation of MTX was increased from 32 to 38 mol MTX/HSA. A more significant difference was that the conjugation method employed to link HSA-MTX to the mAb was altered to reduce the amount of high MW polymers which were produced. This conjugate was shown to be more cytotoxic to target cells, based on a 5 d continuous exposure assay. The higher cytotoxicity of this conjugate compared to the previous one was attributed to both the higher MTX loading and the greater number of HSA-MTX per mAb, while at the same time retaining antigen binding activity. Two of these studies (107,119) also demonstrated

that cytotoxicity was dependent on the presence of mAb in the conjugate since the presence of unconjugated mAb during cytotoxicity assays could completely inhibit cytotoxicity. Studies with direct mAb-MTX conjugates have shown similar results in that conjugated MTX was typically less cytotoxic to target cells than free MTX and that conjugates showed selectivity to the target cells defined by the mAb (77,80,206). In some cases, direct conjugates were reported to be more cytotoxic to target cells than free MTX (123,128).

It is difficult to compare the cytotoxicity of conjugates synthesized in the present study with those of others because of differences in the mAbs and cell lines, as well as the type of cytotoxicity assay used and the purity of conjugates. Based on the finding that the mAb K20-HSA-MTX ternary conjugate retained more antibody activity and was more cytotoxic to target cells than the comparable non-site-specific conjugate, it would be expected that those mAbs which are susceptible to loss of antibody binding activity following acylation of amino groups would yield more potent conjugates by the site-specific conjugation approach reported here.

The finding that cytotoxicity to Caki-1 cells was dependent on the presence of specific mAb (ie. mAb K20), as well as retention of mAb K20 antigen binding activity, illustrates that the toxic effect is exerted by an antibody-mediated mechanism. Such cytotoxicity would be expected to be dependent on a number of factors, including the antigen density and homogeneity of antigen expression on all cells, efficiency of conjugate internalization, as well as the intracellular fate of the internalized conjugate (117). It is generally accepted that free MTX enters cells by different mechanisms than mAb-conjugated MTX. Evidence for this view is that compounds which inhibit MTX transport reduce the cytotoxicity of free MTX but not of conjugates (206), and that conjugate cytotoxicity and not free MTX cytotoxicity is reduced by the presence of unconjugated mAb (107,119). Once bound to cell-associated antigen, mAb conjugates can either be internalized or shed from the cell surface (207). Some controversy exists as to the effect of antibody affinity on the fate of cell-bound antibody. Earlier reports (1,44) indicated that

only mAbs with a certain threshold affinity would be useful as targeting agents, however a recent report by Kyriakos et al. (207) disagrees with this view and proposes that divalent antibody binding to cells can be considered essentially irreversible and that the concept of affinity is therefore not applicable to this situation (207). Cell-bound antibody can either be shed, internalized, or remain bound to the cell surface in the case of non-internalized antigen. The internalization of mAb can proceed either quickly or slowly depending on the receptor and the pathway involved for internalization of that receptor. In the case of receptor-mediated endocytosis by the clathrin coated pit pathway, endocytosis occurs rapidly with recycling of the receptor as, for example, in the case of the transferrin and epidermal growth factor receptors (208).

The majority of mAbs against cell surface antigens are internalized via non-clathrin-dependent endocytosis (207). The physiological significance of this pathway is not fully understood but it has been proposed that the process is responsible for the normal turnover of cell surface components (209). It is likely that, once internalized by this pathway, the mAb is routed to lysosomes for degradation. Evidence for such catabolism comes from studies showing that inhibitors of lysosomal enzymes prevent degradation of mAbs (207) or of mAb-drug conjugates (79), or decrease the cytotoxicity of mAb-drug conjugates (80,119). The presence of intracellular low MW drug-containing species have also been demonstrated following binding of antibody-drug conjugates (122). The mode of action of the ternary conjugates prepared in the present study is likely to follow a similar process, i.e. binding of conjugate, internalization, lysosomal degradation to release either free MTX or MTX bound to peptides derived from HSA, possible polyglutamation of MTX, and inhibition of DHFR and other target enzymes by MTX or MTX-containing fragments.

#### **4. Future Directions**

Conjugates synthesized in the present study using HSA as a drug carrier and with the carrier linked site-specifically to the carbohydrate moiety of mAb K20 were clearly superior to both direct conjugates as well as carrier-based conjugates with the carrier linked non-site-specifically to the mAb. These findings support the view that drug load as well as retention of antibody activity are important factors in the preparation of potent conjugates, and indicate that this method of drug-targeting is a worthwhile avenue of pursuit. For such conjugates to be useful for future studies, a number of improvements in the synthesis are required. The foremost of these is the need for a more hydrophilic site-specific spacer, the use of which would be predicted to result in yields of ternary conjugates comparable to that of non-site-specific conjugates. It is also likely that the use of a mAb which has a high initial IRF would yield conjugates with greater cytotoxicity, and the use of a smaller carrier protein may reduce the loss of antigen binding activity which was found with the present site-specific conjugates. Another approach to increase the potency of these conjugates is the introduction of specific lysosomotropic spacers between HSA and MTX which would be expected to facilitate intracellular release of MTX in an active form.

## **V. Conclusions**

- 1. The site-specific conjugation of HSA or HSA-MTX to the carbohydrate moiety of mAb K20 yielded conjugates with greater antigen binding activity compared to conjugates containing HSA or HSA-MTX linked non-site-specifically.**
- 2. The site-specific ternary mAb K20 conjugates showed greater cytotoxicity to target Caki-1 cells than the non-site-specific mAb K20 ternary conjugates. The increased cytotoxicity was likely due to the greater retention of antibody binding activity. Both conjugates were more cytotoxic than a non-specific mAb IgG1 ternary conjugate.**
- 3. Both site-specific and non-site-specific mAb K20 ternary conjugates were more cytotoxic to target Caki-1 cells than direct mAb K20-MTX conjugates.**
- 4. The greater antigen binding activity of the site-specific ternary conjugates also resulted in greater selectivity between target and non-target cell lines.**
- 5. The hydrazone bond used to link mAb K20 with HSA and HSA-MTX was unstable, but could be stabilized by reduction with cyanoborohydride with full retention of antibody activity.**
- 6. Comparison of HPDP and AUPDP for use in conjugation of HSA-SH and HSA-SPDP-SH to the carbohydrate moiety of mAb K20 suggested that the efficiency of conjugation was dependent on the total length of the spacer moiety between the two proteins.**
- 7. Site-specific incorporation of hydrazides was restricted to the carbohydrate moiety in the Fc portion of mAb K20. The non-site-specific spacers were preferentially incorporated into the Fab fragments of mAb K20, and this explains the differences in antibody activity between site-specific and non-site-specific conjugates.**

## VI. References

1. Ghose, T. and Blair, A.H. (1987) The design of cytotoxic-agent-antibody conjugates. *CRC Crit. Rev. Ther. Drug Carrier Sys.* **3**, 263-361.
2. van Berkel, T.J.C., De Smidt, P.C., van Kijk, M.C.M., Ziene, G.J. and Bijsterbosch, M.K. (1990) 1. Drug targeting by endogenous transport vesicles 2. Antibody-directed enzyme/prodrug therapy (ADEPT) . *Biochem. Soc. Trans.* **18**, 748-750.
3. Bejaoui, N., Pagé, M. and Noel, C. (1991) Cytotoxicity of transferrin-daunorubicin conjugates on small cell carcinoma of the lung (SCCL) cell line NCI-H69. *Anticancer Res.* **11**, 2211-2214.
4. Waldmann, T.A., Pastan, I.H., Gansow, O.A. and Junghans, R.P. (1992) The multichain interleukin-2 receptor: a target for immunotherapy. *Ann. Intern. Med.* **116**, 148-160.
5. De Smidt, P.C., Bijsterbosch, M.K. and van Berkel, M.K. LDL as a carrier in site-specific drug delivery. In: *Targeted therapeutic systems*, Tyle, P. and Ram, B.P. eds. New York: Marcel Dekker, Inc, 1990, pp. 355-383.
6. Micoux, P., Negre, E., Roche, A.C., Mayer, R., Monsigny, M., Balzarini, J., De Clercq, E., Mayer, E., Ghaffar, A. and Gangemi, J.D. (1990) Drug targeting-anti HSV-1 activity of mannosylated polymer-bound 9-(2-phosphomethoxyethyl)adenine. *Biochem. Biophys. Res. Comm.* **167**, 1044-1049.
7. Varga, J.M., Asato, N. and Lande, S. (1977) Melanotropin-daunomycin conjugate shows receptor mediated cytotoxicity in cultured murine melanoma cells. *Nature* **267**, 56-58.
8. Ghose, T. and Nigam, S. (1972) Antibody as carrier of chlorambucil. *Cancer* **29**, 1398-1400.
9. Uadia, P., Blair, A.H. and Ghose, T. (1983) Uptake of methotrexate linked to an anti-EL4-lymphoma antibody by EL4 cells. *Cancer Immunol. Immunother.* **16**, 127-129.
10. Edelman, G.M. (1991) Antibody structure and molecular immunology. *Scand. J. Immunol.* **34**, 1-22.
11. Klein, J. *Immunology. The science of self-nonsel self discrimination*, New York:John Wiley and Sons, 1982. pp. 156-255.
12. Coco-Martin, J.M., Brunink, F., van der Velden-de Groot, T.A.M. and Beuvery, E.C. (1992) Analysis of glycoforms present in two mouse IgG2a monoclonal antibody preparations. *J. Immunol. Meth.* **155**, 241-248.
13. Burton, D.R. (1990) Antibody: the flexible adaptor molecule. *TIBS* **15**, 64-69.

14. Schumaker, V.N., Phillips, M.L. and Hanson, D.C. (1991) Dynamic aspects of antibody structure. *Molec. Immunol.* **28**, 1347-1360.
15. Kabat, E.A., Wu, T.T., Perry, H.M., Gottesman, K.S. and Foeller, C. *Sequences of proteins of immunological interest*, Washington, D.C.:Public Health Service, NIH, 1991.
16. Wright, A., Tao, Mi-hua, Kabat, E.A. and Morrison, S.L. (1991) Antibody variable region glycosylation: position effects on antigen binding and carbohydrate structure. *EMBO J.* **10**, 2717-2723.
17. Grebenau, R.C., Goldenberg, D.M., Chang, C.-H., Koch, G.A., Gold, D.V., Kunz, A. and Hansen, H.J. (1992) Microheterogeneity of a purified IgG1 due to asymmetric Fab glycosylation. *Molec. Immunol.* **29**, 751-758.
18. Hobbs, S.M., Jackson, L.E. and Hoadley, J. (1992) Interaction of aglycosyl immunoglobulins with the IgG Fc transport receptor from neonatal rat gut: comparison of deglycosylation by tunicamycin treatment and genetic engineering. *Molec. Immunol.* **29**, 949-956.
19. Wawrzynczak, E.J., Cumber, A.J., Parnell, G.D., Jones, P.T. and Winter, G. (1992) Blood clearance in the rat of a recombinant mouse monoclonal antibody lacking the N-linked oligosaccharide side chains of the CH2 domains. *Molec. Immunol.* **29**, 213-220.
20. Lund, J., Tanaka, T., Takahashi, N., Sarmay, G., Arata, Y. and Jefferis, R. (1990) A protein structural change in aglycosylated IgG3 correlates with loss of huFcGRI and huFcGRIII binding and/or activation. *Molec. Immunol.* **27**, 1145-1153.
21. Burton, D.R. (1985) Immunoglobulin G: functional sites. *Molec. Immunol.* **22**, 161-206.
22. Parham, P. (1983) On the fragmentation of monoclonal IgG1, IgG2a, and IgG2b from BALB/c mice. *J. Immunology* **131**, 2895-2902.
23. Mizuochi, T., Hamako, J. and Titani, K. (1987) Structures of the sugar chains of mouse immunoglobulin G1. *Arch. Biochem. Biophys.* **257**, 387-394.
24. Patel, T.P., Parelj, R.B., Moellering, B.J. and Prior, C.P. (1992) Different culture methods lead to differences in glycosylation of a murine IgG monoclonal antibody. *Biochem. J.* **285**, 839-845.
25. Sutton, B. and Phillips, D. (1983) The three-dimensional structure of the carbohydrate within the Fc fragment of immunoglobulin G. *Biochem. Soc. Trans.* **11**, 130-132.
26. Deisenhofer, J. (1981) Crystallographic refinement and atomic models of a human Fc fragment and its complex with fragment B of protein A from *Staphylococcus aureus* at 2.9- and 2.8-Å resolution. *Biochemistry* **20**, 2361-2370.
27. Rademacher, T.W., Homans, S.W., Fernandes, D.L., Dwek, R.A., Mizuochi, T., Taniguchi, T. and Kobata, A. (1985) Structural and conformational analysis of immunoglobulin-derived N-linked oligosaccharides. *Biochem. Soc. Trans.* **11**, 132-134.

28. Srivastava, P.K. (1991) Protein tumor antigens. *Curr. Opinion Immunol.* **3**, 654-658.
29. Srivastava, P.K. and Old, L.J. (1988) Individually distinct transplantation antigen of chemically induced mouse tumors. *Immunology Today* **9**, 78-83.
30. DeLeo, A.B., Jay, G., Apella, E., Dubois, G.C., Law, L.W. and Old, L.J.. (1979) Detection of a transformation-related antigen in chemically induced sarcomas and other transformed cells of the mouse. *Proc. Natl. Acad. Sci.* **76**, 2420-2424.
31. Urban, J.L. and Schreiber, H. (1992) Tumor antigens. *Ann. Rev. Immunol.* **10**, 617-644.
32. Taetle, R. and Honeysett, J.M. (1987) Effects of monoclonal anti-transferrin receptor antibodies on in vitro growth of human solid tumor cells. *Cancer Res.* **47**, 2040-2044.
33. Herlyn, M., Menrad, A. and Koprowski, H. (1990) Structure, function, and clinical significance of human tumor antigens. *JNCI* **82**, 1883-1889.
34. Juranka, P.F., Zastawny, R.L. and Ling, V. (1989) P-glycoprotein: Multidrug-resistance and a superfamily of membrane-associated transport proteins. *FASEB J.* **3**, 2583-2592.
35. Benchimol, S., Fuks, A. and Jothy, S. (1989) Carcinoembryonic antigen, a human tumor marker, functions as an intercellular adhesion molecule. *Cell* **57**, 327-334.
36. Johnson, J.P., Stade, B.G. and Holzmann, B. (1989) *De novo* expression of intercellular-adhesion molecule 1 in melanoma correlates with increased risk of metastasis. *Proc. Natl. Acad. Sci.* **86**, 641-644.
37. Kramer, R.H., McDonald, K.A. and Vu, M.P. (1989) Human melanoma cells express a novel integrin receptor for laminin. *J. Biol. Chem.* **264**, 15642-15649.
38. Boon, T. (1983) Antigenic tumor variants obtained with mutagens. *Adv. Cancer Res.* **39**, 121-151.
39. Harris, A.L. (1991) Telling changes of base. *Nature* **350**, 377-378.
40. Hakamori, S. (1989) Abberant glycosylation in tumors and tumor-associated carbohydrate antigens. *Adv. Cancer Res.* **52**, 257-331.
41. Harris, A.L. (1990) The epidermal growth factor receptor as a target for therapy. *Cancer Cells* **2**, 321-323.
42. Kaufman, E.N. and Jain, R.K. (1992) Effect of bivalent interaction upon apparent antibody affinity: experimental confirmation of theory using fluorescence photobleaching and implications for antibody binding assays. *Cancer Res.* **52**, 4157-4167.
43. Herlyn, M., Steplewski, A. and Herlyn, D. (1986) CO 17-1A and related monoclonal antibodies: Their production and characterization. *Hybridoma* **5**, Suppl 1, S3-S10.

44. Kennel, S.J., Foote, L.J., Lankford, P.K., Johnson, P.K., Mitchell, T. and Braslawsky, G.R. (1983) Direct binding of radioiodinated monoclonal antibody to tumor cells: significance of antibody purity and affinity for drug targeting and tumor imaging. *Hybridoma* **2**, 297.
45. Lindmo, T. and Bunn, P.A.Jr. (1986) Determination of the true immunoreactive fraction of monoclonal antibodies after radiolabeling. *Methods in Enzymology* **121**, 678-691.
46. Dux, R., Kindler-Rohrborn, A., Lennartz, K. and Rajewsky, M.F. (1991) Determination of immunoreactive fraction and kinetic parameters of a radiolabeled monoclonal antibody in the absence of antigen excess. *J. Immunol. Meth.* **144**, 175-183.
47. Ghose, T., Guclu, A., Raman, R.R. and Blair, A.H. (1982) Inhibition of a mouse hepatoma by the alkylating agent Trenimon linked to immunoglobulins. *Cancer Immunol. Immunother.* **13**, 185-189.
48. Press, O.W., Farr, A.G., Borroz, K.I., Anderson, S.K. and Martin, P.J. (1989) Endocytosis and degradation of monoclonal antibodies targeting human B-cell malignancies. *Cancer Res.* **49**, 4906-4912.
49. Matthey, K.K., Abai, A.M., Cobb, S., Hong, K., Papahadjopoulos, D. and Straubinger, R.M. (1989) Role of ligand in antibody-directed endocytosis of liposomes by human T-leukemia cells. *Cancer Res.* **49**, 4879-4886.
50. Bagshawe, K.D. (1990) Antibody-directed enzyme/prodrug therapy (ADEPT). *Biochem. Soc. Trans.* **18**, 750-752.
51. Wallace, P.M. and Senter, P.D. (1991) *In vitro* and *in vivo* activities of monoclonal antibody-alkaline phosphatase conjugates in combination with phenol mustard phosphate. *Bioconjugate Chem.* **2**, 349-352.
52. Senter, P.D. (1990) Activation of prodrugs by antibody-enzyme conjugates: a new approach to cancer therapy. *FASEB J.* **4**, 188-193.
53. Senter, P.D., Schreiber, G.J., Hirschberg, D.L., Ashe, S.A., Hellstrom, K.E. and Hellstrom, I. (1989) Enhancement of the *in vitro* and *in vivo* antitumor activities of phosphorylated mitomycin C and etoposide derivatives by monoclonal antibody-alkaline phosphatase conjugates. *Cancer Res.* **49**, 5789-5792.
54. Haenseler, E., Esswein, A., Vitols, K.S., Montejano, Y., Mueller, B.M., Reisfeld, R.A. and Huennekens, F.M. (1992) Activation of methotrexate-  $\alpha$ -alanine by carboxypeptidase A-monoclonal antibody conjugate. *Biochemistry* **31**, 891-897.
55. Grunicke, H. and Hofmann, J. (1992) Cytotoxic and cytostatic effects of antitumor agents induced at the plasma membrane level. *Pharmac. Ther.* **55**, 1-30.
56. Goldenberg, D.M. (1993) Monoclonal antibodies in cancer detection and therapy. *Am. J. Med.* **94**, 297-312.

57. Mendelsohn, J. Antibodies in cancer therapy: clinical applications. Antibodies to growth factors and receptors. In: *Biologic therapy of cancer*, DeVita Jr., V.T., Hellman, S. and Rosenberg, S.A. eds. Philadelphia: J.B. Lippincott, 1991, pp. 601-612.
58. Masui, H., Kawamoto, T., Sato, J.D., Wolf, B., Sato, G. and Mendelsohn, J. (1984) Growth inhibition of human tumor cells in athymic mice by anti-epidermal growth factor receptor monoclonal antibodies. *Cancer Res.* **44**, 1002-1007.
59. Waldman, T.A., Goldman, C.K., Bongiovanni, K.F., Sharrow, S.O., Davey, M.P., Cease, K.B., Greenberg, S.J. and Longo, D.L. (1988) Therapy of patients with human T-cell lymphotropic virus 1-induced adult T-cell leukemia with anti-Tac, a monoclonal antibody to the receptor for interleukin-2. *Blood* **72**, 1805-1816.
60. Dyer, M.J.S., Hale, G., Hayhoe, F.G.J. and Waldmann, H. (1989) Effects of CAMPATH-1 antibodies *in vivo* in patients with lymphoid malignancies: influence of antibody isotype. *Blood* **73**, 1431-1439.
61. Lefranc, G. and Lefranc, M.P. (1990) Antibody engineering and perspectives in therapy. *Biochimie* **72**, 639-651.
62. Co, M.S. and Queen, C. (1991) Humanized antibodies for therapy. *Nature* **351**, 501-502.
63. Songsivilai, S. and Lachmann, P.J. (1990) Bispecific antibody: a tool for diagnosis and treatment of disease. *Clin. exp. Immunol.* **79**, 315-321.
64. Wawrzynczak, E.J. and Davies, A.J.S. (1990) Strategies in antibody therapy of cancer. *Clin. exp. Immunol.* **82**, 189-193.
65. Brown, S.L., Miller, R.A., Horning, S.J., Czerwinski, D., Hart, S.M., McElderry, R., Basham, T., Warnke, R.A., Merigan, T.C. and Levy, R. (1989) Treatment of B-cell lymphomas with anti-idiotypic antibodies alone and in combination with alpha interferon. *Blood* **73**, 651-661.
66. Levy, R. and Miller, R.A. Antibodies in cancer therapy. B-cell lymphomas. In: *Biologic therapy of cancer*, DeVita Jr., V.T., Hellman, S. and Rosenberg, S.A. eds. Philadelphia: J.M. Lippincott, 1991, pp. 512-522.
67. Herlyn, D., Wettendorff, M., Schmoll, E., Iliopoulos, D., Schedel, I., Dreikhausen, U., Raab, R., Ross, A.H., Jaksche, H., Scriba, M. and Koprowski, H. (1987) anti-idiotypic immunization of cancer patients: modulation of the immune response. *Proc. Natl. Acad. Sci.* **84**, 8055-8059.
68. Waldmann, T.A. (1991) Monoclonal antibodies in diagnosis and therapy. *Science* **252**, 1657-1662.
69. Larson, S.M., Cheung, N.-K.V. and Leibel, S.A. Antibodies in cancer therapy: basic principles of monoclonal antibodies. Radioisotope conjugates. In: *Biologic therapy of cancer*, DeVita Jr., V.T., Hellman, S. and Rosenberg, S.A. eds. Philadelphia: J.B. Lippincott Co., 1991, pp. 496-511.

70. Upešlaciš, J. and Hinman, L. Chemical modification of antibodies for cancer chemotherapy. In: *Annual Reports in Medicinal Chemistry*, Salzman, ed. Academic Press Inc., 1988, pp. 151-160.
71. Ghose, T., Blair, A.H. and Kulkarni, P.N. (1983) Preparation of antibody-linked-cytotoxic agents. *Methods in Enzymology* **93**, 280-333.
72. Endo, N., Umemoto, N., Kato, Y., Takeda, Y. and Hara, T. (1987) A novel covalent modification of antibodies at their amino groups with retention of antigen-binding activity. *J. Immunol. Meth.* **104**, 253-258.
73. Kulkarni, P.N., Blair, A.H. and Ghose, T. (1981) Covalent binding of methotrexate to immunoglobulins and the effect of antibody-linked drug on tumor growth *in vivo*. *Cancer Res.* **41**, 2700-2706.
74. Shen, W.-C. and Ryser, J.P. (1981) Cis-aconityl spacer between daunomycin and macromolecular carriers: a model of pH-sensitive linkage releasing drug from a lysosomotropic conjugate. *Biochem. Biophys. Res. Comm.* **102**, 1048-1054.
75. Greenfield, R.S., Kaneko, T., Daves, A., Edson, M.A., Fitzgerald, D.A., Olech, L.J., Grattan, J.A., Spitalny, G.L. and Braslawsky, G.R. (1990) Evaluation *in vitro* of adriamycin immunoconjugates synthesized using an acid-sensitive hydrazone linker. *Cancer Res.* **50**, 6600-6607.
76. Trouet, A., MasQuelier, M., Baurain, R. and Campeneere, D.D-De. (1982) A covalent linkage between daunorubicin and proteins that is stable in serum and reversible by lysosomal hydrolases, as is required for a lysosomotropic drug-carrier conjugate: *in vitro* and *in vivo* studies. *Proc. Natl. Acad. Sci.* **79**, 626-629.
77. Umemoto, N., Kato, Y. and Hara, T. (1989) Cytotoxicities of two disulfide-bond-linked conjugates of methotrexate with monoclonal anti-MM46 antibody. *Cancer Immunol. Immunother.* **28**, 9-16.
78. Shih, L.B., Xuan, H., Sharkey, R.M. and Goldenberg, D.M. (1990) A fluorouridine-anti-CEA immunoconjugate is therapeutically effective in a human colonic cancer xenograft model. *Int. J. Cancer* **46**, 1101-1106.
79. Uadia, P.O., Blair, A.H. and Ghose, T. (1988) Hydrolysis of methotrexate-immunoglobulin conjugates by liver homogenates and characterization of catabolites. *Cancer Chemother. Pharm.* **22**, 175-177.
80. Endo, N., Takeda, Y., Kishida, K., Kato, Y., Saito, M., Umemoto, N. and Hara, T. (1987) Target-selective cytotoxicity of methotrexate conjugated with monoclonal anti-MM46 antibody. *Cancer Immunol. Immunother.* **25**, 1-6.
81. Rowland, A.J., Pietersz, G.A. and McKenzie, I.F.C. (1993) Preclinical investigation of the antitumor effects of anti-CD19-idarubicin immunoconjugates. *Cancer Immunol. Immunother.* **37**, 195-202.
82. Pagé, M., Thibeault, D., Noel, C. and Dumas, L. (1990) Coupling a preactivated daunorubicin derivative to antibody. A new approach. *Anticancer Res.* **10**, 353-358.

83. Trail, P.A., Willner, D., Lasch, S.J., Henerson, A.J., Hofstead, S., Casazza, A.M., Firestone, R.A., Hellstrom, I. and Hellstrom, K.E. (1993) Cure of xenografted human carcinomas by BR96-doxorubicin immunoconjugates. *Science* **261**, 212-215.
84. Pagé, M., Delorme, F., Lafontaine, F. and Dumas, L. (1985) Treatment of human colon adenocarcinoma heterografted into nude mice with anti-CEA-daunorubicin conjugates. *Eur. J. Cancer Clin. Oncol.* **21**, 1405.
85. Kato, Y., Tsukada, Y., Hara, T. and Hirai, H. (1983) Enhanced antitumor activity of mitomycin C conjugated with anti- $\alpha$ -fetoprotein antibody by a novel method of conjugation. *J. Appl. Biochem.* **5**, 313-319.
86. Smyth, M.J., Pietersz, G.A. and McKenzie, I.F.C. (1987) Selective enhancement of antitumor activity of N-acetyl melphalan upon conjugation to monoclonal antibodies. *Cancer Res.* **47**, 62-69.
87. Pagé, M. and Bernier, L.G. (1985) A new derivative for targeting chlorambucil to cancer cells. *Eur. J. Cancer Clin. Oncol.* **21**, 1405.
88. Rowland, G.F., Simmonds, R.G., Gore, V.A., Marsden, C.H. and Smith, W. (1986) Drug localisation and growth inhibition studies of vindesine-monoclonal anti-CEA conjugates in a human tumour xenograft. *Cancer Immunol. Immunother.* **21**, 183-187.
89. Chu, E. and Takimoto, C.H. Antimetabolites. In: *Cancer: Principles and practice of oncology*, DeVita Jr., V.T., Hellman, S. and Rosenberg, S.A. eds. Philadelphia: J.B. Lippincott Company, 1993, pp. 358-362.
90. Allegra, C.J. Antifolates. In: *Cancer chemotherapy. Principles and practice*, Chabner, B.A. and Collins, J.M. eds. Philadelphia: J.B. Lippincott Company, 1990, pp. 110-153.
91. Blaney, J.M., Hansch, C., Silipo, C. and Vittoria, A. (1984) Structure-activity relationships of dihydrofolate reductase inhibitors. *Chem. Rev.* **84**, 333-407.
92. Stone, S.R. and Morrison, J.F. (1986) Mechanism of inhibition of DHFRs from bacterial and vertebrate sources by various classes of folate analogues. *Biochim. Biophys. Acta* **869**, 275-285.
93. Cohen, M., Bender, R.A., Donehower, R., Myers, C.E. and Chabner, B.A. (1978) Reversibility of high-affinity binding of methotrexate in L1210 murine leukemia cells. *Cancer Res.* **38**, 2866-2870.
94. Maherly, L.H., Angeles, S.M. and Csajkowski, C.A. (1992) Characterization of transport-mediated methotrexate resistance in human tumor cells with antibodies to the membrane carrier for methotrexate and tetrahydrofolate. *J. Biol. Chem.* **267**, 23253-23260.
95. Jansen, G., Westerhof, G.R., Jarmuszewski, J.A., Kathmann, I., Rijksen, kG. and Schornagel, J.H. (1990) Methotrexate transport in variant human CCRF-CEM leukemia cells with elevated levels of the reduced folate carrier. *J. Biol. Chem.* **265**, 18272-18277.

96. Warren, R.D., Nichols, A.P. and Bender, R.A. (1978) Membrane transport of methotrexate in human lymphoblastoid cells. *Cancer Res.* **38**, 668-671.
97. Morrison, P.F. and Allegra, C.J. (1989) Folate cycle kinetics in human breast cancer cells. *J. Biol. Chem.* **264**, 10552-10566.
98. Jolivet, J. and Chabner, B.A. (1983) Intracellular pharmacokinetics of methotrexate polyglutamates in human breast cancer cells. *J. Clin. Invest.* **72**, 773-778.
99. Chu, E., Drake, J.C., Boarman, D., Baram, J. and Allegra, C.J. (1990) Mechanism of thymidylate synthase inhibition by methotrexate in human neoplastic cell lines and normal human myeloid progenitor cells. *J. Biol. Chem.* **265**, 8470-8478.
100. Allegra, C.J., Hoang, K., Yeh, G.C., Drake, J.C. and Baram, J. (1987) Evidence for direct inhibition of *de novo* purine synthesis in human MCF-7 breast cells as a principal mode of metabolic inhibition by methotrexate. *J. Biol. Chem.* **262**, 13520-13526.
101. Wang, F.S., Aschele, C., Sobrero, A., Chang, Y.M. and Bertino, J.R. (1993) Decreased folylpolyglutamate synthetase expression: a novel mechanism of fluorouracil resistance. *Cancer Res.* **53**, 3677-3680.
102. Kaufman, R.J., Bertino, J.R. and Schimke, R.T. (1978) Quantitation of dihydrofolate reductase in individual parental and methotrexate-resistant murine cells: use of a fluorescence activated cell sorter. *J. Biol. Chem.* **253**, 5852-5860.
103. Robinson, D.A., Whiteley, J.M. and Harding, G.L. (1973) Cell-directed antitumorites: alternative syntheses of cytotoxic methotrexate-containing macromolecules. *Biochem. Soc. Trans.* **1**, 722-726.
104. DeCarvalho, S., Rand, J.J. and Lewis, A. (1964) Coupling of cyclic chemotherapeutic compounds to immune gamma-globulins. *Nature* **202**, 255-258.
105. Burstein, S. and Knapp, R. (1977) Chemotherapy of murine ovarian carcinoma by methotrexate-antibody conjugates. *J. Med. Chem.* **20**, 950-952.
106. Manabe, Y., Tsubota, Y., Kataoka, K., Okazaki, M., Haisa, S., Nakamura, K. and Kimura, I. (1984) Production of a monoclonal antibody-methotrexate conjugate utilizing dextran T-40 and its biological activity. *J. Lab. Clin. Med.* **104**, 445-454.
107. Garnett, M.C., Embleton, M.J., Jacobs, E. and Baldwin, R.W. (1983) Preparation and properties of a drug-carrier-antibody conjugate showing selective antibody-directed cytotoxicity *in vitro*. *Int. J. Cancer* **31**, 661-670.
108. Halbert, G.W., Florence, A.T. and Stuart, B.B. (1987) Characterization of *in vitro* drug release and biological activity of methotrexate-bovine serum albumin conjugates. *J. Pharm. Pharmacol.* **39**, 871-876.
109. Chu, B.C.F. and Whiteley, J.M. (1977) High molecular weight derivatives of methotrexate as chemotherapeutic agents. *Mol. Pharmacol* **13**, 80-88.
110. Garnett, M.C. and Baldwin, R.W. (1986) An improved synthesis of a methotrexate-albumin 79IT/36 monoclonal antibody conjugate cytotoxic to human osteogenic sarcoma cell lines. *Cancer Res.* **46**, 2407-2421.

111. Embleton, M.J., Garnett, M.C., Jacobs, E. and Baldwin, R.W. (1984) Antigenicity and drug susceptibility of human osteogenic sarcoma cells "escaping" a cytotoxic methotrexate-albumin-monoclonal antibody conjugate. *Br. J. Cancer* **49**, 559-565.
112. Chakraborty, P., Bhaduri, A.N. and Das, P.K. (1990) Sugar receptor mediated drug delivery to macrophages in the therapy of experimental visceral leishmaniasis. *Biochem. Biophys. Res. Comm.* **166**, 404-410.
113. Chaudhuri, G., Mukhopadhyay, A. and Basu, S.K. (1989) Selective delivery of drugs to macrophages through a highly specific receptor. *Biochem. Pharmacol.* **38**, 2995-3002.
114. Galivan, J., Balinska, M. and Whiteley, J.M. (1982) Interaction of methotrexate poly(L-lysine) with transformed hepatic cells in culture. *Arch. Biochem. Biophys.* **216**, 544-550.
115. Hudecz, F., Clegg, J.A., Kajtar, J., Embleton, M.J., Pimm, M.V., Sederde, M. and Baldwin, R.W. (1993) Influence of carrier on biodistribution and *in vitro* cytotoxicity of methotrexate-branched polypeptide conjugates. *Bioconjugate Chem.* **4**, 25-33.
116. Shen, W.-C., Ryser, H.J.-P. and LaManna, L. (1985) Disulfide spacer between methotrexate and poly(D-lysine). *J. Biol. Chem.* **260**, 10905-10908.
117. Shih, L.B., Sharkey, R.M., Primus, F.J. and Goldenberg, D.M. (1988) Site-specific linkage of methotrexate to monoclonal antibodies using an intermediate carrier. *Int. J. Cancer* **41**, 832-839.
118. Endo, N., Takeda, Y., Umemoto, N., Kishida, K., Watanabe, K., Saito, M., Kato, Y. and Hara, T. (1988) Nature of linkage and mode of action of Methotrexate conjugated with antitumor antibodies: implications for future preparation of conjugates. *Cancer Res.* **48**, 3330-3335.
119. Endo, N., Kato, Y., Takeda, Y., Saito, M., Umemoto, N., Kishida, K. and Hara, T. (1987) *In vitro* cytotoxicity of a human serum albumin-mediated conjugate of methotrexate with anti-MM46 monoclonal antibody. *Cancer Res.* **47**, 1076-1080.
120. Pimm, M.V., Clegg, J.A., Caten, J.E., Ballantyne, K.D., Perkins, A.C., Garnett, M.C. and Baldwin, R.W. (1987) Biodistribution of methotrexate-monoclonal antibody conjugates and complexes: experimental and clinical studies. *Cancer Treat. Rev.* **14**, 411-420.
121. Pimm, M.V., Clegg, J.A., Garnett, M.C. and Baldwin, R.W. (1988) Biodistribution and tumour localization of a methotrexate-monoclonal-antibody 79IT/36 conjugate in nude mice with human tumour xenografts. *Int. J. Cancer* **41**, 886-891.
122. Uadia, P., Blair, A.H., Ghose, T. and Ferrone, S. (1985) Uptake of methotrexate linked to polyclonal and monoclonal antimelanoma antibodies by a human melanoma cell line. *JNCI* **74**, 29-35.
123. Singh, M., Kralovec, J., Mezei, M. and Ghose, T. (1989) Inhibition of human renal cancer by methotrexate linked to a monoclonal antibody. *J. Urology* **141**, 428-431.

124. Uadia, P., Blair, A.H. and Ghose, T. (1984) Tumor and tissue distribution of a methotrexate-anti-EL4 immunoglobulin conjugate in EL4 lymphoma-bearing mice. *Cancer Res.* **44**, 4263-4266.
125. Embleton, M.J., Charleston, A. and Affleck, K. (1991) Efficacy and selectivity of monoclonal-antibody-targeted drugs and free methotrexate in fluorescence-labelled multicellular spheroids. *Int. J. Cancer* **49**, 566-572.
126. Ghose, T., Blair, A.H., Uadia, P., Kulkarni, P.N., Goundalkar, A., Mezei, M. and Ferrone, S. (1985) Antibodies as carriers of cancer chemotherapeutic agents. *Ann. NY Acad. Sci.* **446**, 213-227.
127. Singh, M., Ghose, T., Kralovec, J., Blair, A.H. and Belitsky, P. (1991) Inhibition of human renal cancer by monoclonal-antibody-linked methotrexate in an ascites tumor model. *Cancer Immunol. Immunother.* **32**, 331-334.
128. Kralovec, J., Singh, M., Mammen, M., Blair, A.H. and Ghose, T. (1989) Synthesis of site-specific methotrexate-IgG conjugates: comparison of stability and antitumor activity with active-ester based conjugates. *Cancer Immunol. Immunother.* **29**, 293-302.
129. Lopes, A.W., Radcliffe, R.D., Coughlin, D.J., Lee, L.S., McKearn, T.J. and Rodwell, J.D. Site-selective methotrexate-antibody conjugates yield a superior therapeutic effect in tumor xenograft-bearing nude mice. In: *Clinical Immunology*, Pruzanski, W. and Seligmann, M. eds. New York: Elsevier, 1987, pp. 303-307.
130. Wong, S.S. *Chemistry of protein conjugation and cross-linking*, Boca Raton: CRC Press, 1991. pp. 1-6.
131. Ellman, G.L. (1959) Tissue sulfhydryl groups. *Arch. Biochem. Biophys.* **82**, 70-77.
132. Wong, S.S. *Chemistry of protein conjugation and cross-linking*, Boca Raton: CRC Press, 1991. pp. 295-317.
133. Carlsson, J., Drevin, H. and Axen, R. (1978) Protein thiolation and reversible protein-protein conjugation: N-succinimidyl 3-(2-pyridyldithio)propionate, a new heterobifunctional reagent. *Biochem. J.* **173**, 723-737.
134. Duncan, R.J.S., Weston, P.D. and Wrigglesworth, R. (1983) A new reagent which may be used to introduce sulfhydryl groups into proteins, and its use in the preparation of conjugates for immunoassay. *Anal. Biochem.* **132**, 68-73.
135. Traut, R.R., Bollen, A., Sun, T.T., Hershey, J.W.B., Sundberg, J. and Pierce, L.R. (1973) Methyl-4-mercaptobutyrimidate as a cleavable crosslinking reagent and its application to the Escherichia coli 30S ribosome. *Biochemistry* **12**, 3266-3273.
136. Dugaiczky, A., Law, S.W. and Dennison, O.E. (1982) Nucleotide sequence and the encoded amino acids of human serum albumin mRNA. *Proc. Natl. Acad. Sci.* **79**, 71-75.
137. He, X.M. and Carter, D.C. (1992) Atomic structure and chemistry of human serum albumin. *Nature* **358**, 209-215.

138. Umemoto, N., Kato, Y., Takeda, Y., Saito, M., Hara, T., Seto, M. and Takahashi, T. (1984) Conjugates of mitomycin C with the immunoglobulin M monomer fragment of a monoclonal anti-MM46 immunoglobulin M antibody with or without serum albumin as intermediary. *J. Appl. Biochem.* **6**, 297-307.
139. Andersson, L.-O. (1966) The heterogeneity of bovine serum albumin. *Biochim. Biophys. Acta* **117**, 115-133.
140. Arnon, R. and Sela, M. (1982) *In vitro* and *in vivo* efficacy of conjugates of daunomycin with anti-tumor antibodies. *Immunol. Rev.* **62**, 5-27.
141. Hurwitz, E., Kashi, R., Arnon, R., Wilchek, M. and Sela, M. (1985) The covalent linking of two nucleotide analogues to antibodies. *J. Med. Chem.* **28**, 137-140.
142. Manabe, Y., Tsubota, T., Haruta, Y., Kataoka, K., Okazaki, M., Haisa, S., Nakamura, K. and Kimura, I. (1985) Production of a monoclonal antibody-mitomycin C conjugate, utilizing dextran T-40, and its biological activity. *Biochem. Pharmacol.* **34**, 289-291.
143. Manabe, Y., Tsubota, T., Haruta, Y., Okazaki, M., Haisa, S., Nakamura, K. and Kimura, I. (1983) Production of a monoclonal antibody-bleomycin conjugate utilizing dextran T-40 and the antigen-targeting cytotoxicity of the conjugate. *Biochem. Biophys. Res. Comm.* **115**, 1009-1014.
144. Hurwitz, E., Wilchek, M. and Pitha, J. (1980) Soluble macromolecules as carriers for daunorubicin. *J. Appl. Biochem.* **2**, 25-35.
145. Richard, F.M. and Knowles, J.R. (1968) Glutaraldehyde as a protein cross-linking reagent. *J. Mol. Biol.* **37**, 231-233.
146. Rowland, G.F., O'Neill, G.J. and Davies, D.A.L. (1975) Suppression of tumour growth in mice by a drug-antibody conjugate using a novel approach to linkage. *Nature* **255**, 487-488.
147. Kato, Y., Umemoto, N., Kayama, Y., Fukushima, H., Takeda, Y., Hara, T. and Tsukada, Y. (1984) A novel method of conjugation of daunomycin with antibody with a poly-L-glutamic acid derivative as intermediate drug carrier. An anti- $\alpha$ -fetoprotein antibody-daunomycin conjugate. *J. Med. Chem.* **27**, 1602-1607.
148. Trubetskoy, V.S., Torchilin, V.P., Kennel, S.J. and Huang, L. (1992) Use of N-terminal modified poly(L-lysine)-antibody conjugate as a carrier for targeted gene delivery in mouse lung endothelial cells. *Bioconjugate Chem.* **3**, 323-327.
149. Pastan, I., Chaudhary, V. and Fitzgerald, D.J. (1992) Recombinant toxins as novel therapeutic agents. *Ann. Rev. Biochem.* **61**, 331-354.
150. Ross, W.C.J., Thorpe, P.E., Cumber, A.J., Edwards, D.C., Hinson, C.A. and Davies, A.J.S. (1980) Increased toxicity of diphtheria toxin for human lymphoblastoid cells following covalent linkage to anti(human lymphocyte)globulin or its F(ab)<sub>2</sub> fragment. *Eur. J. Biochem.* **104**, 381-390.

151. Batra, J.K., Jinno, Y. and Chaudhary, V.K. (1989) Antitumor activity in mice of an immunotoxin made with antitransferrin receptor and a recombinant form of pseudomonas exotoxin. *Proc. Natl. Acad. Sci.* **86**, 8445-8549.
152. Chaudhary, V.K., Queen, C. and Junghans, R.P. (1988) A recombinant immunotoxin consisting of two antibody variable domains fused to pseudomonas exotoxin. *Nature* **339**, 394-397.
153. Szoka, F.C.Jr. (1990) The future of liposomal drug delivery. *Biotech. Appl. Biochem.* **12**, 496-500.
154. Singh, M., Faulkner, G., Ghose, T. and Mezei, M. (1988) Antibody directed targeting of methotrexate-containing small unilamellar vesicles. *Cancer Immunol. Immunother.* **27**, 17-25.
155. Singh, M., Ghose, T., Faulkner, G., Kralovec, J. and Mezei, M. (1989) Targeting of methotrexate-containing liposomes with a monoclonal antibody against human renal cancer. *Cancer Res.* **49**, 3976-3984.
156. Singh, M., Ghose, T., Mezei, M. and Belitsky, P. (1991) Inhibition of human renal cancer by monoclonal antibody targeted methotrexate-containing liposomes in an ascites tumor model. *Cancer Letters* **56**, 97-102.
157. Domen, P.I., Nevens, J.R., Mallia, A.K., Hermanson, G.T. and Klenk, D.C. (1990) Site-directed immobilization of proteins. *J. Chrom.* **510**, 293-302.
158. O'Shannessy, D.J. (1990) Hydrazido-derivatized supports in affinity chromatography. *J. Chrom.* **510**, 13-21.
159. O'Shannessy, D.J. and Wilchek, M. (1990) Immobilization of glycoconjugates by their oligosaccharides: use of hydrazido-derivatized matrices. *Anal. Biochem.* **191**, 1-8.
160. O'Shannessy, D.J. and Hoffman, W.L. (1987) Site-directed immobilization of glycoproteins on hydrazide-containing solid supports. *Biotech. Appl. Biochem.* **9**, 488-496.
161. Radparvar, S., Fung, G. and Ngo, T.T. (1990) Simple, quick and efficient site-directed antibody immobilization in a cartridge. *BioTechniques* **9**, 632-638.
162. Schwartz, D.A., Abrams, M.J., Hauser, M.M., Gaul, F.E., Larsen, S.K., Rauh, D. and Zubieta, J.A. (1991) Preparation of hydrazino-modified proteins and their use for the synthesis of <sup>99m</sup>Tc-protein conjugates. *Bioconjugate Chem.* **2**, 333-336.
163. Rodwell, J.D., Alvarez, V.L., Lee, C., Lopes, A.D., Goers, J.W.F., King, H.D., Powsner, H.J. and McKearn, T.J. (1986) Site-specific covalent modification of monoclonal antibodies: *in vitro* and *in vivo* evaluations. *Proc. Natl. Acad. Sci.* **83**, 2632-2636.

164. Rosenstraus, M.J., Davis, W.L., Lopes, A.D., D'Aleo, C.J. and Gilman, S.C. (1990) Carbohydrate-derivatized immunoconjugate of the anti-(carcinoembryonic antigen) monoclonal antibody C46: immunohistological reactivity and pharmacokinetic comparison with a randomly derivatized C46 immunoconjugate. *Cancer Immunol. Immunother.* **32**, 207-213.
165. Braslawsky, G.R., Kadow, K., Knipe, J., McGoff, K., Edson, M., Kaneko, T. and Greenfield, R.S. (1991) Adriamycin(hydrazone)-antibody conjugates require internalization and intracellular acid hydrolysis for antitumor activity. *Cancer Immunol. Immunother.* **33**, 367-374.
166. Miralles, F., Takeda, Y. and Escribano, M.J. (1991) Comparison of carbohydrate and peptide biotinylation of the immunological activity of IgG1 murine monoclonal antibodies. *J. Immunol. Meth.* **140**, 191-196.
167. Wilchek, M. and Bayer, E.A. (1990) Labeling glycoconjugates with hydrazide reagents. *Methods in Enzymology* **138**, 429-442.
168. Gershoni, J.M., Bayer, E.A. and Wilchek, M. (1985) Blot analyses of glycoconjugates: Enzyme-hydrazide-a novel reagent for the detection of aldehydes. *Anal. Biochem.* **146**, 59-63.
169. Zara, J.J., Wood, R.D., Boon, P., Kim, C.H., Pomato, N., Bredehorst, R. and Vogel, C.-W. (1991) A carbohydrate-directed heterobifunctional cross-linking reagent for the synthesis of immunoconjugates. *Anal. Biochem.* **194**, 156-162.
170. Avigad, G., Amaral, D., Asensio, C. and Horecker, B.L. (1962) The D-galactose oxidase of *Polyporus circinatus*. *J. Biol. Chem.* **237**, 2736-2741.
171. Rothfus, J.A. and Smith, E.L. (1963) Glycopeptides iv. The periodate oxidation of glycopeptides from human G-globulin. *J. Biol. Chem.* **238**, 1402-1410.
172. Lenten, L.V. and Ashwell, G. (1971) Studies on the chemical and enzymatic modification of glycoproteins. *J. Biol. Chem.* **246**, 1889-1894.
173. Jencks, W.P. (1959) Studies on the mechanism of oxime and semicarbazone formation. *J. Am. Chem. Soc.* **81**, 475-481.
174. Cordes, E.H. and Jencks, W.P. (1962) On the mechanism of schiff base formation and hydrolysis. *J. Am. Chem. Soc.* **84**, 832-837.
175. Anderson, B.M and Jencks, W.P. (1960) The effect of structure on reactivity in semicarbazone formation. *J. Am. Chem. Soc.* **82**, 1773-1777.
176. O'Shannessy, D.J. and Quarles, R.H. (1987) Labeling of the oligosaccharide moieties of immunoglobulins. *J. Immunol. Meth.* **99**, 153-161.
177. Chamow, S.M., Kogan, T.P., Peers, D.H., Hastings, R.C., Byrn, R.A. and Ashkenazi, A. (1992) Conjugation of soluble CD4 without loss of biological activity via a novel carbohydrate-directed cross-linking reagent. *J. Biol. Chem.* **267**, 15916-15922.
178. King, T.P., Zhao, S.W. and Lam, T. (1986) Preparation of protein conjugates via intermolecular hydrazone linkage. *Biochemistry* **25**, 5774-5779.

179. Chua, W.M., Fan, S.T. and Karush, F. (1984) Attachment of immunoglobulin to liposomal membrane via protein carbohydrate. *Biochim. Biophys. Acta* **800**, 291-300.
180. Lowry, O.H., Rosebrough, N.J., Farr, A.L. and Randall, R.J. (1951) Protein measurement with the Folin phenol reagent. *J. Biol. Chem.* **193**, 265-275.
181. Peterson, G.L. (1983) Determination of total protein. *Methods in Enzymology* **91**, 95-119.
182. Laemmli, U.K. (1970) Cleavage of structural proteins during the assembly of the head of bacteriophage T4. *Nature* **227**, 680-685.
183. McConahey, P.J. and Dixon, F.J. (1980) Radioiodination of proteins by the use of the chloramine-T method. *Methods in Enzymology* **70**, 210-247.
184. Fogh, J. and Trempe, G. New human tumour cell lines. In: *Human tumour cells in vitro*, Fogh, J. ed. New York: Plenum Press, 1975, pp. 115-141.
185. Luner, S.J., Ghose, T., Chatterjee, S., Nolido-Cruz, H. and Belitsky, P. (1986) Monoclonal antibodies to kidney and tumor-associated surface antigens of human renal cell carcinoma. *Cancer Res.* **46**, 5816-5820.
186. McKinney, M.M. and Parkinson, A. (1987) A simple, non-chromatographic procedure to purify immunoglobulins from serum and ascites fluid. *J. Immunol. Meth.* **96**, 271-278.
187. Riddles, P.W., Blakeley, R.L. and Zerner, B. (1983) Reassessment of Ellman's Reagent. *Methods in Enzymology* **91**, 49-60.
188. Kueng, W., Silber, E. and Eppenberger, U. (1989) Quantification of cells cultured on 96-well plates. *Anal. Biochem.* **182**, 16-19.
189. Peterson, D.L., Gleisner, J.M. and Blakley, R.L. (1975) Bovine liver dihydrofolate reductase: purification and properties of the enzyme. *Biochemistry* **14**, 5261-5266.
190. Ghose, T., Blair, A.H., Kralovec, J., Mammen, M. and Uadia, P.O. Synthesis and testing of antibody-antifolate conjugates for drug targeting. In: *Antibody-mediated delivery systems*, Rodwell, J.D. ed. New York: Marcel Dekker, Inc., 1988, pp. 81-122.
191. Nakao, H., Nishikawa, A., Nishiura, T., Kanayama, Y., Tarui, S. and Taniguchi, N. (1991) Hypogalactosylation of immunoglobulin G sugar chains and elevated serum interleukin 6 in Castleman's disease. *Clinica Chimica Acta.* **197**, 221-228.
192. Rudd, P.M., Leatherbarrow, R.J., Rademacher, T.W. and Dwek, R.A. (1991) Diversification of the IgG molecule by oligosaccharides. *Molec. Immunol.* **28**, 1369-1378.
193. Rosowsky, A. and Yu, C.-S. (1978) Methotrexate analogues. 10. Direct coupling of methotrexate and diethyl L-glutamate in the presence of peptide forming reagents. *J. Med. Chem.* **21**, 170-175.

194. Kralovc, J., Spencer, G., Blair, A.H., Mammen, M., Singh, M. and Ghose, T. (1989) Synthesis of methotrexate-antibody conjugates by regiospecific coupling and assessment of drug and antitumor activities. *J. Med. Chem.* **32**, 2426-2431.
195. Rochu, D., Crespeau, H. and Fine, J.M. (1991) Albumin Paris 2: a new genetic variant distinguished by isoelectric focusing. *Biochimie* **73**, 617-619.
196. Clamp, J.R. and Hough, L. (1965) The periodate oxidation of amino acids with reference to studies on glycoproteins. *Biochem. J.* **94**, 17-24.
197. Krotoski, W.A. and Weimer, H.E. (1966) Peptide-associated and antigenic changes accompanying periodic acid oxidation of human plasma orosomucoid. *Arch. Biochem. Biophys.* **115**, 337-344.
198. O'Shannessy, D.J. and Quarles, R.H. (1985) Specific conjugation reactions of the oligosaccharide moieties of immunoglobulins. *J. Appl. Biochem.* **7**, 347-355.
199. Bumol, T.F., Baker, A.L., Andrews, E.L., et al. KS1/4-DAVLB, a monoclonal antibody-vinca alkaloid conjugate for site-directed therapy of epithelial malignancies. In: *Antibody-mediated delivery systems*, Rodwell, J.D. ed. New York: Marcel Dekker, Inc., 1988, pp. 55-79.
200. Jeanson, A., Cloes, J.M., Bouchet, M. and Rentier, B. (1988) Comparison of conjugation procedures for the preparation of monoclonal antibody-enzyme conjugates. *J. Immunol. Meth.* **111**, 261-270.
201. Ramjeesingh, M., Zywuiko, M., Rothstein, A., Whyte, R. and Shami, E.Y. (1990) Antigen protection of monoclonal antibodies undergoing labelling. *J. Immunol. Meth.* **133**, 159-167.
202. Myers, D.E., Uckun, F.M., Swaim, S.E. and Vallera, D.A. (1989) The effects of aromatic and aliphatic maleimide crosslinkers on anti-CD5 ricin immunotoxins. *J. Immunol. Meth.* **121**, 129-142.
203. Rose, K., Vilaseca, L.A., Werlen, R., Meunier, A., Fisch, I., Jones, R.M.L. and Offord, R.E. (1991) Preparation of well-defined protein conjugates using enzyme-assisted reverse proteolysis. *Bioconjugate Chem.* **2**, 154-159.
204. Hamilton, R.G., Reimer, C.B. and Rodkey, L.S. (1987) Quality control of murine monoclonal antibodies using isoelectric focusing affinity immunoblot analysis. *Hybridoma* **6**, 205-217.
205. Awdeh, Z.L., Williamson, R. and Askonas, B.A. (1970) One cell-one immunoglobulin: Origin of limited heterogeneity of myeloma proteins. *Biochem. J.* **116**, 241-248.
206. Smyth, M.J., Pietersz, G.A. and McKenzie, I.F.C. (1987) The mode of action of methotrexate-monoclonal antibody conjugates. *Immunol. Cell Biology* **65**, 189-200.
207. Kyriakos, R.J., Shih, L.B., Ong, G.L., Patel, K., Goldenberg, D.M. and Mattes, M.J. (1992) The fate of antibodies bound to the surface of tumor cells *in vitro*. *Cancer Res.* **52**, 835-842.

208. Basu, S.K. (1990) Receptor-mediated endocytosis of macromolecular conjugates in selective drug delivery. *Biochem. Pharmacol.* **40**, 1941-1946.
209. Scanlin, T.F. and Glick, M.C. Turnover of mammalian surface membranes. In: *Mammalian cell membranes*, Jamieson, G.A. and Robinson, D.M. eds. London: Butterworths, 1977, pp. Vol 5, 1-28.